

Random Interval Distillation for Detecting Multiple Changes in General Dependent Data

Xinyuan Fan¹ and Weichi Wu¹

¹Center for Statistical Science, Department of Industrial Engineering, Tsinghua University

Abstract

We propose a new and generic approach for detecting multiple change-points in general dependent data, termed random interval distillation (RID). By collecting random intervals with sufficient strength of signals and reassembling them into a sequence of informative short intervals, our new approach captures the shifts in signal characteristics across diverse dependent data forms including locally stationary high-dimensional time series and dynamic networks with Markov formation. We further propose a range of secondary refinements tailored to various data types to enhance the localization precision. Notably, for univariate time series and low-rank autoregressive networks, our methods achieve the minimax optimality as their independent counterparts. For practical applications, we introduce a clustering-based and data-driven procedure to determine the optimal threshold for signal strength, which is adaptable to a wide array of dependent data scenarios utilizing the connection between RID and clustering. Additionally, our method has been extended to identify kinks and changes in signals characterized by piecewise polynomial trends. We examine the effectiveness and usefulness of our methodology via extensive simulation studies and a real data example, implementing it in the R-package `rid`.

Keywords: Change-point detection; Locally stationary time series; Network; Data-driven threshold.

1 Introduction

Change-point detection methods have significant prospects for applications in various fields, including finance [8; 40], climatology [27; 55], geoscience [10], biology [50], epidemiology [13; 31], neuroscience [3; 33], chemistry [19], to name a few. With technology development for data collection, the types and volumes of data have become increasingly diverse and massive with complex dependent structures. Practical examples include high-dimensional data [39], locally stationary time series [36], dependent network sequence [44], and integer time series [9] among others. However, most existing multiple change-point detection methods are developed with theoretical guarantees for low-dimensional and mainly independent data, which are not directly applicable to investigating the structure changes for the aforementioned data types. To bridge this gap, in this paper, we aim to develop a novel and general approach for multiple change-point detection that can encompass those types of data under general dependence. To better understand the novelty of our approach, we first present some literature reviews on popular change-point detection methods.

Existing multiple change-point estimation methods primarily include three branches, which are loss and penalization based methods, moving sum (MOSUM) based methods, and binary segmentation based methods. A typical form for the first class of methods is to employ a loss function, which is often the \mathcal{L}_2 loss or certain one that is related to likelihood or quasi-likelihood, together

with some regularization to estimate the best piecewise constant signals, and hence changes. For independent data, various penalties, including l_0 penalty and l_1 penalty can lead to consistent estimations, see for example [60; 22; 38; 32; 28]. Other related works include [20] which employed the constraint optimization, and [70] which utilized projection in addition to penalization. For time series, change-point detection methods belonging to this class include [4; 37; 67; 14] among others. Most of the above-mentioned methods are proven to be valid only when applied to data that fulfill certain specific parametric assumptions or possess unscalable computational complexity. It is hard in general to generalize those methods, making them applicable to various types of data such as high-dimensional time series, integer time series, and dynamic networks as discussed in Section 3 of our paper.

The second popular class of detection methods is based on the moving sum (MOSUM), which can be dated back to [2]. Recent progress on MOSUM includes but is not limited to [17] for theoretical properties of univariate stationary data, and [71] which improves univariate MOSUM via PULSE criterion. Works beyond univariate series, among others, include [41; 11] for stationary high-dimensional data, and [25] for independent tensor data. [34] proposed a general framework for non-stationary data based on estimating equations. To apply the MOSUM-type methods in practice, a key ingredient is to choose the window size or bandwidth, which is difficult, especially under temporal dependence and general time series nonstationarity or under multi-dimensionality. Moreover, to the best of the authors' knowledge, there are no available MOSUM-based methods for network sequence.

The third class of multiple change-point detection methods is based on the Binary Segmentation (BS) [59; 57]. BS does not require choosing the window size or bandwidth, however, the effectiveness of the algorithm critically depends on the pattern of signals, see for example [21]. [21] further proposed the seminal Wild Binary Segmentation (WBS) algorithm, augmenting BS via binary segmented random intervals based on their signals to achieve the (nearly) minimax detection bound with i.i.d. Gaussian noises when the number of change-points is bounded. However, when the number of change-points is unbounded, WBS requires the prior knowledge of minimal spacing to retain this optimality [60]. Following WBS, many subsequent works consider conducting binary segmentation on specific random intervals or sub-intervals. Some prominent examples include [7; 35; 72]. A few works extend WBS to identify the changes in high-dimensional or non-Euclidian data. For example, [61] considered dynamic networks, where networks at different times are assumed to be independent. [63] proposed a self-normalize test for high-dimensional time series, briefly discussing possible extensions to detecting multiple changes with WBS. However, the theoretical justification and essential issues for implementation including the choice of threshold for the WBS extensions seemed not to have been investigated by [63].

In this paper, we propose a new framework for the change-point detection problem that is distinct from the above-mentioned three classes of methods, which is the random interval distillation (RID) to get RID of the influence of structural changes. Motivated by WBS, we sample random intervals and calculate some statistics for signals on the intervals. As in the previous research, the absence of change-points within this interval generally results in a relatively small value while the existence of one change-point will yield a large one. Different from BS-based methods, such as WBS, RID does not rely on BS to separate the random intervals sequentially. Instead, we process the random intervals altogether to yield a new sequence of informative intervals. The new intervals need not be any of the original intervals, however, each of them contains exactly one change-point with probability tending to 1, and is very short with a high probability. We term the process 'distillation' since the new sequence carries the full information of changes as the original massive random intervals that could be noisy and be without or with more than one change-point. Briefly speaking, we first perform a preliminary selection removing those with too small statistical values

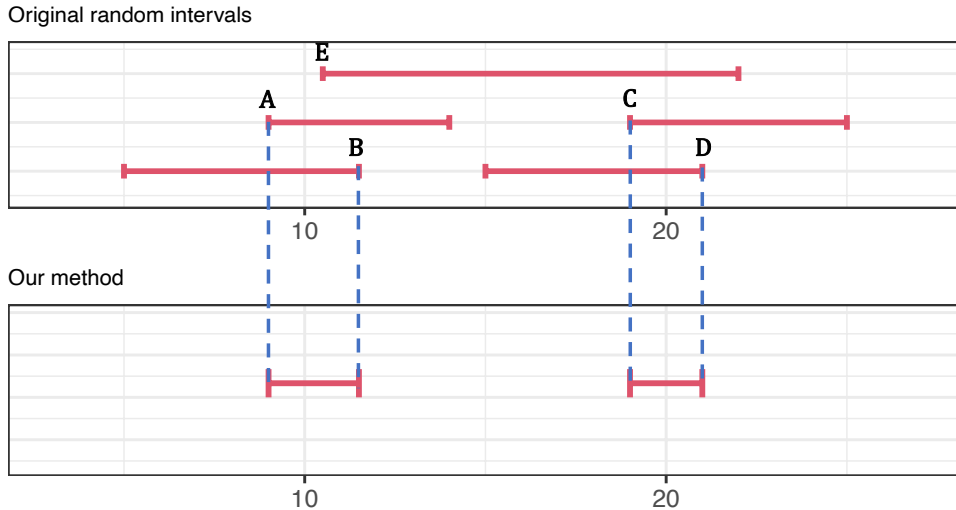


Figure 1: Suppose that there are two change-points $\eta_1 = 10, \eta_2 = 20$. The first figure displays the random intervals (5 intervals in total, represented by horizontal lines) all with signals exceeding the threshold. Our distillation begins with finding the right endpoint B (the smallest right endpoint), then the intervals corresponding to A and E are removed due to the overlap, and we select D . Similarly, for the left endpoints, we successively choose C and A . Therefore, the final constructed intervals are $[A, B]$ and $[C, D]$. We mention that our method appropriately avoids generating $[E, B]$ which does not contain η_1 .

while preserving those containing change-point information. Our Theorem 3.4 shows the existence of clustering boundary for the informative intervals and noninformative intervals under general conditions for various types of data, which motivates us to determine the threshold via a data-driven clustering algorithm. As pointed out by [41], the existing three classes of detection methods listed in the previous paragraphs relate the change-point problem to either model fittings or testing. Different from previous works, and to the best of the authors' knowledge, RID is the first method that connects change-point detection to clustering with theoretical justification. After preliminary screening, we rearrange the endpoints of intervals according to certain positional relationships, and use qualified endpoints to 'distill' new intervals that contain exactly one change-point (see Figure 1 for an illustration) with short lengths. We then find the change-points through the signal statistics on each distilled new interval. We defer the detailed procedure in Section 2 of the paper. For univariate short-range dependent time series data and low-rank autoregressive networks, we can achieve a (nearly) minimax optimal detection bound and a (nearly) minimax optimal localization bound after refinements without any prior knowledge of the minimum spacing. We generalize our methods for piecewise polynomial signals, finding new low-complexity statistics and providing the relevant theoretical results for this scenario. The implementation of RID is encapsulated in the R-package `rid`.

1.1 Advantages of RID

We summarize the advantages of RID as follows.

1. (*Flexibility.*) RID is applicable to the change-point analysis for various types of data under general dependence, such as high-dimensional time series, locally stationary time series, inte-

ger time series, and dynamic network data. For multivariate and high-dimensional data, there are no restrictions on the dependence across different dimensions. The theoretical framework allows different dependence measures, including Markov chain dependence, mixing condition, and physical dependence measure.

2. (*Nearly minimax optimality.*) For univariate short-range time series and low-rank autoregressive network [29], with refinement our methods achieve a minimax optimal condition except for a logarithm factor as their independent counterparts. We mention that for our method, to achieve optimality allowing diverging number of changes, we do not need any prior knowledge about the minimal spacing of change-points, which is a benefit brought by the ‘distillation’ process.
3. (*Data adaptive thresholds.*) For piecewise constant signals, RID gives a data-driven approach to determine the threshold which is based on a density-based clustering method and is valid for various types of dependent data including m -dependent sequences, Markov chains, locally stationary time series, ϕ -mixing and strong mixing sequences, and dynamic networks. Moreover, to improve the finite sample performance under local stationarity, we propose a customized refinement method that has advantages over self-normalization-based methods designed for stationarity.
4. (*Computational efficiency.*) The computational complexity of interval distillation is of $O(M \log M)$ where M is the number of random intervals, which is usually much smaller than T . For univariate sequences, the total computational cost is $O(MT)$, which is the same as NOT [7]. In practice, RID often achieves good performance with relatively very small M since the distilled intervals are often shorter than the interval produced by NOT. Finally, the computation of signal statistics within each interval and each dimension can be easily parallelized, which shows the potential applicability of RID to large-scale data.

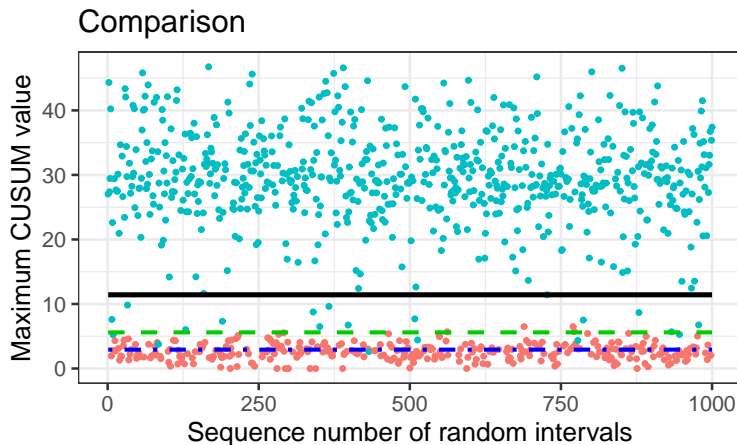


Figure 2: The samples are from a model with piecewise constant signals and AR(1) errors with the AR coefficient 0.5 and centered $\chi^2(2)$ errors. The density of maximum CUSUM values is bimodal. The solid line represents our threshold. The dashed line and dotted line are thresholds obtained by NOT and WBS respectively. Both of them are too small, which leads to an overestimation of the number of change-points K .

The rest of the paper is structured as follows. Section 2 presents a general framework, including

the evaluation criteria, algorithms, signal-to-noise ratio condition, and theoretical properties for multiple change-point detection. In Section 3, the conditions for different types of dependent data and the corresponding consistent results are discussed. Furthermore, a fully data-driven method for choosing the threshold is proposed. Moreover, refinements for dynamic networks and locally stationary time series are presented in Section 3.3 and Section 3.4 respectively. In Section 4, we introduce a new statistic for processing piecewise polynomial signals and present the theoretical results. In Section 5, we conduct numerical studies comparing our method with the state-of-the-art approaches, while in Section 6, we analyze a real data example via RID. Section 7 contains the conclusion. The results of extra simulation studies, an additional real data example, useful concentration inequalities, and all detailed derivations and proofs are relegated to the appendix.

1.2 Notations

In this paper, we write \mathbb{X} to emphasize that X is a vector. For a vector $\mathbb{X} \in \mathbb{R}^p$, $|\mathbb{X}|_\infty = \max_i |X_i|$. For $q \in \mathbb{N}^*$, $|\mathbb{X}|_q = (\sum_{i=1}^p |X_i|^q)^{1/q}$. For a sub-Gaussian random variable X , define $\|X\|_{\psi_2} = \inf \left\{ t > 0 : \mathbb{E} \exp \left(\frac{X^2}{t^2} \right) \leq 2 \right\}$. For a random variable X , $\|X\|_{\mathcal{L}_p} = (\mathbb{E}|X|^p)^{\frac{1}{p}}$ is the usual p -norm. For a set S , $|S|$ is the number of elements in S . For a real number x , $\lfloor x \rfloor$ represents the largest integer that is less than or equal to x , and $\text{sign}(x) = I(x > 0) - I(x < 0)$ where $I(\cdot)$ is the indicator function. For two positive real numbers a, b , write $a \vee b = \max(a, b)$, $a \wedge b = \min(a, b)$. For two matrices A and B , define the inner product $\langle A, B \rangle = \sum_{i=1}^n \sum_{j=1}^n A_{ij} B_{ij}$ where A_{ij}, B_{ij} are the elements in i th row and j th column of A and B , respectively. For two sequences of positive real numbers a_n, b_n , $a_n = o(b_n)$ if $a_n/b_n \rightarrow 0$ as $n \rightarrow \infty$, $a_n = O(b_n)$ if there exists two positive constants N and C such that $a_n/b_n \leq C$ when $n > N$, and $a_n = \Omega(b_n)$ if there exists three positive constants N, C_1, C_2 such that $C_1 \leq a_n/b_n \leq C_2$ when $n > N$. Let $C_i, c_i, i = 1, 2, \dots$ denote absolute constants and C_x, c_x represent constants related to some variable x . We use the convention that $0/0 = 0$ in this paper.

2 A general framework for detecting change-points

2.1 Model setups

Let $\{\mathbb{X}_t, \mathbb{X}_t \in \mathbb{R}^p\}_{t=1}^T$ be a sequence of p -dimensional samples of time series. For $1 \leq i \leq p$, let $X_{t,i}$ denote the i th dimension of \mathbb{X}_t . Let $\eta = \{\eta_1, \dots, \eta_K\}$ be the collection of K change-points $\eta_i, 1 \leq i \leq K$, such that $1 < \eta_1 < \dots < \eta_K < T + 1$. The multiple detection problem is to detect both the total number K and the locations $\{\eta_1, \dots, \eta_K\}$. Let \hat{K} and $\hat{\eta}_i$ s be the estimators of K and η_i s. We shall first consider the change-point detection for piecewise constant signals, i.e.,

$$\mathbb{E}\mathbb{X}_t \neq \mathbb{E}\mathbb{X}_{t-1} \text{ if and only if } t = \eta_k \text{ for } 1 \leq k \leq K. \quad (1)$$

We then discuss the extension to piecewise polynomial signals in Section 4. For ease of reference, we abbreviate them as PC and PP respectively. An estimator is consistent if it satisfies the following definition.

Definition 2.1 (Consistency). *Denote $\Delta = \min_{k=1, \dots, K-1} \{\eta_{k+1} - \eta_k\} \wedge (\eta_1 - 1) \wedge (T + 1 - \eta_K)$. The estimator $(\hat{\eta}_1, \dots, \hat{\eta}_{\hat{K}})$ is consistent with respect to (η_1, \dots, η_K) iff*

$$\mathbb{P} \left(\hat{K} = K \quad \text{and} \quad \max_{k=1, \dots, K} |\hat{\eta}_k - \eta_k| \leq \epsilon \right) \rightarrow 1,$$

where $\epsilon/\Delta \rightarrow 0$ as $T \rightarrow \infty$.

The main work of this paper is to give a new algorithm that consistently estimates K and $\eta_k s$ under mild conditions.

Table 1: Summary of notations

Notation	Meaning
T	Length of time
p	Dimension of data
\mathbb{X}_t	p -dimensional sample at time t
K	Number of change-points
$\eta = \{\eta_k\}_{k=1}^K$	Change-points
Δ	Minimal spacing
q	An arbitrary but fixed positive number
τ	Detecting threshold
$(s, e]$	(Random) interval
$\tilde{f}_{s,e}(X)$	p -dimensional statistic on $(s, e]$, with the i_{th} coordinate being $\tilde{f}_{s,e,i}(X)$
$\tilde{g}_{s,e}^t(X)$	p -dimensional statistic on $(s, e]$ at time t , with the i_{th} coordinate being $\tilde{g}_{s,e,i}^t(X)$ ($\tilde{f}_{s,e}$ and $\tilde{g}_{s,e}^t$ are usually related)

2.2 Methodology

Different from methods that require recursion or iterative optimization, we propose a Random Interval Distillation procedure to detect $\eta_k s$. It consists of the distillation and localization step. In the first step, we construct for each change-point η_k a small enough interval $[u_k, v_k]$ that covers it. In the second step, we localize the specific position of η_k in the interval $[u_k, v_k]$.

For any interval $(s, e] \subset (0, T]$ where s, e are integers, $s < e$ and any dimension i , define a measurable function $\tilde{f}_{s,e,i} : \mathbb{R}^{e-s} \mapsto \mathbb{R}$. Let $\tilde{f}_{s,e,i}(X) := \tilde{f}_{s,e,i}(X_{s+1,i}, \dots, X_{e,i})$ denote a statistic and let $\tilde{f}_{s,e}(X) = (\tilde{f}_{s,e,1}(X), \dots, \tilde{f}_{s,e,p}(X))^\top$ be the vector version. Here $\tilde{f}_{s,e,i}$ is a general statistic and is chosen according to the type of data and the type of signals, i.e., the piecewise constant or the piecewise polynomial signals. For example, if we have a univariate time series with the piecewise constant signal then we can set $\tilde{f}_{s,e,i}$ as the conventional maximum value of the CUSUM statistics. We discuss the choices of $\tilde{f}_{s,e,i}$ in detail for general piecewise constant signals and piecewise polynomial signals in Section 3 and Section 4, respectively.

Our Algorithm 1 takes the data $\{\mathbb{X}_t\}$, threshold τ and number of random intervals M as inputs and outputs \hat{K} and a set of intervals S^* . In Line 2 in Algorithm 1, we draw each random interval by sampling two endpoints, s, e , independently and identically following the uniformly distributed random variable Z on $\{1, \dots, T\}$, i.e $\mathbb{P}(Z = z) = 1/T$ for $1 \leq z \leq T$. Then the interval is $[s \wedge e, s \vee e]$. In Lines 3-7 in Algorithm 1, we gather into the set S the intervals $(s_m, e_m]$ in which $|\tilde{f}_{s_m, e_m}(X)|_q$ is larger than τ . The main purpose of this step is to exclude intervals that contain no change-point. Note that RID does not impose any requirements on the relationships or dependencies between different dimensions.

In Lines 8-21 in Algorithm 1, we select from S some endpoints and use them to form new intervals. In lines 8-14, a greedy method is employed to find the right endpoints $\{r_i\}$ of the newly created intervals. By reversing the time axis and applying the same method, we get the left endpoints $\{l_i\}$. It is straightforward to show that the numbers of r_i and l_i are equal and they both equal to the maximum sizes of subsets of S with non-overlapping intervals, and the number of r_i and l_i is \hat{K} . It is proved in Lemma C.2 that $l_j < r_j$ whenever $1 \leq j \leq \hat{K}$, which makes $[l_j, r_j]$ our new distilled intervals. Moreover, with a probability tending to 1, $\hat{K} = K$ and $[l_j, r_j]$ only covers

Algorithm 1 Distillation Step

Require: $\{\mathbb{X}_t\}_{t=1}^T$, τ , M , $\tilde{f}_{s,e}$

- 1: $S = \emptyset$
 - 2: Take M random intervals $\{(s_m, e_m)\}_{m=1}^M$ independently and uniformly
 - 3: **while** $1 \leq m \leq M$ **do**
 - 4: **if** $|\tilde{f}_{s_m, e_m}(X)|_q > \tau$ **then**
 - 5: $S = S \cup \{(s_m, e_m)\}$
 - 6: **end if**
 - 7: **end while**
 - 8: $\tilde{S} = S, i = 1$
 - 9: **while** $|\tilde{S}| > 0$ **do**
 - 10: $r_i = \min\{v : \exists u, (u, v) \in \tilde{S}\}$
 - 11: $v^* = r_i, u^* = \max\{u : (u, v^*) \in \tilde{S}\}$
 - 12: $\tilde{S} = \tilde{S} \cap \{(u, v) \in \tilde{S} : (u, v) \cap (u^*, v^*) \neq \emptyset\}^c$
 - 13: $i = i + 1$
 - 14: **end while**
 - 15: $\hat{K}_0 = i - 1, \tilde{S} = S, i = 1$
 - 16: **while** $|\tilde{S}| > 0$ **do**
 - 17: $l_{\hat{K}_0+1-i} = \max\{u : \exists v, (u, v) \in \tilde{S}\}$
 - 18: $u^* = l_{\hat{K}_0+1-i}, v^* = \min\{v : (u^*, v) \in \tilde{S}\}$
 - 19: $\tilde{S} = \tilde{S} \cap \{(u, v) \in \tilde{S} : (u, v) \cap (u^*, v^*) \neq \emptyset\}^c$
 - 20: $i = i + 1$
 - 21: **end while**
 - 22: $\hat{K} = i - 1, S^* = \{[l_j, r_j]\}_{j=1}^{\hat{K}}$
 - 23: Output \hat{K} and S^*
-

η_j , which is guaranteed in Theorem 2.2. q is a pre-specified fixed number. In the literature, q is usually set as 1 or 2. For instance, [21] choose $q = 1$ and [61] choose $q = 2$.

In summary, Algorithm 1 gives \hat{K} disjoint intervals, each of which covers exactly one change-point. We then utilize the following localization step to estimate the location of the changes in each distilled interval. For every $s_k < t \leq e_k$, define a measure function $\tilde{g}_{s_k, e_k, i}^t : \mathbb{R}^{e_k - s_k} \mapsto \mathbb{R}$ with the property that η_k is the only local maximum of $|\mathbb{E}\tilde{g}_{s_k, e_k, i}^t(X)|$ when $s_k \in (\eta_{k-1}, \eta_k)$ and $e_k \in (\eta_k, \eta_{k+1})$. Here, $\tilde{g}_{s_k, e_k, i}^t(X) := \tilde{g}_{s_k, e_k, i}^t(X_{s_k+1, i}, \dots, X_{e_k, i})$ and $\tilde{g}_{s_k, e_k}^t(X) := (\tilde{g}_{s_k, e_k, 1}^t(X), \dots, \tilde{g}_{s_k, e_k, i}^t(X))^\top$. We use $\arg \max_t |\tilde{g}_{s_k, e_k}^t(X)|_q$ to estimate η_k . For the PC case, we can choose $\tilde{g}_{s, e, i}^t$ to be the CUSUM statistic at time t in the interval $(s, e]$ (see (13)). In our paper, for detecting changes in

Algorithm 2 Localization Step

Require: $\{\mathbb{X}_t\}_{t=1}^T$, S^* , $\tilde{g}_{s,e}^t$

- 1: $i = 1, \hat{K} = |S^*|$. Suppose $S^* = \{[s_k, e_k]\}_{k=1}^{\hat{K}}$.
 - 2: **while** $i \leq \hat{K}$ **do**
 - 3: $\hat{\eta}_i = \arg \max_{t: s_i < t \leq e_i} |\tilde{g}_{s_i, e_i}^t(X)|_q$
 - 4: $i = i + 1$
 - 5: **end while**
 - 6: Output $\hat{\eta} = \{\hat{\eta}_1, \dots, \hat{\eta}_{\hat{K}}\}$
-

PC and PP cases, we impose $\tilde{f}_{s, e, i}^t(X) = \max_{t: s < t \leq e} |\tilde{g}_{s, e, i}^t(X)|$ for $p = 1$ and $\tilde{f}_{s, e, i} = \tilde{g}_{s, e, i}^{t_0}$ where

$t_0 = \arg \max_{s < t \leq e} |\tilde{g}_{s,e}^t(X)|_q$ for $p > 1$, though our theoretical results are more flexible in the sense that Theorem 2.2 and 2.3 posit no assumptions on the relationship between $\tilde{f}_{s,e,i}(\cdot)$ and $\tilde{g}_{s,e,i}(\cdot)$.

The main purpose of sampling random intervals in WBS and NOT is to generate some well-positioned intervals to overcome the signal diminishing in certain intervals during the binary segmentation procedure. NOT augments WBS by further selecting short intervals. RID inherits the benefit of sampling random intervals, and further screens the endpoints of those intervals to form the shortest possible intervals, which are often narrower than intervals in NOT. Therefore, RID produces an accurate estimate of changes for various types of data mentioned in the introduction and Section 3, and can achieve a nearly minimax optimality of signal-to-noise ratio condition (see Section 3 for details), and a nearly minimax optimal localization error rate for the classic scenarios of detecting changes in the univariate mean cases. The time complexity of lines 3-7 in Algorithm 1 is $O(MpT)$ (we consider it $O(T)$ to calculate each $\tilde{f}_{s_m, e_m, i}(X)$). By first sorting the intervals in S according to the right endpoints, lines 8-14 can be computed in $O(M \log(M))$ time. The computational complexity of Algorithm 2 is $O(pT)$ in this paper. Therefore, the total time complexity is $O(MpT)$. We mention that it is possible to combine our algorithm with seeded intervals in [35] to achieve a time complexity of $O(pT \log(T))$.

2.3 Consistency

In this section we establish the consistency of RID. For this purpose, we first define the following quantities for signals and noises. Recall q in Algorithm 1, and define

$$\mathfrak{N} = \sup_{(s,e] \cap \eta = \emptyset} |\mathbb{E} \tilde{f}_{s,e}(X)|_q, \quad (2)$$

$$\mathfrak{J} = \arg \min_{\varepsilon} \{ \Lambda(\varepsilon) \leq T^{-3} \} \quad (3)$$

$$\text{where } \Lambda(\varepsilon) = \sup_{(s,e] \cap \eta \neq \emptyset} \mathbb{P} \left(\left| |\tilde{f}_{s,e}(X)|_q - |\mathbb{E} \tilde{f}_{s,e}(X)|_q \right| \geq \varepsilon \right),$$

$$\mathfrak{S} = \inf_{1 \leq k \leq K} \inf_{\substack{s \in (\eta_k - \Delta/4, \eta_k - \Delta/8) \\ e \in (\eta_k + \Delta/8, \eta_k + \Delta/4)}} |\mathbb{E} \tilde{f}_{s,e}(X)|_q. \quad (4)$$

To detect the changes, we shall consider $\tilde{f}_{s,e}$ which has the property that $|\mathbb{E} \tilde{f}_{s,e}(X)|_q$ is small in intervals where there is no change-point, and large in the neighborhood of the changes. This requirement is motivated, and clearly satisfied by the popular CUSUM statistics where $\tilde{f}_{s,e} = \tilde{g}_{s,e}^{t_0}$ and $t_0 = \arg \max_{s < t \leq e} |\tilde{g}_{s,e}^t(X)|_q$, $\tilde{g}_{s,e}^t(X) = \sqrt{\frac{e-t}{(e-s)(t-s)}} \sum_{r=s+1}^t \mathbb{X}_r - \sqrt{\frac{t-s}{(e-s)(e-t)}} \sum_{r=t+1}^e \mathbb{X}_r$ for PC means. Notice that in some sense the magnitudes of $\tilde{f}_{s,e}$ in the intervals without change-points can be measured by \mathfrak{N} , and in the interval with one change-point can be measured by \mathfrak{S} . Therefore, \mathfrak{S} symbolizes the signals resulting from changes, and \mathfrak{N} represents one source of the noises. Similarly, \mathfrak{J} measures the proximity of $|\tilde{f}_{s,e}(X)|_q$ to $|\mathbb{E} \tilde{f}_{s,e}(X)|_q$ with a controlled probability, and denotes another source of the noises. In Remark 9 of the appendix, we provide concrete formulas of \mathfrak{J} for Markov chains, locally stationary time series, and strong mixing sequences.

Theorem 2.2 (Properties of distilled intervals). *Assume that*

$$\mathfrak{S} > \mathfrak{N} + 2\mathfrak{J}. \quad (5)$$

Then if τ satisfies

$$\mathfrak{J} + \mathfrak{N} < \tau < \mathfrak{S} - \mathfrak{J}, \quad (6)$$

we have

$$\mathbb{P} \left(\left\{ \hat{K} = K \right\}, \bigcap_{j=1}^{\hat{K}} \left\{ [l_j, r_j] \text{ covers } \eta_j \text{ and } r_j - l_j \leq \frac{\Delta}{2} \right\} \right) \geq 1 - T^{-1} - \frac{T}{\Delta} \exp \left\{ -\frac{M\Delta^2}{32T^2} \right\}, \quad (7)$$

where \hat{K} and $\{[l_j, r_j]\}_{j=1}^{\hat{K}}$ are yielded by Algorithm 1 with input parameters τ and M .

Theorem 2.2 shows that under suitable signal and noise condition (5), with a high probability that our distilled intervals will consist of K disjoint intervals with each length smaller than $\Delta/2$, and each interval cover one change-point. Notice that condition (5) allows both fixed and diverging p and K . Compared with [60] assuming independence and sub-gaussianity, the range $(\mathfrak{J} + \mathfrak{N}, \mathfrak{S} - \mathfrak{J})$ in (6) is affected by the additionally dependence among $\{\mathbb{X}_t\}$.

Remark 1. Condition (5) is the signal-to-noise condition, which can be verified for Markov chains, locally stationary time series, and strong mixing sequences as discussed in Section 3 and Section D.1 of the appendix. Equation (6) derives a range for threshold τ such that the distilled intervals satisfy the desired property (7), and is further simplified in (17) of Corollary 3.2, tailor to the dependence structure. We further propose a data-driven method for selecting τ for PC signals in Section 3.2.

The probability (7) will tend to 1 if

$$\frac{32T^2}{\Delta^2} \log \left(\frac{T}{\Delta} \right) = o(M). \quad (8)$$

For WBS-based algorithms, (8) is commonly assumed, as discussed in [21] among others. When $\Delta = \Omega(T)$ such that the number of changes is bounded, equation (8) will hold with M diverging at an arbitrarily slow rate.

To further obtain the consistent estimation of η via Algorithm 2, additional conditions (regarding $\tilde{g}_{s,e,i}^t$) are needed. Recall that by the definition of $\tilde{g}_{s,e,i}^t$, for any $s_k \in (\eta_{k-1}, \eta_k)$, $e_k \in (\eta_k, \eta_{k+1})$, η_k is the only local maximum of $|\mathbb{E}\tilde{g}_{s_k,e_k}^t(X)|_q$. Define

$$\mathfrak{N}^* := \inf_{k=1,\dots,K} \inf_{\substack{s_k \in (\eta_k - \Delta/2, \eta_k) \\ e_k \in (\eta_k, \eta_k + \Delta/2)}} \inf_{b \in (s_k, e_k), b \neq \eta_k} \frac{|\mathbb{E}\tilde{g}_{s_k,e_k}^{\eta_k}(X)|_q - |\mathbb{E}\tilde{g}_{s_k,e_k}^b(X)|_q}{|\eta_k - b|}. \quad (9)$$

$$\mathfrak{J}^* := \arg \min_{\varepsilon} \{ \Lambda^*(\varepsilon) \leq \Delta^{-1}T^{-1} \} \quad (10)$$

$$\text{where } \Lambda^*(\varepsilon) = \sup_{(s,e]: |(s,e] \cap \eta| \leq 1, e-s \leq \frac{\Delta}{2}} \sup_{t: t \in (s,e]} \mathbb{P} (|\tilde{g}_{s,e}^t(X)|_q - |\mathbb{E}\tilde{g}_{s,e}^t(X)|_q \geq \varepsilon).$$

By (9), we have $|\eta_k - b| \leq \mathfrak{N}^*(|\mathbb{E}\tilde{g}_{s_k,e_k}^{\eta_k}(X)|_q - |\mathbb{E}\tilde{g}_{s_k,e_k}^b(X)|_q)$. Since η_k is the only maximizer of $|\mathbb{E}\tilde{g}_{s_k,e_k}^t(X)|_q$, $|\eta_k - \hat{\eta}_k|$ will be small if $|\tilde{g}_{s_k,e_k}^{\hat{\eta}_k}(X)|_q$ is close to the maximum if \mathfrak{J}^* , which measures the proximity of $|\tilde{g}_{s_k,e_k}^t(X)|_q$ to $|\mathbb{E}\tilde{g}_{s_k,e_k}^t(X)|_q$, is small. This holds under many circumstances since $\hat{\eta}_k$ is the sample maximizer of $|\tilde{g}_{s_k,e_k}^t(X)|_q$. We calculate \mathfrak{N}^* in Section D.1 of the appendix for the PC case. To calculate \mathfrak{J}^* , the procedure is similar to the previous calculations for \mathfrak{J} in Section B of the appendix. In this paper we set $\tilde{g}_{s,e}^t$ as the CUSUM statistic (13) for the PC case and as a linear function (see (24)) for the PP case. We list some specific results of \mathfrak{J}^* in Table 13 of the appendix. With \mathfrak{J}^* , \mathfrak{N}^* , we have the following results for the localization error.

Theorem 2.3 (Consistency of RID). *Assume that the conditions of Theorem 2.2 hold and that*

$$\frac{\mathfrak{J}^*}{\mathfrak{R}^* \Delta} \rightarrow 0 \quad \text{as} \quad T \rightarrow \infty. \quad (11)$$

Then the estimates \hat{K} and $\hat{\eta}_1, \dots, \hat{\eta}_{\hat{K}}$ given by Algorithm 1 and Algorithm 2 satisfy

$$P \left(\hat{K} = K, \max_{k=1, \dots, K} |\hat{\eta}_k - \eta_k| \leq \varepsilon \right) \geq 1 - \frac{K+1}{T} - \frac{T}{\Delta} \exp \left\{ -\frac{M \Delta^2}{32 T^2} \right\}, \quad (12)$$

where $\frac{\varepsilon}{\Delta} \leq \frac{2\mathfrak{J}^*}{\mathfrak{R}^* \Delta} \rightarrow 0$.

In Section 3 and Section 4 we give the exact formulas for $\tilde{f}_{s,e,i}$, $\tilde{g}_{s,e,i}^t$, and τ . For the PC case with univariate independent sub-gaussian variables, our signal-to-noise ratio matches that in Lemma 1 in [60], which is nearly minimax optimal up to a logarithmic factor, see Remark 2 below. Moreover, using a refined argument (see Proposition 1), we show that our localization bound also matches that in Lemma 2 of [60], which is also nearly minimax optimal. For the PP case, our detection condition is weaker than [70] with lower computational complexity, and the localization error rate can be further improved by the second-stage localization (equation (7)) of [70].

3 Multiple change-point detection for the PC signal

In this section, we discuss the multiple change-point detection for general dependent and multivariate data. The types of such data include m -dependent sequences, Markov chains, ϕ -mixing processes, strong mixing processes, piecewise locally stationary time series, and piecewise stationary Poisson INGARCH. For practical applications, we propose a data-adaptive approach to select the suitable threshold through clustering, which is different from previous methods that choose thresholds by model selection, e.g., most of the penalization and WBS-based methods, and by test, e.g., most of the MOSUM-based methods. Moreover, in Section 3.3 and Section 3.4, second-stage refinements for dynamic networks and locally stationary time series are given. Throughout this section, we assume that $T \geq 3$.

3.1 Statistics and model assumptions

Let $\{\mathbb{X}_t\}_{t=1}^T$ be a sequence of p -dimensional vectors, where $\mathbb{X}_t = (X_{t,1}, \dots, X_{t,p})^\top$. Recall the forward definition (1) for PC signals. For any tripe (s, t, e) with $(s, e] \subset (0, T]$ and $s < t \leq e$, let

$$\tilde{g}_{s,e,i}^t(X) = \sqrt{\frac{e-t}{(e-s)(t-s)}} \sum_{r=s+1}^t X_{r,i} - \sqrt{\frac{t-s}{(e-s)(e-t)}} \sum_{r=t+1}^e X_{r,i}. \quad (13)$$

Let $\tilde{f}_{s,e,i} = \tilde{g}_{s,e,i}^{t_0}$ where $t_0 = \arg \max_{s < t \leq e} |\tilde{g}_{s,e,i}^t(X)|_q$. Formula (13) is well known as the CUSUM statistic [48]. We mention that if $(s, e] \cap \eta = \eta_k$ for some k , $\mathbb{E} \tilde{g}_{s,e,i}^t(X)$ reaches its maximum at $t = \eta_k - 1$. In this case we set $\hat{\eta}_k = 1 + \arg \max_{t: s_k < t \leq e_k} |\tilde{g}_{s_k, e_k}^t(X)|_q$.

Let $\kappa_{\eta_k} := |\mathbb{E} \mathbb{X}_{\eta_k} - \mathbb{E} \mathbb{X}_{\eta_k - 1}|_q$ be the magnitude of changes and $\kappa_q := \min_k \kappa_{\eta_k} / p$. In this paper, we consider two classes of distributions. Class A and the associated parameters are listed in Table 2. Let $\alpha = \Omega(\max_i \alpha_i)$ where α_i s are the variance proxies in Table 2. Class B and the associated assumptions are also summarized, with those assumptions guaranteeing that the $\alpha = \Omega(\max_i 1) = \Omega(1)$ for Class B.

Table 2: Models for $\{X_{t,i}\}_{t=1}^T$ and expressions of α_i (see Section B of the appendix for derivation details and for the complete definition of the notation)

Class	Time series	Parameters	α_i
A	m-dependent sub-gaussian (Example 1)	$\sigma_i = \max_t \ X_{t,i}\ _{\psi_2}$, let $\gamma = 2$	$m\sigma_i^2$
A	Markov chains (Theorem B.3)	$B_i = \max_{1 \leq t \leq T} X_{t,i} - \mathbb{E}X_{t,i} $, let $\gamma = 2$	$B_i^2 \inf_{0 < y < 1} \bar{t}_{mix}(y) \left(\frac{2-y}{1-y}\right)^2$ (See (30))
A	ϕ -mixing process (Example 3)	Mixing coefficients $\{\phi_{k,i}\}_{k=1}^\infty$, let $\gamma = 2$	$(\sum_{k=1}^\infty \sqrt{\phi_{k,i}})^2$
A	Piecewise locally stationary time series (Inequality 2 in Section B of the appendix)	Physical dependence measure $\{\Omega_p\}_{p=1}^\infty$ with parameter $\gamma \in (0, 2]$	$(\limsup_{p \rightarrow \infty} p^{1/2-1/\gamma} \Omega_p)^\gamma$

Class	Time series	Assumptions
B	Strong mixing process (Example 4)	$\mathbb{E}(X_{t,i})^\xi \leq c_\xi < \infty$ for some even integer $\xi \geq 2$, and mixing coefficients $\alpha(j) \leq Cr^j$ for some $C > 0$ and $0 < r < 1$.
B	Piecewise stationary Poisson INGARCH(p_0, q_0) (Example 5)	Positive parameters $\{\gamma_{u,i,k}, \delta_{v,i,k}\}_{u=0,v=1}^{p_0,q_0}$ satisfying $\max_{i,k} \left(\sum_{j=1}^{p_0} \gamma_{u,j,k} + \sum_{k=1}^{q_0} \delta_{v,i,k}\right) < 1$, and let ξ be an arbitrary positive even integer

Assumption 3.1 (Signal-to-noise condition for PC case). *For models in Class A, the signal-to-noise condition*

$$p^{\frac{1}{q}-1} (\alpha \log(T \vee p))^{1/\gamma} = o(\kappa_q \sqrt{\Delta}). \quad (14)$$

holds. For models in Class B, condition

$$p^{\frac{1}{\xi} + \frac{1}{q} - 1} T^{\frac{4}{\xi}} = o(\kappa_q \sqrt{\Delta}) \quad (15)$$

holds, and that assumptions in Table 2 are satisfied.

In fact, Assumption 3.1 is the specific form of (5) in the PC case, and we put the detailed derivations in Section D.1 of the appendix.

Remark 2 (Minimax detection bound for univariate independent sub-gaussian variables). *When $p = 1$ and $\{X_t\}$ are independent sub-gaussian variables with the maximum ψ_2 -norm $\sigma = \max_t \|X(t)\|_{\psi_2}$, (14) in Assumption 3.1 reduces to*

$$\sigma \log^{\frac{1}{2}}(T) = o(\kappa_1 \sqrt{\Delta}). \quad (16)$$

By Lemma 1 in [60], if T is sufficiently large and the joint distribution F_X of (X_1, \dots, X_T) satisfies $\kappa_1 \sqrt{\Delta} < \frac{1}{2} \sigma \sqrt{\log(T)}$, we have $\inf_{\hat{\eta}} \sup_{F_X} \mathbb{E}(H(\eta, \hat{\eta})) \geq \frac{\Delta}{8}$ where H is the Hausdorff distance (see (25) for the exact definition), which indicates that (16) is necessary (up to a logarithmic factor) for the existence of a consistent estimator.

Remark 3 (Comparison with WBS). *WBS [21] achieves the minimax detection bound when K is bounded for independent sub-gaussian data. [60] further shows that [21] can achieve a minimax*

detection bound when K diverges if $\max_{1 \leq m \leq M} (e_m - s_m) \leq C_1 \Delta$ almost surely for an absolute constant $C_1 > 1$. As a comparison, RID can achieve the minimax detection bound without prior knowledge of the minimal spacing Δ . Moreover, we achieve the same rate on K as in [60].

Corollary 3.2 (Consistency result for the PC case). *Under Assumption 3.1, choose τ such that*

$$\begin{aligned} c_2 p^{\frac{1}{q}} (\alpha \log(T \vee p))^{1/\gamma} < \tau < C_2 \kappa_q p \sqrt{\Delta} \text{ for models in Class A} \\ c_2 T^{4/\xi} p^{1/\xi+1/q} < \tau < C_2 \kappa_q p \sqrt{\Delta} \text{ for models in Class B} \end{aligned} \quad (17)$$

where c_2, C_2 are two absolute constants. Apply Algorithm 1 and Algorithm 2 with input parameters τ and M to get \hat{K} and $\hat{\eta}_1, \dots, \hat{\eta}_{\hat{K}}$. Then

$$P \left(\hat{K} = K, \max_{k=1, \dots, K} |\hat{\eta}_k - \eta_k| \leq \varepsilon \right) \geq 1 - \frac{2}{T} - \frac{T}{\Delta} \exp \left\{ -\frac{M \Delta^2}{32 T^2} \right\},$$

where

$$\begin{aligned} \frac{\varepsilon}{\Delta} &\leq C_4 \frac{p^{\frac{1}{q}-1} (\alpha \log(T \vee p))^{1/\gamma}}{\kappa_q \sqrt{\Delta}} \rightarrow 0 \text{ for models in Class A} \\ \frac{\varepsilon}{\Delta} &\leq C_4 \frac{T^{4/\xi} p^{1/\xi+\frac{1}{q}-1}}{\kappa_q \sqrt{\Delta}} \rightarrow 0 \text{ for models in Class B} \end{aligned}$$

for some absolute constant C_4 , and α, ξ can be found in Table 2 for different types of data.

Corollary 3.2 shows that $\{\hat{\eta}_k\}$ is consistent. The localization error rate can be further reduced to a nearly minimax optimal rate through a refinement advocated by [21]. Concretely, we set $\tilde{s}_k = \lfloor \frac{1}{2}(\hat{\eta}_{k-1} + \hat{\eta}_k) \rfloor$, $\tilde{e}_k = \lfloor \frac{1}{2}(\hat{\eta}_k + \hat{\eta}_{k+1}) \rfloor$ for $k = 1, \dots, \hat{K}$ where $\hat{\eta}_k$ are the estimates from Algorithm 1 and Algorithm 2 (set $\hat{\eta}_0 = 0$ and $\hat{\eta}_{\hat{K}+1} = T + 1$). Apply Algorithm 2 with $\{(\tilde{s}_k, \tilde{e}_k)\}_{1 \leq k \leq \hat{K}}$ again, and we get new estimators $\{\hat{\eta}_k^*\}_{1 \leq k \leq \hat{K}}$. The nearly minimax optimality of $\{\hat{\eta}_k^*\}_{1 \leq k \leq \hat{K}}$ for univariate series is shown in the following proposition.

Proposition 1 (Minimax localization error bound for univariate independent sub-gaussian variables). *Under the scenario of Remark 2 and condition (16), we have that with a probability tending to 1, $\sup_k |\eta_k - \hat{\eta}_k^*| = O(\frac{\sigma^2 \log(T)}{\kappa_1^2})$, which is nearly minimax optimal up to a logarithmic factor (by Lemma 2 in [60], the minimax lower bound is of order $\frac{\sigma^2}{\kappa_1^2}$).*

3.2 A clustering-based data-driven approach for τ

We need to choose two parameters, namely, threshold τ and number of random intervals M . We recommend choosing the largest possible M under computational constraints. A similar treatment has been adopted by [7; 47] among others. In this paper, we choose $M = 1000$ for simulation studies. The selection of τ is more involved and critical in change-point detection [21; 7]. Notice that we derive the theoretical range of τ in (17), of which the key quantities α and κ_q are difficult to estimate, especially when $\{\mathbb{X}_t\}$ are dependent. Moreover, the sSIC criterion advocated by [21; 7] are designed for independent data, and it often underestimates the threshold when correlation exists. In this section, we are devoted to developing a change-point threshold selection method, valid for general dependent data without the need of calculating α and κ_q . For this purpose, define

$$\tau_{ref} = \max_{j=1, \dots, T-h} |\tilde{f}_{j, j+h}(X)|_q e_T \text{ where } h = \lfloor 3 \log(T) \rfloor$$

and e_T is a divergent sequence that grows slowly (for example, we implement with $e_T = \log \log(T)$). The magnitude of order of τ_{ref} will asymptotically in the range of (17), exceeding its lower bound by a factor of e_T , which guarantee the good performance of RID when there are no change-points. For illustrations, note that h is small such that when $(j, j+h]$ contains no change-points, $\max_j |\tilde{f}_{j,j+h}(X)|_q$ is an approximation of the left-hand side of (17). On the contrary, $|\tilde{f}_{j,j+h}(X)|_q e_T$ cannot exceed the right-hand side of (17) even if it contains change-points because h is small. In fact, one can use τ_{ref} as a rule of thumb threshold. For refinements, we propose a clustering-based data-driven threshold utilizing τ_{ref} . We first set the interval $[0.1\tau_{ref}, 10\tau_{ref}]$ and employ a clustering-based machine learning approach to search a candidate threshold inside the interval. To see the equivalence between choosing a threshold and clustering, notice that heuristically if $|\tilde{f}_{s_m, e_m}(X)|_q$ is large, it is highly probable that (s_m, e_m) contains change-points (one can refer to the blue points in Figure 2). Conversely, a small $|\tilde{f}_{s_m, e_m}(X)|_q$ indicates that with a high probability (s_m, e_m) contains no change-point (one can refer to the red points in Figure 2). Figure 5 in Section D.2 of the appendix illustrates this phenomenon graphically in more detail. We assume the following assumption for Theorem 3.4 which proves the above observation.

Assumption 3.3. *Recall that M is the number of random intervals with a theoretical range (8). For models from Class A, in addition to (14), assuming*

$$\frac{K\sqrt{M}}{\sqrt{T}} p^{\frac{1}{q}-1} (\alpha \log(T \vee p))^{1/\gamma} = o(\kappa_q).$$

For models from Class B, in addition to (15) and assumptions in Table 2, assuming

$$\frac{K\sqrt{M}}{\sqrt{T}} T^{\frac{4}{\xi}} p^{\frac{1}{\xi} + \frac{1}{q} - 1} = o(\kappa_q).$$

Assumption 3.3 is a technical condition, which is a strengthened version of conditions (14) and (15), with an additional term $K\sqrt{M\Delta/T}$ in the left-hand side. When $\Delta = \Omega(T)$, this assumption reduces to Assumption 3.1 because K is bounded and M is allowed to diverge at an arbitrarily slow rate in this case.

Theorem 3.4. *Let \mathcal{P} be the class of joint distributions in Table 2 for which the corresponding \mathfrak{J} are listed in Table 13 in the appendix. Recall that $\tilde{g}_{s,e}^t(X)$ is the CUSUM statistic (13) and $|\tilde{f}_{s,e}(X)|_q = \max_t |\tilde{g}_{s,e}^t(X)|_q$. Let $\mathbb{E}_X(\cdot) = \mathbb{E}(\cdot | s_m, e_m)$ denote the conditional expectation. Then the event*

$$\mathcal{A}_* := \left\{ \sup_{(s,e] \subset (0,T]} \left| |\tilde{f}_{s,e}(X)|_q - \max_t |\mathbb{E}_X \tilde{g}_{s,e}^t(X)|_q \right| \leq C_3 \mathfrak{J} \sqrt{K} \right\}$$

satisfies $\mathbb{P}(\mathcal{A}_) \geq 1 - T^{-1}$ for some sufficiently large absolute constant $C_3 > 0$. Let b be an arbitrary real number such that $b = o(\kappa_q p \sqrt{T} / \sqrt{KM})$. Under Assumption 3.3, we have with a probability tending to 1,*

1. $\mathbb{E} \left(\left| \tilde{f}_{s_m, e_m}(X) \right|_q \middle| \{ |(s_m, e_m] \cap \eta| = 0 \}, \mathcal{A}_* \right) < C_3 \mathfrak{J} \sqrt{K}.$
2. $\mathbb{E} \left(\left| \tilde{f}_{s_m, e_m}(X) \right|_q \middle| \{ |(s_m, e_m] \cap \eta| > 0 \}, \mathcal{A}_* \right) > b/2.$
3. $\mathbb{P} \left(\bigcup_{m=1}^M \left\{ C_3 \mathfrak{J} \sqrt{K} < \left| \tilde{f}_{s_m, e_m}(X) \right|_q < b/2 \right\} \middle| \mathcal{A}_* \right) \rightarrow 0.$

Theorem 3.4(1)(2) suggest that $|\tilde{f}_{s_m, e_m}(X)|_q$ s can be grouped into two categories based on whether $(s_m, e_m]$ s contain change-points, with the categories exhibiting well-separated conditional expectations. Theorem 3.4(3) shows that with probability tending to 1, all the $|\tilde{f}_{s_m, e_m}(X)|_q$ s fall into $[0, C_3\mathfrak{I}\sqrt{K}] \cup [b/2, \infty)$. Therefore, there is a ‘gap’ $(C_3\mathfrak{I}\sqrt{K}, b/2)$, which is presented graphically in Figure 2. Moreover, by Corollary 3.2 all values in the interval $(C_3\mathfrak{I}\sqrt{K}, b/2)$ are qualified thresholds (note that we can take a large enough C_3). Therefore, Theorem 3.4 indicates that we could find a decision boundary for clustering $|\tilde{f}_{s_m, e_m}(X)|_q$ according to whether the random intervals contain change-points as a threshold, which can fall into (17).

Remark 4. *Theorem 3.4 remains valid for unbounded K when the popular sSIC criteria [21] fails. The quantity $\mathfrak{I}\sqrt{K}$ arises since one needs to consider arbitrary $(s, e] \subset (0, T]$, see (50) in Section B of the appendix for more details.*

To extract a valid threshold, we employ a clustering-based approach [53], which recognizes the cluster centers by finding density peaks, and is flexible and suitable for our general settings which allow heteroscedasticity and non-gaussianity. If one of the clustering boundaries falls into the candidate range $[0.1\tau_{ref}, 10\tau_{ref}]$, we set it as the threshold, or we use τ_{ref} as the threshold. Moreover, since τ_{ref} is always larger than the left hand side of (17) by a factor of e_T , RID will identify no changes with high probability if there are no change-points. From our numerical studies, the clustering-based method is effective for a wide range of practical data. The approach consists of three steps.

- (a) For each point $|\tilde{f}_{s_m, e_m}(X)|_q$, calculate its density ρ_m through the kernel density estimation

$$\rho_m = \frac{1}{Mh} \sum_{i=1}^M K \left(\frac{|\tilde{f}_{s_m, e_m}(X)|_q - |\tilde{f}_{s_i, e_i}(X)|_q}{h} \right)$$

where $K(\cdot)$ is the kernel function and h is a bandwidth.

- (b) Define

$$\delta_m := \min_{j: \rho_j > \rho_m} \left| |\tilde{f}_{s_j, e_j}(X)|_q - |\tilde{f}_{s_m, e_m}(X)|_q \right|. \quad (18)$$

If $\{j : \rho_j > \rho_m\} = \emptyset$, define $\delta_m = \max_j \left| |\tilde{f}_{s_j, e_j}(X)|_q - |\tilde{f}_{s_m, e_m}(X)|_q \right|$. Construct the decision graph (see [53]) $\{(\rho_m, \delta_m)\}_{m=1}^M$. Points with high δ_m and high ρ_m are regarded as cluster centers.

- (c) Assigning the rest points to the same cluster as its nearest neighbor of higher density. For detailed allocation, we refer to [53].

We propose a visualization as well as comparisons to [21] and [7] in Figure 5 in the appendix. The simulation studies in Section 5 demonstrate that our method for choosing thresholds works reasonably well under various conditions.

3.3 Local refinement in dynamic networks

To detect change-points in dynamic networks, a straightforward method is to vectorize the adjacency matrices and perform the methods in Section 3.1. However, when the network data has a low-rank structure such as the ubiquitous community structure, the aforementioned estimation can be sub-optimal and the accuracy of the estimation can be further improved. To address this issue, [61] first identify the change-points using CUSUM methods which are analogous to our Algorithm 1

and 2 but with threshold tailored to the independent objects, and then apply the Universal Singular Value Thresholding (USVT) method to the data around estimated changes for further refinement. They show that their method is nearly minimax rate optimal in terms of the localization error. In this section, we extend the USVT approach to dependent dynamic networks. Specifically, we consider detecting changes in a general dynamic network model which includes the independent networks [61] and autoregressive networks [29] as special cases.

Definition 3.5 (Markov chain Bernoulli network). *Let $\{A(t)\}_{t=1}^T$ be a series of adjacency matrices with size n . For $1 \leq i, j \leq n, 1 \leq t \leq T$, the entity $A_{ij}(t) \in \{0, 1\}$ are Bernoulli random variables and $A_{ij}(t) = 1$ if the i th and j th nodes are connected at time t . $\{A(t)\}_{t=1}^T$ is a Markov chain Bernoulli network if*

1. For any $(i, j) \neq (i', j')$ and any $t, t', A_{ij}(t)$ is independent of $A_{i'j'}(t')$.
2. For $1 \leq i, j \leq n, \{A_{ij}(t)\}_{t=1}^T$ are Markov chains.

Markov chain Bernoulli network allows the recent Autoregressive Networks [29]. When the chain is homogeneous, detecting changes in connection probabilities is equivalent to that in transition probabilities, and [29] studies the latter for cases that contain exactly one change-point. In this paper, we allow the number of change-points to diverge and further allow Markov chains to be heterogeneous when testing whether $\mathbb{E}A(t)$ stays constant across time.

Many network models such as the stochastic block model [24] have low-rank features, which enables us to further enhance the estimation accuracy through matrix decomposition. Specifically, after applying Algorithm 1 we take a data point every $\tau_3 \log(T)$ (τ_3 is determined in Theorem 3.7 and $\tau_3 \log(T)$ is an integer) and further split the sequence into two sub-sequences. Let $A(t_i) = A(s+1+\tau_3 \log(T)(i-1)), 1 \leq i \leq 1 + \lfloor \frac{e-s-1}{\tau_3 \log(T)} \rfloor$. We first apply the CUSUM statistics (i.e., equation (13)) on the sequence $\{A(t_{2i-1})\}_{i \geq 1}$, and apply the USVT step. Concretely, for a symmetric matrix A , suppose that $(\kappa_i(A), v_i)$ is the i th eigen-pair of A with $|\kappa_1(A)| \geq \dots \geq |\kappa_n(A)|$, then $\text{USVT}(A, \tau_2, \infty) = \sum_{i: |\kappa_i(A)| \geq \tau_2} \kappa_i(A) v_i v_i^\top$ with τ_2 be a positive threshold, and $\text{USVT}(A, \tau_2, c_0)_{ij} = (|\text{USVT}(A, \tau_2, \infty)_{ij}| \wedge c_0) \text{sign}(\text{USVT}(A, \tau_2, \infty)_{ij})$ for some positive parameter c_0 . For the formal algorithm we refer to Algorithm D.4. We then calculate the CUSUM statistics on the sequence $\{A(t_{2i})\}_{i \geq 1}$, and get the position where the inner product reaches the maximum. We present our algorithm in Algorithm 4 of the appendix. We next posit an assumption for this procedure and give the theoretical results.

Recall that $\mathbb{E}A(t)$ is piecewise constant. Let $r = \max_{1 \leq k \leq K} \text{rank}(\mathbb{E}A(\eta_k) - \mathbb{E}A(\eta_k - 1))$. Let $\beta = \sup_{i,j,t} |\mathbb{P}(A_{ij}(t) = 1 | A_{ij}(t-1) = 1) - \mathbb{P}(A_{ij}(t) = 1 | A_{ij}(t-1) = 0)| \vee \frac{1}{2} \in [\frac{1}{2}, 1]$. Let $\tilde{\kappa} = \min_{1 \leq k \leq K} |\mathbb{E}A(\eta_k) - \mathbb{E}A(\eta_k - 1)|_F / n \in (0, 1]$. Let n be the network size. We mention that for networks with community structure, r is typically small because $r \leq 2 \max_t \text{rank}(\mathbb{E}A(t))$.

Assumption 3.6. *Assume that (a) $\{A(t)\}$ follows Definition 3.5. (b) There exists a constant $c_7 > 1$ such that $n \leq T^{c_7 - \frac{1}{2}}$. Moreover, $T^{-c_7} \leq \mathbb{E}A_{ij}(t) \leq 1 - T^{-c_7}$ for all $1 \leq i, j \leq n, 1 \leq t \leq T$. (c) $\frac{\log(T)}{-\log \beta} = o(\Delta)$. (d) $\frac{\log^2(T)r}{-n\Delta \log \beta} = o(\tilde{\kappa}^2)$.*

Assumption 3.6 (b) restricts the divergence rate of the network size n . When the networks are independent, following the proof in the appendix, especially the fact that (62) is zero under independence, (b) is not needed. (c) ensures that $\tau_3 \log(T)$ is small enough, which is necessary for the localization step. (d) is the signal-to-noise ratio condition. When $r = \Omega(n)$, it is asymptotically equivalent to condition (14) with $q = 2$. When $\beta < 1 - \delta_0$ for some $\delta_0 > 0$, (d) matches the Assumption 3 in [61].

Theorem 3.7 (Theoretical result of local refinement). *Assume that the conditions for Theorem 2.2 and Assumption 3.6 hold. Apply Algorithm 1 to get \hat{K} and S^* , and then apply Algorithm 4 in the appendix with input parameters S^*, τ_2, τ_3 to get $\{b_k\}_{k=1}^{\hat{K}}$ where*

$$\tau_2 = C_7(\sqrt{n} + \sqrt{\log(T)}), \quad \tau_3 = \lfloor \frac{c_7 \log(T)}{-\log \beta} \rfloor / \log(T),$$

for a positive constant $C_7 > 8$. Then we have $P\left(\hat{K} = K, \max_{k=1, \dots, K} |b_k - \eta_k| \leq \varepsilon\right) \rightarrow 1$ as $T \rightarrow \infty$, where

$$0 < \varepsilon \leq C_4^* \frac{c_7 \log^3(T)}{-(\log \beta) \tilde{\kappa}^2 n^2}, \quad (19)$$

and C_4^* is an absolute constant.

In practice the performance of Algorithm 4 is not sensitive to the choice of c_7 , and we recommend choosing $c_7 = 1$ for network with moderate size.

Remark 5. *By Assumption 3.6, we have $\frac{\varepsilon}{\Delta} = o\left(\frac{-\log \beta}{rn}\right) = o(1)$. Hence, the estimator in Theorem 3.7 is consistent. Furthermore, when β is bounded away from 1, the localization bound (19) matches with [61], which is also nearly minimax optimal up to a logarithmic factor, following Lemma 2 in [61].*

It is often assumed that there is no self-loop, i.e., $A_{ii}(t) = 0$ for all i, t , in which case the rank of $\mathbb{E}A(t)$ is not low. To fix this problem, assume that there exists a $B(t)$ such that $\mathbb{E}A(t) = B(t) - \text{diag}(B(t))$. Let $\tilde{r} = \max \text{rank}(B(t))$. We modify Assumption 3.6 to the following assumption with further restrictions on $B(t)$.

Assumption 3.8. *Assume that (a) $\{A(t)\}$ follows Definition 3.5. (b) There exists a constant $c_7 > 1$ such that $n \leq T^{c_7 - \frac{1}{2}}$. Moreover, $T^{-c_7} \leq B_{ij}(t) \leq 1 - T^{-c_7}$ for all $1 \leq i, j \leq n, 1 \leq t \leq T$. (c) $\frac{\log(T)}{-\log \beta} = o(\Delta)$. (d) $\frac{\log^2(T) \tilde{r}}{n \Delta \log \beta} = o(\tilde{\kappa}^2)$. (e) $\|B(t)\|_F \geq C \|\text{diag} B(t)\|_F$ for all t and a large enough absolute constant $C > 0$.*

Notice that Assumption 3.8(e) is also considered in [61].

Theorem 3.9. *Under Assumption 3.8, Theorem 3.7 still holds.*

3.4 Refinement for local stationarity

Remark 2 shows that our signal-to-noise ratio is already nearly minimax optimal. However, at a finite sample size, the performance of the algorithm could be further influenced by heteroscedasticity. Recall Algorithm 1 where we use a threshold τ to separate the signal and noise. Under heteroscedasticity, it requires a larger threshold to account for the noise when the variance is large than when the variance is small. Hence adjusting the threshold to the volatility will benefit the finite sample performance. Consider the model

$$X_{t,i} = \mathbb{E}X_{t,i} + \varepsilon_{t,i}, \quad 1 \leq i \leq p, 1 \leq t \leq T,$$

where each $\mathbb{E}X_{t,i}$ is a piecewise constant mean functions with common change-points $\{\eta_1, \dots, \eta_K\}$, and $(\varepsilon_{t,i})$ is a centered locally stationary process defined as follows.

Assumption 3.10. The error processes $\epsilon_{t,i} = G_i(t/T, \mathcal{F}_t)$ where $G_i(u, \mathcal{F}_t) : [0, 1] \times \mathcal{S}^{\mathbb{Z}} \rightarrow \mathbb{R}$ is a filter, $\mathcal{F}_t = (\epsilon_{-\infty}, \dots, \epsilon_{t-1}, \epsilon_t)$ and (ϵ_t) are i.i.d. random elements defined on \mathcal{S} . Define $\mathcal{F}_t^* = (\epsilon_{-\infty}, \dots, \epsilon_{-1}, \epsilon_0^*, \dots, \epsilon_t)$ where (ϵ_t^*) is an i.i.d. copy of (ϵ_t) . Moreover, $\mathbb{E}G_i(u, \mathcal{F}_0) = 0$ and there exists $\bar{q} > 4$ such that

1. $\sup_i \sup_{t \in [0, 1]} \|G_i(t, \mathcal{F}_0)\|_{\mathcal{L}_{\bar{q}}} < \infty, \sup_{t,i} |\mathbb{E}X_{t,i}| < \infty$
2. $\max_i \delta_{\bar{q}}(G_i, k) = O(\chi^k)$ for some $0 < \chi < 1$ where $\delta_{\bar{q}}(G_i, k)$ is the physical dependence measure defined as $\delta_{\bar{q}}(G_i, k) = \sup_{u \in [0, 1]} \|G_i(u, \mathcal{F}_k) - G_i(u, \mathcal{F}_k^*)\|_{\mathcal{L}_{\bar{q}}}$.
3. There exists a constant C such that for all u_1, u_2 , $\sup_i \sup_{0 \leq u_1 < u_2 \leq 1} \|G_i(u_1, \mathcal{F}_0) - G_i(u_2, \mathcal{F}_0)\|_{\mathcal{L}_2} / |u_1 - u_2| \leq C$.
4. The long-run variance $\sigma_i^2(u) = \sum_{k=-\infty}^{\infty} \text{Cov}(G_i(u, \mathcal{F}_0), G_i(u, \mathcal{F}_k))$ satisfies $\inf_{u,i} \sigma_i^2(u) > 0$ for $u \in [0, 1]$.

The G_i s are locally stationary processes when satisfying Assumption 3.10. Under Assumption 3.10 and the null hypothesis that there is no change-point, straightforward calculations show that for $t \in (s, e]$,

$$\begin{aligned} \text{Var} \left(\frac{\sqrt{(t-s)(e-t)}}{e-s} \tilde{g}_{s,e,i}^t(X) \right) &= \frac{1}{e-s} \left(\left(\frac{e-t}{e-s} \right)^2 \sum_{r=s+1}^t \sigma_i^2(r/T) \right. \\ &\quad \left. + \left(\frac{t-s}{e-s} \right)^2 \sum_{r=t+1}^e \sigma_i^2(r/T) \right) \xrightarrow{e-s \rightarrow \infty} 0. \end{aligned}$$

Therefore, we shall normalize $\tilde{g}_{s,e,i}^t(X)$ by the square root of

$$\frac{e-t}{(e-s)(t-s)} \sum_{r=s+1}^t \sigma_i^2(r/T) + \frac{t-s}{(e-s)(e-t)} \sum_{r=t+1}^e \sigma_i^2(r/T).$$

Let $\hat{\sigma}_i^2(t)$ be an consistent estimator of $\sigma_i^2(t)$. We define

$$\check{g}_{s,e,i}^t(X) := \frac{\tilde{g}_{s,e,i}^t(X)}{\sqrt{\sum_{r=s+1}^e \hat{\sigma}_i^2(r/T) a_{r,t}^2}} \text{ where } a_{r,t} = \begin{cases} \sqrt{\frac{e-t}{(e-s)(t-s)}}, & s < r \leq t \\ \sqrt{\frac{t-s}{(e-s)(e-t)}}, & t < r \leq e \end{cases} \quad (20)$$

and replace $\tilde{g}_{s,e,i}^t(X)$ with $\check{g}_{s,e,i}^t(X)$ for detecting the change-points. To estimate $\sigma_i^2(t)$, we refer to equation (4.7) in [15] which is robust to the changes in mean. Specifically, define $S_{k,r}^{(i)} = \sum_{t=k}^r X_{t,i}$ and for $m \geq 2$, $\Delta_j^{(i)} = \frac{S_{j-m+1,j}^{(i)} - S_{j+1,j+m}^{(i)}}{m}$. For $u \in [m/T, 1 - m/T]$,

$$\hat{\sigma}_i^2(u) = \sum_{j=1}^T \frac{m(\Delta_j^{(i)})^2}{2} \omega(u, j) \quad (21)$$

where for some bandwidth τ_T ,

$$\omega(u, j) = K \left(\frac{j/T - u}{\tau_T} \right) / \sum_{j=1}^T K \left(\frac{j/T - u}{\tau_T} \right).$$

For $u \in [0, m/T)$ and $(1 - m/T, 1]$, we define $\hat{\sigma}_i^2(u) = \hat{\sigma}_i^2(m/T)$ and $\hat{\sigma}_i^2(1 - m/T)$ respectively.

Proposition 2. *Under Assumption 3.10 and assume $p^{\frac{1}{q}}/m \rightarrow 0, p^{\frac{1}{q}}\tau_T \rightarrow 0, p^{\frac{2}{q}}\frac{m^2K}{T\tau_T} \rightarrow 0, p^{\frac{1}{q}}m\tau_T^{-1-2/q}/T \rightarrow 0$. If, additionally, the function $\sigma_i^2(u)$ is twice continuously differentiable, then the estimate defined in (21) satisfies*

$$\max_i \sup_{u \in [0,1]} |\hat{\sigma}_i^2(u) - \sigma_i^2(u)| = O_p \left(p^{\frac{1}{q}} \left(\sqrt{\frac{m}{T\tau_T}} \tau_T^{-\frac{1}{q}} + \frac{1}{m} + \tau_T \right) + p^{\frac{2}{q}} \frac{m^2K}{T\tau_T} \right). \quad (22)$$

For stationary time series, the self-normalization approach for detecting change-points are considered by for example [63; 72] to avoid estimating the long-run variance $\sigma_i^2(t)$ above. Under local stationarity, the self-normalization method could be invalid and less effective in practice.

Remark 6. *Suppose $\sigma_i^2(u)$ are all upper bounded and bounded away from 0, then the adjustment terms are all bounded with probability tending to 1, in which case the asymptotic performance of RID remain unchanged. Meanwhile, the refinement has good performance under finite sample cases for locally stationary time series, which is supported by numerical studies in Section 5.*

4 The piecewise polynomial case

In this section, we study RID for PP signals. Let $\{\mathbb{X}_t\}_{t=1}^T$ be a sequence of p -dimensional time series. Consider

$$\mathbb{E}\mathbb{X}_t = \sum_{i=0}^K Q_l^{(i)}(t - \eta_i) I(t \geq \eta_i). \quad (23)$$

where $1 < \eta_1 < \dots < \eta_K < T + 1$ are change-points, $Q_l^{(i)}(t) = \sum_{j=0}^l a_j^{(i)} t^j$, and $a_j^{(i)}$ are coefficient vectors. We assume that all elements of the leading coefficients $\{a_l^{(i)}\}_{i=0}^K$ are not zero. When $l = 1$, (23) reduces to the piecewise linear signal. Moreover, if there is no change, $\mathbb{E}\mathbb{X}_t = Q_l^{(0)}(t)$, $1 \leq t \leq T$. A related problem is the detection of abrupt changes. The abrupt changes are discontinuous points of trends. Before and after the abrupt changes the means are smoothly changing, allowing piecewise polynomial means. The problem and the associate nonparametric tests have received considerable attention recently, see for example [64; 42]. The difference between the PP case and the abrupt changes lies in the fact that η_i here could be a kink.

We first construct the functions $\tilde{g}_{s,e,i}^t$ defined in Section 2. For any tripe (s, t, e) with $(s, e] \subset (0, T]$ and $s < t \leq e$, let

$$\tilde{g}_{s,e,i}^t(X) = \sum_{r=s+1}^e \tilde{w}_{s,e}^t(r) X_{r,i}, \quad (24)$$

where the coefficients $\{\tilde{w}_{s,e}^t(r)\}_{r=s+1}^e$ are defined through the following projection procedure. Let

$$U = \begin{pmatrix} 1 & s+1 & (s+1)^2 & \dots & (s+1)^l \\ 1 & s+2 & (s+2)^2 & \dots & (s+2)^l \\ \vdots & \vdots & \vdots & \vdots & \vdots \\ 1 & e & e^2 & \dots & e^l \end{pmatrix}, P_U = U(U^\top U)^{-1}U^\top, \\ W = (I - P_U)_{(e-s) \times (e-s)} \begin{pmatrix} 0 & \dots & 0 & 1^l & 2^l & \dots & (e-t)^l \end{pmatrix}_{(e-s) \times 1}^\top.$$

Then $(\tilde{w}_{s,e}^t(s+1), \dots, \tilde{w}_{s,e}^t(e))^\top = \frac{W}{|W|_2}$. Let $\tilde{f}_{s,e,i} = \tilde{g}_{s,e,i}^{t_0}$ where $t_0 = \arg \max_{s < t \leq e} |\tilde{g}_{s,e}^t(X)|_q$ as in Section 3.1. For $l = 1$, $\{\tilde{w}_{s,e}^t(r)\}$ reduce to those in Section B.2 in the appendix of [7]. By construction, $\sum_{r=s+1}^e (\tilde{w}_{s,e}^t(r))^2 = 1$ and $\sum_{r=s+1}^e r^k \tilde{w}_{s,e}^t(r) = 0$ whenever $0 \leq k \leq l$.

Theorem 4.1 (Consistency result for PP cases). *Assume that*

1. l is fixed with $1 \leq l \leq 50$;
2. $\log(T) \leq H_T = o(\Delta)$ where H_T is an arbitrary positive number, serving as a trade-off term;
- 3.

$$\frac{H_T^{l+\frac{1}{2}} \mathfrak{J}}{\min_{k=1, \dots, K} |a_l^{(\eta_k)}|_q \Delta^{l+\frac{1}{2}}} \rightarrow 0 \quad \text{as } T \rightarrow \infty.$$

4. $\frac{32T^2 H_T^2}{\Delta^2} \log\left(\frac{T}{\Delta}\right) = o(M)$.

Suppose the threshold τ satisfies $\mathfrak{J} = o(\tau)$ and $\tau = o\left(\min_{k=1, \dots, K} |a_l^{(\eta_k)}|_q \left(\frac{\Delta}{H_T}\right)^{l+\frac{1}{2}}\right)$. Apply Algorithm 1 with input parameters τ and M to get \hat{K} and S^* . Let $\hat{\eta}_k = \frac{1}{2}(l_k + r_k)$. Then as $T \rightarrow \infty$, we have $P\left(\hat{K} = K, \max_{k=1, \dots, K} |\hat{\eta}_k - \eta_k| \leq \varepsilon\right) \rightarrow 1$, where $\frac{\varepsilon}{\Delta} = O\left(\frac{1}{H_T}\right)$.

The first condition that $l \leq 50$ is sufficiently flexible for most practical scenarios, though it's possible to derive the formula for any fixed l with substantially more involved mathematical arguments. The third assumption is the signal-to-noise condition in the PP signals, and we put more illustrations in Section E.1 of the appendix. \mathfrak{J} is also listed in Table 13 in the appendix for those types of data listed in Table 2. When H_T diverges slowly (e.g., $H_T = \log(T)$), this condition is weaker than [69] (Theorem 5).

Remark 7 (Refinement for the PP case). [70] proposed a two-step method for detecting piecewise polynomial mean changes in a univariate series by dynamic programming. Their first step minimizes a objection function and get the initial estimator $\tilde{\eta}_k$. The second step performs a refinement, as described in (7) of [70]. The computation complexity of their first step for fixed l is $O(T^3)$. As a comparison, the computational complexity of our method for fixed l and $p = 1$ is $O(MT)$. One can refer to simulations in Section 5 for the comparisons of computational costs. For the refinement, we can follow (6) and (7) in [70] after we get our $\{\hat{\eta}_k\}$, yielding the same localization error bound as [70].

For parameter choice in the PP case, we recommend choosing the largest possible M under computational constraints. For τ , the clustering method in Section 3.2 is no longer applicable, and we recommend using a similar rule of thumb as discussed in Section 3.2, which is taking $\tau = \max_j |f_{j, j+h}(X)|_q e_T$ for $j = 1, 2, \dots, T-h$ where $h = \lfloor c \log(T) \rfloor$ and e_T is a divergent sequence that grows slowly.

5 Simulation studies

In this section, we compare the performances of RID with representative existing methods. For univariate data, we compare RID with WBS(sSIC) [21] using thresholds selected via sSIC, NOT(sSIC) [7] with thresholds chosen by sSIC, PELT.NP(SIC) [23], e.cp3o [28], B & P [5], SMUCE [20], cum-Seg [45]. For network data we compare RID with NBS [61]. For univariate piecewise polynomial cases, we compare RID with DP [70]. For multivariate locally stationary time series we compare RID with WBS-SN [63]. We adopt four measurements to evaluate these methods, which are also commonly used in literature mentioned above.

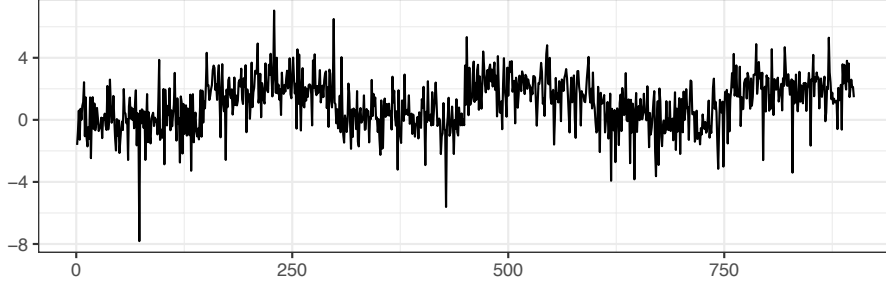


Figure 3: An illustration of samples for the third case in scenario 1.

- A list of $\hat{K} - K$, where \hat{K} and K are numbers of estimated change-points and true change-points.
- $H(\hat{\eta}, \eta)/T$, the normalized Hausdorff distance defined as

$$\frac{H(\hat{\eta}, \eta)}{T} := \frac{1}{T} \max \left\{ \max_{x \in \hat{\eta}} \min_{y \in \eta} |x - y|, \max_{y \in \hat{\eta}} \min_{x \in \eta} |x - y| \right\}. \quad (25)$$

A smaller $H(\hat{\eta}, \eta)/T$ indicates a better performance.

- Averaged Rand Index [51; 26], which is denoted by ARI, and ranges between 0 and 1. A higher value corresponds to a more accurate estimation.
- Time: The time required per detection (in seconds).

We use default parameters for both RID (i.e., first sample random intervals and follow Section 3.2 for the threshold, then put them into Algorithm 1 and 2) and other methods (provided by their original codes). For each scenario, we repeat 200 times and report the mean of $H(\hat{\eta}, \eta)/T$, ARI, time used and a list of $\hat{K} - K$. Due to the page limitation, we list the results and interpretations for the first three scenarios in Section A.1 of the appendix.

(Scenario 1.) $\Delta = 150, 300, K = 5, p = 1, T = \Delta(K + 1)$, change-points are equally spaced. \mathbb{X}_t are independent with distributions switching between

1. $N(0, 1)$ and $N(1, 1)$;
2. $(\chi^2(2) - 2)/2$ and $2 + (\chi^2(2) - 2)/2$;
3. $t(5)$ and $2 + t(5)$.

(Scenario 2.) $\Delta = 150, 300, K = 3, p = 1, T = \Delta(K + 1)$, change-points are equally spaced. \mathbb{X}_t are AR(1) $\mathbb{X}_t = \mu_t + \rho\mathbb{X}_{t-1} + \epsilon_t$ with

1. $\rho = 0.3$, ϵ_t being independent $N(0, 1)$ variables, μ_t switching between 0 and 1;
2. $\rho = 0.5$, ϵ_t being independent $(\chi^2(2) - 2)/2$, μ_t switching between 0 and 2;
3. $\rho = 0.3$, ϵ_t being independent $t(5)$ variables, μ_t switching between 0 and 2.

(Scenario 3.) $\Delta = 50, 100, 150, 200, K = 2, p = 1, T = \Delta(K + 1)$, change-points are equally spaced. \mathbb{X}_t are piecewise polynomial sequence $\mathbb{X}_t = \mu_t + \epsilon_t$ with $\epsilon_t \sim U(-5, 5)$ independently and identically and

$$\mu_t = Q_2^{(0)}(t) + Q_2^{(1)}(t - \eta_1)I(t \geq \eta_1) + Q_2^{(2)}(t - \eta_2)I(t \geq \eta_2),$$

where $Q_2^{(0)}(t) = 0.002t^2 - 0.05t$, $Q_2^{(1)}(t) = -0.005t^2 + 0.01t$, $Q_2^{(2)}(t) = 0.005t^2 - 0.02t$. We first apply our Algorithm 1 with the statistic defined in (24), then we use (7) in [70] for refinement. For comparisons, we apply [70] by first selecting their tuning parameter λ through the cross-validation method, and then using their Algorithm 1. We report both the detecting accuracy and the time cost (For [70], the time for cross-validation is not included).

(Scenario 4.) $\Delta = 30, 60, 90, 120, K = 2, p = 2, T = 4\Delta$, change-points are placed at $\eta_1 = \Delta, \eta_2 = 3\Delta$. \mathbb{X}_t are locally stationary time series $\mathbb{X}_t = \mu_t + \epsilon_t$ with $\epsilon_{t,1} = \sqrt{\frac{2000t}{T}}\xi_{t,1}, \epsilon_{t,2} = \sqrt{\frac{1000(T-t)}{T}}\xi_{t,2}, \xi_{t,1} = 0.5(t/T - 0.5)\xi_{t-1,1} + \xi_{t,1}^*, \xi_{t,1}^* \stackrel{i.i.d.}{\sim} N(0, 1), \xi_{t,2}^* \stackrel{i.i.d.}{\sim} (\chi^2(2) - 2)/2, \mu_{t,1} = 20I(\eta_1 \leq t < \eta_2) - 20I(t \geq \eta_2), \mu_{t,2} = 20I(\eta_1 \leq t < \eta_2) + 10I(t \geq \eta_2)$. We apply RID with (and without) the refinement in Section 3.4. For comparisons, we apply [63] (WBS-SN) by following their Section 5, but due to the computational burden of their method in the multiple change-points case, we are unable to obtain results. (One can also refer to Table 6 for their running time.)

(Scenario 5.) We detect changes in the Block Model [24]. Let $K = 2, n$ (network size) = 12, $\Delta = 80, 120, 160, 200, \rho = 0.5$. Change-points are equally spaced. The mean (denoted as Θ) of Markov chain Bernoulli networks are

$$\Theta_t = \begin{cases} (I_3 \otimes \mathbb{1}_4)\rho \begin{pmatrix} 0.2 & 1 & 0.2 \\ 1 & 0.2 & 0.2 \\ 0.2 & 0.2 & 0.2 \end{pmatrix} (I_3 \otimes \mathbb{1}_4^\top) & 1 \leq t < \eta_1 \text{ or } \eta_2 \leq t \leq T \\ (I_3 \otimes \mathbb{1}_4)\rho \begin{pmatrix} 0.2 & 0.2 & 1 \\ 0.2 & 0.2 & 0.2 \\ 1 & 0.2 & 0.2 \end{pmatrix} (I_3 \otimes \mathbb{1}_4^\top) & \eta_1 \leq t < \eta_2 \end{cases}$$

where I_3 is the diagonal matrix of size 3, $\mathbb{1}_4 = (1, 1, 1, 1)^\top$, and \otimes denotes the Kronecker product. That is, there are three communities in the network and each community contains four nodes. For each $1 \leq i, j, \leq n$, the transition kernel is

$$P_{ij}(t) = \begin{pmatrix} 1 - 0.2\Theta_{ij}(t) & 0.2\Theta_{ij}(t) \\ 0.2 - 0.2\Theta_{ij}(t) & 0.8 + 0.2\Theta_{ij}(t) \end{pmatrix}.$$

It is easy to show that within each segment,

$$\Theta_{ij}(t+1) = \Theta_{ij}(t)(0.8 + 0.2\Theta_{ij}(t)) + 0.2\Theta_{ij}(t)(1 - \Theta_{ij}(t)) = \Theta_{ij}(t).$$

Meanwhile, The correlation of $\Theta_{ij}(t)$ and $\Theta_{ij}(t-1)$ is not zero. To detect change-points, for RID without refinement, $X_{ij}(t)$ is vectorized, for NBS, $X_{ij}(t)$ is split into two sequences. We further apply the refinement described in Section 3.3.

(Scenario 6.) $\Delta = 50, 100, 150, 200, K = 3, p = 3, T = \Delta(K+1)$, change-points are equally spaced. \mathbb{X}_t are piecewise polynomial sequence $\mathbb{X}_t = \mu_t + 5\epsilon_t$. Here, $\epsilon_{t,1}$ is a ARMA(2,2) sequence with coefficients for the AR part being (0.8, -0.5) and coefficients for the MA part being (-0.2, 0.25). $\epsilon_{t,2}$ is a MA(1) sequence with the coefficient -0.5. $\epsilon_{t,3}$ is the i.i.d. $t(8)$ random variables. For the mean $\mu_t = (\mu_{t,1}, \mu_{t,2}, \mu_{t,3})^\top$,

$$\mu_{t,1} = \mu_{t,2} = Q_2^{(0)}(t) + Q_2^{(1)}(t - \eta_1)I(t \geq \eta_1) + Q_2^{(2)}(t - \eta_2)I(t \geq \eta_2) + Q_2^{(3)}(t - \eta_3)I(t \geq \eta_3),$$

$\mu_{t,3} = 0$, where $Q_2^{(0)}(t) = 0.002t^2 - 0.05t$, $Q_2^{(1)}(t) = -0.005t^2 + 0.01t$, $Q_2^{(2)}(t) = 0.005t^2 - 0.02t$, $Q_2^{(3)}(t) = -0.005t^2 + 0.01t$. We apply our Algorithm 1 with the statistic defined in (24).

(**Scenario 7.**) $\Delta = 50, 100, p = 100, 200, K = 2, T = 4\Delta$, change-points are placed at $\eta_1 = \Delta, \eta_2 = 2\Delta$. $\mathbb{X}_t = \mu_t + \epsilon_t$ with $\epsilon_t \stackrel{i.i.d.}{\sim} N(0, \Sigma), \Sigma_{ij} = 0.99^{|i-j|}, \mu_t = I(\eta_1 \leq t < \eta_2)$. For comparison, we apply [63] (WBS-SN) by following their Section 5.

We mention that $H(\cdot)$ and ARI exhibit a higher tolerance for overestimation of K than for underestimation of K . Therefore, it is meaningful to compare their $H(\cdot)$ and ARI only when the estimates of K by two methods are both close to the true value. From Table 3, it is evident that applying the refinement procedure for locally stationary time series further enhances the estimation accuracy. Table 4 shows that NBS becomes less effective in Markov chain Bernoulli networks, and our refinement method is useful when the sample size is large ($T \geq 480$ in this case), which is reasonable since we need a large $\log(T)$ to ensure a sufficient number of data points, as described in Section 3.3. Table 5 shows that RID estimates change-points consistently in the multivariate PP case. Finally, Table 6 demonstrates that RID seems to outperform WBS-SN method in the sense that it can rapidly and accurately estimate change-points in high-dimensional scenarios.

Table 3: Results for Scenario 4 (for locally stationary time series with non equally-spaced change-points).

(T, K)	Method	$\hat{K} - K$						$H(\hat{\eta}, \eta) \cdot 10^2/T$	ARI	time (seconds)
		-2	-1	0	1	2	≥ 3			
(120,2)	RID (wr) ¹	7	60	106	18	7	2	21.412	0.824	0.095
	RID (wor) ²	17	75	80	22	4	2	29.167	0.776	0.083
(240,2)	RID (wr)	2	21	161	15	1	0	8.693	0.914	0.119
	RID (wor)	0	46	130	19	5	0	14.014	0.891	0.090
(360,2)	RID (wr)	0	6	183	9	2	0	3.561	0.957	0.131
	RID (wor)	0	16	170	13	1	0	5.800	0.946	0.108
(480,2)	RID (wr)	0	3	190	5	1	1	2.014	0.973	0.153
	RID (wor)	0	7	182	11	0	0	3.278	0.969	0.127

Table 4: Results for Scenario 5 (for network).

(T, K)	Method	$\hat{K} - K$						$H(\hat{\eta}, \eta) \cdot 10^2/T$	ARI	time (seconds)
		-2	-1	0	1	2	≥ 3			
(240,2)	RID(with refinement)	0	14	183	0	0	3	8.345	0.914	0.363
	RID (without refinement)	0	14	183	0	0	3	1.731	0.978	0.353
	NBS(with refinement)	0	0	0	0	0	200	27.337	0.739	4.985
(360,2)	RID(with refinement)	0	1	199	0	0	0	0.991	0.990	0.521
	RID (without refinement)	0	1	199	0	0	0	0.159	0.997	0.501
	NBS(with refinement)	0	0	0	0	0	200	29.238	0.714	11.688
(480,2)	RID(with refinement)	0	0	200	0	0	0	0.029	0.999	0.700
	RID (without refinement)	0	0	200	0	0	0	0.041	0.999	0.653
	NBS(with refinement)	0	0	0	0	0	200	30.266	0.702	20.976
(600,2)	RID(with refinement)	0	0	200	0	0	0	0.006	0.999	0.866
	RID (without refinement)	0	0	200	0	0	0	0.046	0.999	0.821
	NBS(with refinement)	0	0	0	0	0	200	30.910	0.695	32.729

¹‘wr’ is an abbreviation for ‘with refinement’.

²‘wor’ is an abbreviation for ‘without refinement’.

Table 5: Results for Scenario 6 (for the multivariate PP case).

(T, K)	Method	$\hat{K} - K$							$H(\hat{\eta}, \eta) \cdot 10^2/T$	ARI	Time(s)
		≤ -3	-2	-1	0	1	2	≥ 3			
(200,3)	RID	2	173	25	0	0	0	0	32.272	0.692	0.659
(400,3)	RID	0	0	151	49	0	0	0	13.032	0.832	2.298
(600,3)	RID	0	0	0	198	2	0	0	4.328	0.932	4.597
(800,3)	RID	0	0	0	199	1	0	0	3.486	0.942	8.289

Table 6: Results for Scenario 7 (for high-dimensional data with non equally-spaced change-points).

(T, K, p) and p	Method	$\hat{K} - K$						$H(\hat{\eta}, \eta) \cdot 10^2/T$	ARI	time (seconds)
		-2	-1	0	1	2	≥ 3			
(200,2,100)	RID	1	24	159	13	2	1	7.470	0.937	0.603
	WBS-SN	0	0	0	0	0	200	37.332	0.737	132.402
(200,2,200)	RID	0	11	182	6	1	0	4.182	0.959	0.705
	WBS-SN	0	0	0	0	0	200	37.092	0.739	124.141
(400,2,100)	RID	0	1	197	2	0	0	1.850	0.976	0.635
	WBS-SN	0	0	0	0	0	200	37.056	0.743	483.824
(400,2,200)	RID	0	1	196	3	0	0	1.381	0.981	1.133
	WBS-SN	0	0	0	0	0	200	36.902	0.744	475.781

6 Real data examples

In this section, we apply our method to detect change-points of mean in ant societies. To investigate the evolution of ant societies, [44] utilized an automated video tracking system to monitor every individual in six colonies of the ant *Camponotus fellah*. They recorded all social interactions that occurred among the ants over 41 days. To simplify data analysis, they divided the 41-day experiment into four periods of 11, 10, 10, and 10 days respectively. Using community detection algorithms they discovered three distinct groups, and each group represents a functional behavioral unit. We now detect whether there are change-points in social interactions among these six colonies and identify the locations of them to support or refine their division of the time period. For the i_{th} colony, let $X^{(i)}(t)$ denotes the ant social interaction matrix for the t_{th} day, i.e.,

$$X_{kl}^{(i)}(t) = \begin{cases} 1 & \text{ants } k \text{ and } l \text{ from colony } i \text{ interacted on the } t_{th} \text{ day} \\ 0 & \text{otherwise} \end{cases}$$

Notably, during these 41 days, some ants might have died. In such cases, we consider the social interactions of the dead ants with other ants to be 0. In this example, $X_{kl}^{(i)}(t)$ and $X_{k'l'}^{(i)}(t')$ are not necessarily independent, and we have no knowledge of the dependency structure of social interactions between different individuals and days. We perform a change-point detection on the expected probability of social interactions (namely $\mathbb{E}X^{(i)}(t)$ for $i = 1, 2, \dots, 6$). Results are summarized in Table 7.

The results indicate that in terms of the first and sixth colonies, the data segmentation [44] used is fairly reasonable. This also corresponds to Fig 3(A) therein. For the second, third, and fifth colonies, $t = 31$ is not identified as a change-point, but we find that there are indeed changes in the social network of ants at $t = 11$ and $t = 21$. Therefore, for these three colonies, we suggest that it is reasonable to divide the data into three periods of 11, 10, and 20 days respectively. Moreover, The

Table 7: Change-point locations for the social interactions of ants in the six colonies.

Colony	Change-points for ant interactions
1	{11,21,31}
2	{11,21}
3	{11,21}
4	{11}
5	{11,22}
5	{12,22,31}

social dynamics of the fourth colony appear to be the most stable, as it has only one change-point identified at $t = 11$.

7 Conclusion

We have proposed a flexible approach, RID, for multiple change-point detection for general dependent data allowing the number of change-points and dimension of data to diverge. RID generates informative intervals from random intervals, without performing segmentation as many existing literature. We further propose a novel clustering-based threshold selection procedure that is adaptive to various types of dependent data for detecting change-points. To the best of our knowledge, RID is the first method for general dependent data with a theoretical guaranteed threshold. We also propose second-stage refinements for different data types to improve localization accuracy. Together with RID, we show that for general univariate time series data and autoregressive network, our methods achieve the almost minimax optimality as their independent counterparts. We also extend RID to data with piecewise polynomial signals. RID has the potential to combine with state-of-the-art single change-point detection methods, such as the self-normalization method [63; 72], in the context of multiple change-point detection, akin to WBS.

There are some directions for future work. First, for scenarios other than the piecewise constant case, it remains challenging to find the clustering-based threshold. Second, it is of practical interest and importance to extend RID to the identification of changes in the second order structure such as the covariance matrix, and to the detection of asynchronous changes in different dimensions for multivariate data.

Acknowledgments

Weichi Wu is the corresponding author and is supported by NSFC 12271287. The authors thank Prof. Stanislav Volgushev for providing code of [63].

References

- [1] A. Aknouche and C. Francq. Count and duration time series with equal conditional stochastic and mean orders. *Econometric Theory*, 37(2):248–280, 2021.
- [2] J. Antoch, M. Hušková, and D. Jarušková. Change point detection. 5th ers iasc summer school, 2000.
- [3] J. A. Aston and C. Kirch. Evaluating stationarity via change-point alternatives with applications to fmri data. *The Annals of Applied Statistics*, 6(4):1906–1948, 2012.

- [4] J. Bai and P. Perron. Estimating and testing linear models with multiple structural changes. *Econometrica*, pages 47–78, 1998.
- [5] J. Bai and P. Perron. Computation and analysis of multiple structural change models. *Journal of applied econometrics*, 18(1):1–22, 2003.
- [6] A. S. Bandeira and R. van Handel. Sharp nonasymptotic bounds on the norm of random matrices with independent entries. *The Annals of Probability*, 2016.
- [7] R. Baranowski, Y. Chen, and P. Fryzlewicz. Narrowest-over-threshold detection of multiple change points and change-point-like features. *Journal of the Royal Statistical Society: Series B (Statistical Methodology)*, 81(3):649–672, 2019.
- [8] L. Bardwell, P. Fearnhead, I. A. Eckley, S. Smith, and M. Spott. Most recent changepoint detection in panel data. *Technometrics*, 61(1):88–98, 2019.
- [9] R. Bormann, M. Gulde, A. Weismann, S. V. Yalunin, and C. Ropers. Tip-enhanced strong-field photoemission. *Physical review letters*, 105(14):147601, 2010.
- [10] V. Brovkin, E. Brook, J. W. Williams, S. Bathiany, T. M. Lenton, M. Barton, R. M. DeConto, J. F. Donges, A. Ganopolski, J. McManus, et al. Past abrupt changes, tipping points and cascading impacts in the earth system. *Nature Geoscience*, 14(8):550–558, 2021.
- [11] H. Cho, H. Maeng, I. A. Eckley, and P. Fearnhead. High-dimensional time series segmentation via factor-adjusted vector autoregressive modeling. *Journal of the American Statistical Association*, pages 1–13, 2023.
- [12] Y. Cui, R. Wu, and Q. Zheng. Estimation of change-point for a class of count time series models. *Scandinavian Journal of Statistics*, 48(4):1277–1313, 2021.
- [13] J. Dehning, J. Zierenberg, F. P. Spitzner, M. Wibral, J. P. Neto, M. Wilczek, and V. Priesemann. Inferring change points in the spread of covid-19 reveals the effectiveness of interventions. *Science*, 369(6500):eabb9789, 2020.
- [14] H. Dette, T. Ecker, and M. Vetter. Multiscale change point detection for dependent data. *Scandinavian Journal of Statistics*, 47(4):1243–1274, 2020.
- [15] H. Dette and W. Wu. Detecting relevant changes in the mean of nonstationary processes—a mass excess approach. *The Annals of Statistics*, 47(6):3578–3608, 2019.
- [16] H. Dette, W. Wu, and Z. Zhou. Change point analysis of correlation in non-stationary time series. *Statistica Sinica*, 29(2):611–643, 2019.
- [17] B. Eichinger and C. Kirch. A MOSUM procedure for the estimation of multiple random change points. *Bernoulli*, 24(1):526 – 564, 2018.
- [18] R. Ferland, A. Latour, and D. Oraichi. Integer-valued garch process. *Journal of time series analysis*, 27(6):923–942, 2006.
- [19] C. S. Ferreira, C. B. Zeller, A. M. Mimura, and J. C. Silva. Partially linear models and their applications to change point detection of chemical process data. *Journal of Applied Statistics*, 44(12):2125–2141, 2017.

- [20] K. Frick, A. Munk, and H. Sieling. Multiscale change point inference. *Journal of the Royal Statistical Society: Series B: Statistical Methodology*, pages 495–580, 2014.
- [21] P. Fryzlewicz. Wild binary segmentation for multiple change-point detection. *The Annals of Statistics*, 42(6):2243–2281, 2014.
- [22] Z. Harchaoui and C. Lévy-Leduc. Multiple change-point estimation with a total variation penalty. *Journal of the American Statistical Association*, 105(492):1480–1493, 2010.
- [23] K. Haynes, P. Fearnhead, and I. A. Eckley. A computationally efficient nonparametric approach for changepoint detection. *Statistics and computing*, 27:1293–1305, 2017.
- [24] P. W. Holland, K. B. Laskey, and S. Leinhardt. Stochastic blockmodels: First steps. *Social networks*, 5(2):109–137, 1983.
- [25] J. Huang, J. Wang, X. Zhu, and L. Zhu. Two ridge ratio criteria for multiple change point detection in tensors. *arXiv preprint [arXiv:2206.13004](https://arxiv.org/abs/2206.13004)*, 2022.
- [26] L. Hubert and P. Arabie. Comparing partitions. *Journal of classification*, 2:193–218, 1985.
- [27] R. Jaiswal, A. Lohani, and H. Tiwari. Statistical analysis for change detection and trend assessment in climatological parameters. *Environmental Processes*, 2:729–749, 2015.
- [28] N. A. James and D. S. Matteson. ecp: An r package for nonparametric multiple change point analysis of multivariate data. *arXiv preprint [arXiv:1309.3295](https://arxiv.org/abs/1309.3295)*, 2013.
- [29] B. Jiang, J. Li, and Q. Yao. Autoregressive networks. *Journal of Machine Learning Research*, 24(227):1–69, 2023.
- [30] B. Jiang, Q. Sun, and J. Fan. Bernstein’s inequality for general markov chains. *arXiv preprint [arXiv:1805.10721](https://arxiv.org/abs/1805.10721)*, 2018.
- [31] F. Jiang, Z. Zhao, and X. Shao. Time series analysis of covid-19 infection curve: A change-point perspective. *Journal of econometrics*, 232(1):1–17, 2023.
- [32] R. Killick, P. Fearnhead, and I. A. Eckley. Optimal detection of changepoints with a linear computational cost. *Journal of the American Statistical Association*, 107(500):1590–1598, 2012.
- [33] C. Kirch, B. Muhsal, and H. Ombao. Detection of changes in multivariate time series with application to eeg data. *Journal of the American Statistical Association*, 110(511):1197–1216, 2015.
- [34] C. Kirch and K. Reckruehm. Data segmentation for time series based on a general moving sum approach. *arXiv preprint [arXiv:2207.07396](https://arxiv.org/abs/2207.07396)*, 2022.
- [35] S. Kovács, P. Bühlmann, H. Li, and A. Munk. Seeded binary segmentation: a general methodology for fast and optimal changepoint detection. *Biometrika*, 110(1):249–256, 2023.
- [36] M. Last and R. Shumway. Detecting abrupt changes in a piecewise locally stationary time series. *Journal of multivariate analysis*, 99(2):191–214, 2008.
- [37] M. Lavielle and E. Moulines. Least-squares estimation of an unknown number of shifts in a time series. *Journal of time series analysis*, 21(1):33–59, 2000.

- [38] C.-B. Lee. Estimating the number of change points in a sequence of independent normal random variables. *Statistics & probability letters*, 25(3):241–248, 1995.
- [39] C. Lévy-Leduc and F. Roueff. Detection and localization of change-points in high-dimensional network traffic data. *The Annals of Applied Statistics*, pages 637–662, 2009.
- [40] B. Li and X. Diao. Structural break in different stock index markets in china. *The North American Journal of Economics and Finance*, 65:101882, 2023.
- [41] J. Li, L. Chen, W. Wang, and W. B. Wu. ℓ^2 inference for change points in high-dimensional time series via a two-way mosum. *arXiv preprint [arXiv:2208.13074](https://arxiv.org/abs/2208.13074)*, 2022.
- [42] W. W. Likai Chen and W. B. Wu. Inference of breakpoints in high-dimensional time series. *Journal of the American Statistical Association*, 117(540):1951–1963, 2022.
- [43] K. Marton. A measure concentration inequality for contracting markov chains. *Geometric & Functional Analysis GAFA*, 6(3):556–571, 1996.
- [44] D. P. Mersch, A. Crespi, and L. Keller. Tracking individuals shows spatial fidelity is a key regulator of ant social organization. *Science*, 340(6136):1090–1093, 2013.
- [45] V. M. Muggeo and G. Adelfio. Efficient change point detection for genomic sequences of continuous measurements. *Bioinformatics*, 27(2):161–166, 2011.
- [46] M. H. Neumann. Bootstrap for integer-valued garch (p, q) processes. *Statistica Neerlandica*, 75(3):343–363, 2021.
- [47] O. H. M. Padilla, Y. Yu, and C. E. Priebe. Change point localization in dependent dynamic nonparametric random dot product graphs. *The Journal of Machine Learning Research*, 23(1):10661–10719, 2022.
- [48] E. S. Page. Continuous inspection schemes. *Biometrika*, 41(1/2):100–115, 1954.
- [49] D. Paulin. Concentration inequalities for markov chains by marton couplings and spectral methods. *Electronic Journal of Probability*, 20:1–32, 2015.
- [50] P. J. Plummer and J. Chen. A bayesian approach for locating change points in a compound poisson process with application to detecting dna copy number variations. *Journal of Applied Statistics*, 41(2):423–438, 2014.
- [51] W. M. Rand. Objective criteria for the evaluation of clustering methods. *Journal of the American Statistical association*, 66(336):846–850, 1971.
- [52] E. Rio. Moment inequalities for sums of dependent random variables under projective conditions. *Journal of Theoretical Probability*, 22(1):146–163, 2009.
- [53] A. Rodriguez and A. Laio. Clustering by fast search and find of density peaks. *science*, 344(6191):1492–1496, 2014.
- [54] M. Rosenblatt. A central limit theorem and a strong mixing condition. *Proceedings of the national Academy of Sciences*, 42(1):43–47, 1956.
- [55] E. Ruggieri. A bayesian approach to detecting change points in climatic records. *International Journal of Climatology*, 33(2):520–528, 2013.

- [56] P.-M. Samson. Concentration of measure inequalities for markov chains and ϕ -mixing processes. *The Annals of Probability*, 28(1):416–461, 2000.
- [57] E. S. Venkatraman. *Consistency results in multiple change-point problems*. Stanford University, 1992.
- [58] R. Vershynin. *High-dimensional probability: An introduction with applications in data science*, volume 47. Cambridge university press, 2018.
- [59] L. Y. Vostrikova. Detecting “disorder” in multidimensional random processes. In *Doklady akademii nauk*, volume 259, pages 270–274, 1981.
- [60] D. Wang, Y. Yu, and A. Rinaldo. Univariate mean change point detection: Penalization, cusum and optimality. *Electronic Journal of Statistics*, 14:1917–1961, 2020.
- [61] D. Wang, Y. Yu, and A. Rinaldo. Optimal change point detection and localization in sparse dynamic networks. *The Annals of Statistics*, 49(1):203–232, 2021.
- [62] D. Wang, Y. Yu, and A. Rinaldo. Optimal covariance change point localization in high dimensions. *Bernoulli*, 27(1):554 – 575, 2021.
- [63] R. Wang, C. Zhu, S. Volgushev, and X. Shao. Inference for change points in high-dimensional data via selfnormalization. *The Annals of Statistics*, 50(2):781–806, 2022.
- [64] W. Wu and Z. Zhou. Multiscale jump testing and estimation under complex temporal dynamics. *arXiv preprint [arXiv:1909.06307](https://arxiv.org/abs/1909.06307)*, 2019.
- [65] W. B. Wu. Nonlinear system theory: Another look at dependence. *Proceedings of the National Academy of Sciences*, 102(40):14150–14154, 2005.
- [66] J. Xu. Rates of convergence of spectral methods for graphon estimation. In *International Conference on Machine Learning*, pages 5433–5442, 2018.
- [67] C. Y. Yau and Z. Zhao. Inference for multiple change points in time series via likelihood ratio scan statistics. *Journal of the Royal Statistical Society Series B: Statistical Methodology*, 78(4):895–916, 2016.
- [68] K.-I. Yoshihara. Moment inequalities for mixing sequences. *Kodai Mathematical Journal*, 1(2):316–328, 1978.
- [69] Y. Yu. A review on minimax rates in change point detection and localisation. *arXiv preprint [arXiv:2011.01857](https://arxiv.org/abs/2011.01857)*, 2020.
- [70] Y. Yu, S. Chatterjee, and H. Xu. Localising change points in piecewise polynomials of general degrees. *Electronic Journal of Statistics*, 16(1):1855 – 1890, 2022.
- [71] W. Zhao, X. Zhu, and L. Zhu. Detecting multiple change points: a pulse criterion. *arXiv preprint [arXiv:2003.01280](https://arxiv.org/abs/2003.01280)*, 2020.
- [72] Z. Zhao, F. Jiang, and X. Shao. Segmenting time series via self-normalisation. *Journal of the Royal Statistical Society Series B: Statistical Methodology*, 84(5):1699–1725, 2022.
- [73] Z. Zhou and W. B. Wu. Simultaneous inference of linear models with time varying coefficients. *Journal of the Royal Statistical Society: Series B (Statistical Methodology)*, 72(4):513–531, 2010.

A Results for simulation studies and another real data example

A.1 Results for simulation studies

Table 8 and Table 9 list the results for Scenario 1. Table 10 and Table 11 list the results for Scenario 2. Table 12 list the results for Scenario 3. Table 8 and 9 show the competitiveness of RID under the independent scenarios. When the sample size is large (e.g., $T = 1800$ in Table 9), results from RID are close to that of the state-of-the-art methods which are specifically designed for independent data. Table 10 and 11 show that in the autoregressive cases, RID outperforms many other methods with a low computational complexity. Table 12 shows that DP [70], with a high computational complexity, often overestimates K . On the other hand, the estimation accuracy of both the \hat{K} and the locations of changes for RID improves as the sample size increases.

Table 8: Results for Scenario 1 with $(T, K) = (900, 5)$

Distribution	Method	$\hat{K} - K$							$H(\hat{\eta}, \eta) \cdot 10^2/T$	ARI	Time(s)
		≤ -3	-2	-1	0	1	2	≥ 3			
Normal	RID	0	0	1	192	7	0	0	1.712	0.983	0.107
	NOT(SSIC)	0	0	0	195	4	1	0	1.117	0.988	0.010
	WBS(SSIC)	0	0	0	193	6	1	0	1.289	0.988	0.023
	PELT.NP(SIC)	0	0	0	114	43	30	13	3.100	0.983	0.012
	e.cp3o	2	2	2	188	5	1	0	1.805	0.981	0.341
	B & P	0	0	0	199	1	0	0	0.921	0.989	4.633
	SMUCE	0	0	0	196	4	0	0	1.076	0.987	0.046
	cumSeg	0	2	0	198	1	0	0	1.402	0.983	0.034
Chisq	RID	0	0	0	176	22	1	1	1.008	0.993	0.103
	NOT(SSIC)	0	0	0	193	6	1	0	0.455	0.998	0.010
	WBS(SSIC)	0	0	0	65	5	57	73	5.381	0.984	0.024
	PELT.NP(SIC)	0	0	0	117	33	36	14	2.913	0.995	0.011
	e.cp3o	0	0	0	200	0	0	0	0.253	0.995	0.284
	B & P	0	0	0	200	0	0	0	0.186	0.998	4.553
	SMUCE	0	0	0	0	0	1	199	12.492	0.925	0.042
	cumSeg	0	0	0	198	2	0	0	0.402	0.994	0.036
t	RID	0	0	0	166	31	3	0	1.596	0.990	0.106
	NOT(SSIC)	0	0	0	189	10	0	1	0.695	0.995	0.011
	WBS(SSIC)	0	0	0	98	4	54	44	3.885	0.988	0.025
	PELT.NP(SIC)	0	0	0	81	29	59	31	3.890	0.987	0.011
	e.cp3o	0	0	0	200	0	0	0	0.471	0.993	0.299
	B & P	0	0	0	200	0	0	0	0.351	0.996	4.533
	SMUCE	0	0	0	13	21	35	131	7.798	0.971	0.042
	cumSeg	0	0	0	199	1	0	0	0.528	0.992	0.036

A.2 Another real data example: change-points in the volatility of the S&P 500 index

In this section, we apply RID to the field of finance. A well-established observation in finance is that stock market volatility is significantly higher during crisis periods than normal periods [72]. In this section, we examine the behavior of the S&P 500 index from 2013-06-18 to 2023-06-14. The

Table 9: Results for Scenario 1 with $(T, K) = (1800, 5)$.

Distribution	Method	$\hat{K} - K$							$H(\hat{\eta}, \eta) \cdot 10^2/T$	ARI	Time(s)
		≤ -3	-2	-1	0	1	2	≥ 3			
Normal	RID	0	0	0	199	1	0	0	0.680	0.992	0.155
	NOT(SSIC)	0	0	0	192	8	0	0	0.583	0.993	0.015
	WBS(SSIC)	0	0	0	193	7	0	0	0.691	0.994	0.037
	PELT.NP(SIC)	0	0	0	93	55	31	21	2.97	0.987	0.039
	e.cp3o	0	3	6	187	4	0	0	1.372	0.986	1.483
	B & P	0	0	0	200	0	0	0	0.491	0.994	20.899
	SMUCE	0	0	0	193	7	0	0	0.700	0.993	0.226
	cumSeg	0	2	0	199	1	0	0	0.931	0.989	0.076
Chisq	RID	0	0	0	194	5	1	0	0.345	0.997	0.168
	NOT(SSIC)	0	0	0	200	0	0	0	0.087	0.999	0.017
	WBS(SSIC)	0	0	0	85	2	42	71	5.577	0.986	0.034
	PELT.NP(SIC)	0	0	0	95	31	54	20	3.034	0.993	0.036
	e.cp3o	0	0	0	200	0	0	0	0.124	0.997	1.074
	B & P	0	0	0	200	0	0	0	0.099	0.999	21.520
	SMUCE	0	0	0	0	0	0	200	14.278	0.895	0.008
	cumSeg	0	0	0	198	2	0	0	0.331	0.996	0.091
t	RID	0	0	0	185	14	0	1	0.672	0.995	0.156
	NOT(SSIC)	0	0	0	197	2	1	0	0.258	0.998	0.017
	WBS(SSIC)	0	0	0	96	1	48	55	4.406	0.987	0.036
	PELT.NP(SIC)	0	0	0	50	20	63	67	4.938	0.987	0.033
	e.cp3o	0	0	1	199	0	0	0	0.340	0.996	1.163
	B & P	0	0	0	200	0	0	0	0.207	0.997	20.977
	SMUCE	0	0	0	1	1	5	193	10.461	0.954	0.008
	cumSeg	0	0	0	197	3	0	0	0.453	0.994	0.079

data consists of daily log returns with $T = 2538$ observations. A mainstream assumption is that the mean and median of log returns are both zero. Our sample mean and median, being 3.86×10^{-4} and 5.47×10^{-4} , confirm this point. We base on $\{|X_t|\}_{t=1}^{2538}$ to detect changes in volatility.

Considering the issue of heteroscedasticity, we utilize the refinement introduced in Section 3.4 with the long-run variance estimation method proposed by [15]. The results indicate that there are five change-points with positions 2015-08-19, 2016-03-01, 2018-02-01, 2020-03-17, and 2021-11-24. In the six periods, the average values of $|X_t|$ are 5.36×10^{-3} , 5.60×10^{-3} , 4.79×10^{-3} , 8.88×10^{-3} , 8.61×10^{-3} and 10.64×10^{-3} . We conclude that the volatility of the S&P 500 index has been increasing over the past decade and is currently in a phase of relatively high volatility.

B Examples of concentration inequalities for time series

In this paper, we need the concentration inequalities for univariate time series. For multivariate data, we discuss it in Remark 9 and list the results in Table 13.

For a univariate time series $\{Y_t\}_{t=1}^T$, its biggest difference from an independent sequence lies in the correlation between Y_i and Y_j , which affects the properties of statistics. Variance proxy is a mapping $\alpha : \{Y_t\}_{t=1}^T \mapsto \mathbb{R}$ that depicts the strength of correlation of the time series $\{Y_t\}_{t=1}^T$. By controlling α , concentration inequalities of the form (26) with $(s, e) \subset (0, T)$ can be obtained,

Table 10: Results for Scenario 2 with $(T, K) = (600, 3)$

Distribution	Method	$\hat{K} - K$							$H(\hat{\eta}, \eta) \cdot 10^2/T$	ARI	Time(s)
		≤ -3	-2	-1	0	1	2	≥ 3			
Normal	RID	0	5	7	163	19	5	1	6.522	0.939	0.104
	NOT(SSIC)	0	0	0	139	28	22	11	5.600	0.956	0.010
	WBS(SSIC)	0	0	0	127	29	22	22	6.496	0.956	0.023
	PELT.NP(SIC)	0	0	0	18	15	24	143	13.124	0.926	0.008
	e.cp3o	0	0	9	148	20	4	19	4.800	0.949	0.159
	B & P	0	0	0	163	36	1	0	4.283	0.961	1.607
	SMUCE	0	0	0	23	42	64	71	12.780	0.925	0.047
	cumSeg	0	7	1	190	2	0	0	4.147	0.954	0.022
Chisq	RID	0	0	0	174	23	3	0	2.905	0.978	0.098
	NOT(SSIC)	0	0	0	66	21	23	90	10.509	0.946	0.009
	WBS(SSIC)	0	0	0	5	4	6	185	18.852	0.893	0.023
	PELT.NP(SIC)	0	0	0	1	1	7	191	17.420	0.914	0.006
	e.cp3o	0	0	0	196	3	0	1	1.267	0.983	0.145
	B & P	0	0	0	130	60	10	0	4.470	0.976	1.658
	SMUCE	0	0	0	0	0	0	200	22.545	0.810	0.040
	cumSeg	0	0	0	164	25	8	3	2.791	0.977	0.020
t	RID	0	1	0	162	33	3	1	3.605	0.976	0.101
	NOT(SSIC)	0	0	0	134	29	23	14	4.275	0.979	0.009
	WBS(SSIC)	0	0	0	53	16	50	81	10.023	0.959	0.022
	PELT.NP(SIC)	0	0	0	12	18	41	129	13.290	0.945	0.007
	e.cp3o	0	0	0	197	3	0	0	1.256	0.983	0.149
	B & P	0	0	0	176	24	0	0	2.110	0.985	1.632
	SMUCE	0	0	0	0	0	2	198	18.054	0.988	0.052
	cumSeg	0	0	0	193	5	2	0	1.533	0.982	0.022

where f is a multivariate function satisfying some conditions. For Markov chains, [30] summarizes various types of variance proxies. We omit the dependency of $h(\varepsilon, \alpha, T)$ on α, T and shorten it as $h(\varepsilon)$ if there is no ambiguity.

$$\mathbb{P}(|f(Y_{s+1}, \dots, Y_e) - \mathbb{E}f(Y_{s+1}, \dots, Y_e)| \geq \varepsilon) \leq h(\varepsilon, \alpha, T). \quad (26)$$

In this section, we review three classical results of variance proxies and concentration inequalities. Then we take f as the linear function (that is, $f(x_1, \dots, x_n) = \sum_{i=1}^n a_i x_i$ for some coefficients $\{a_i\}$ satisfying $\sum_i a_i = 0$ and $\sum_i a_i^2 = 1$) because $\tilde{g}_{s,e}^t$ s in PC and PP cases are both linear, and the corresponding results of m -dependent sub-gaussian sequences, Markov chains, ϕ -mixing sequences, strong mixing sequences, piecewise locally stationary time series and integer-valued time series are derived. Notice that the interval (s, e) may contain change-points, i.e., $(s, e) \cap \eta (= \{\eta_1, \dots, \eta_K\}) \neq \emptyset$. If necessary, we will derive inequalities for both (s, e) such that $|(s, e) \cap \eta| \leq 1$ and arbitrary $(s, e) \subset (0, T)$.

(Inequality 1.) The first measure is given by [56]. Suppose that $Y = (Y_1, \dots, Y_T)$ is defined on $(\Omega^T, \mathcal{F}, P)$ and takes value in \mathcal{G}^T . Y_i^j is used to denote the subsequence (Y_i, \dots, Y_j) and $\mathcal{L}(Z|Z' = y)$ is used to denote the conditional distribution of Z given $Z' = y$. For $1 \leq i < j \leq T$,

Table 11: Results for Scenario 2 with $(T, K) = (1200, 3)$.

Distribution	Method	$\hat{K} - K$							$H(\hat{\eta}, \eta) \cdot 10^2 / T$	ARI	Time(s)
		≤ -3	-2	-1	0	1	2	≥ 3			
Normal	RID	0	0	1	194	5	0	0	1.827	0.979	0.130
	NOT(SSIC)	0	0	0	158	21	11	10	3.436	0.979	0.011
	WBS(SSIC)	0	0	0	133	24	31	12	4.864	0.975	0.030
	PELT.NP(SIC)	0	0	0	8	13	25	154	14.865	0.932	0.018
	e.cp3o	0	0	15	150	18	9	8	4.644	0.954	0.630
	B & P	0	0	0	183	17	0	0	1.983	0.982	9.816
	SMUCE	0	0	0	3	12	14	171	16.090	0.907	0.007
	cumSeg	0	0	0	200	0	0	0	1.570	0.979	0.059
Chisq	RID	0	0	0	194	5	1	0	0.960	0.991	0.129
	NOT(SSIC)	0	0	0	77	18	27	78	8.581	0.960	0.012
	WBS(SSIC)	0	0	0	4	3	10	183	18.363	0.893	0.029
	PELT.NP(SIC)	0	0	0	0	0	1	199	18.959	0.901	0.014
	e.cp3o	0	0	0	197	3	0	0	0.799	0.991	0.504
	B & P	0	0	0	135	54	10	1	4.001	0.983	9.728
	SMUCE	0	0	0	0	0	0	200	23.766	0.785	0.006
	cumSeg	0	0	0	174	20	5	1	1.665	0.986	0.054
t	RID	0	0	0	181	16	3	0	1.714	0.988	0.122
	NOT(SSIC)	0	0	0	157	26	13	4	2.711	0.987	0.011
	WBS(SSIC)	0	0	0	56	14	41	89	10.120	0.962	0.028
	PELT.NP(SIC)	0	0	0	3	7	20	170	15.147	0.936	0.017
	e.cp3o	0	0	0	194	2	1	3	0.986	0.988	0.537
	B & P	0	0	0	177	22	1	0	1.802	0.990	9.687
	SMUCE	0	0	0	0	0	0	200	20.920	0.850	0.007
	cumSeg	0	0	0	198	2	0	0	0.773	0.989	0.059

define

$$\gamma_{ij} := \sup_{y_1^{i-1} \in \mathcal{G}^{i-1}, y_i, y_i' \in \mathcal{G}} \left\| \mathcal{L}(Y_j^T | Y_1^{i-1} = y_1^{i-1}, Y_i = y_i) - \mathcal{L}(Y_j^T | Y_1^{i-1} = y_1^{i-1}, Y_i = y_i') \right\|_{TV}, \quad (27)$$

where $\|\cdot\|_{TV}$ is the total variation distance defined as $\|\mu - \nu\|_{TV} = \sup_{A \subset \mathcal{F}} |\mu(A) - \nu(A)|$ for two probability measures ν and μ . Let

$$\Gamma := \begin{pmatrix} 1 & \sqrt{\gamma_{12}} & \sqrt{\gamma_{13}} & \cdots & \sqrt{\gamma_{1T}} \\ 0 & 1 & \sqrt{\gamma_{23}} & \cdots & \sqrt{\gamma_{2T}} \\ \vdots & \ddots & \ddots & \ddots & \vdots \\ 0 & \cdots & \ddots & 1 & \sqrt{\gamma_{T-1,T}} \\ 0 & \cdots & \cdots & 0 & 1 \end{pmatrix},$$

and define the variance proxy as $\alpha := \left(\sup_{|y|_2=1} |\Gamma y|_2 \right)^2$.

Theorem B.1 (Corollary 4 in [56]). *If $\mathcal{G} \subset [0, 1]$, $f : \mathcal{G}^T \mapsto \mathbb{R}$ is convex and satisfies*

$$|f(X) - f(Y)| \leq |X - Y|_2 \text{ for any } X, Y \in \mathcal{G}^T. \quad (28)$$

Table 12: Results for Scenario 3 (for the univariate PP case).

(T, K)	Method	$\hat{K} - K$						$H(\hat{\eta}, \eta) \cdot 10^2/T$	ARI	time (seconds)
		-2	-1	0	1	2	≥ 3			
(150,2)	RID	55	136	9	0	0	0	41.53	0.585	0.440
	DP	0	0	0	0	0	200	24.63	0.750	0.173
(300,2)	RID	0	32	166	2	0	0	10.365	0.830	1.300
	DP	0	0	0	0	0	200	28.928	0.712	2.075
(450,2)	RID	0	0	195	5	0	0	5.452	0.906	2.799
	DP	0	0	0	0	0	200	30.395	0.698	9.633
(600,2)	RID	0	0	196	4	0	0	3.730	0.930	4.769
	DP	0	0	0	0	0	200	31.042	0.691	28.544

Then for any $\varepsilon > 0$,

$$\mathbb{P}(|f(Y) - \mathbb{E}f(Y)| \geq \varepsilon) \leq 2 \exp\left(-\frac{\varepsilon^2}{2\alpha}\right).$$

(Inequality 2.) Consider the model

$$X_t = \mathbb{E}X_t + \varepsilon_t, 1 \leq t \leq T$$

where $\mathbb{E}X_t$ is piecewise constant mean functions with change-points $\{\eta_1, \dots, \eta_K\}$, and (ε_t) is a centered piecewise locally stationary process defined as follows.

Assumption B.2. For the error processes $\{\varepsilon_t\}_{t=1}^T$, there exist constants $0 = b_0 < b_1 < \dots < b_r < b_{r+1} = 1$ and nonlinear filters G_0, \dots, G_r such that $\varepsilon_t = G_j(t/T, \mathcal{F}_t)$ if $b_j < t/T \leq b_{j+1}$ where $\mathcal{F}_t = (\varepsilon_{-\infty}, \dots, \varepsilon_{t-1}, \varepsilon_t)$ and (ε_t) are i.i.d. random elements. Define $\mathcal{F}_t^* = (\varepsilon_{-\infty}, \dots, \varepsilon_{-1}, \varepsilon_0^*, \dots, \varepsilon_t)$ where (ε_t^*) is an i.i.d. copy of (ε_t) . Assume that there exists a $\bar{q} \geq 4$ such that

1. $\sup_i \sup_{t \in [0,1]} \|G_i(t, \mathcal{F}_0)\|_{\mathcal{L}_{\bar{q}}} < \infty$

2. $\delta_{\bar{q}}(k) = O(\chi^k)$ for some $0 < \chi < 1$ where $\delta_{\bar{q}}(k)$ is the physical dependence measure defined as

$$\delta_{\bar{q}}(k) = \max_{0 \leq i \leq r} \sup_{b_i \leq t \leq b_{i+1}} \|G_i(t, \mathcal{F}_k) - G_i(t, \mathcal{F}_k^*)\|_{\mathcal{L}_{\bar{q}}}.$$

3. There exists a constant C such that for all u_1, u_2 , $\max_{i \in [0,r]} \sup_{b_i \leq u_1 < u_2 \leq b_{i+1}} \|G_i(u_1, \mathcal{F}_0) - G_i(u_2, \mathcal{F}_0)\|_{\mathcal{L}_2} / |u_1 - u_2| \leq C$.

4. The long-run variance

$$\sigma^2(u) = \sum_{k=-\infty}^{\infty} \text{Cov}(G_i(u, \mathcal{F}_0), G_i(u, \mathcal{F}_k))$$

if $u \in (b_i, b_{i+1}]$, $0 \leq i \leq r$. Let $\sigma^2(0) = \lim_{u \downarrow 0} \sigma^2(u)$. Assume that $\inf_{u \in [0,1]} \sigma^2(u) > 0$.

Under Assumption B.2, let $\Omega_p = \sum_{n=0}^{\infty} \delta_p(n) < \infty$ and assume that

$$\alpha := \left(\limsup_{p \rightarrow \infty} p^{\frac{1}{2} - \frac{1}{\gamma}} \Omega_p \right)^{\gamma} < \infty$$

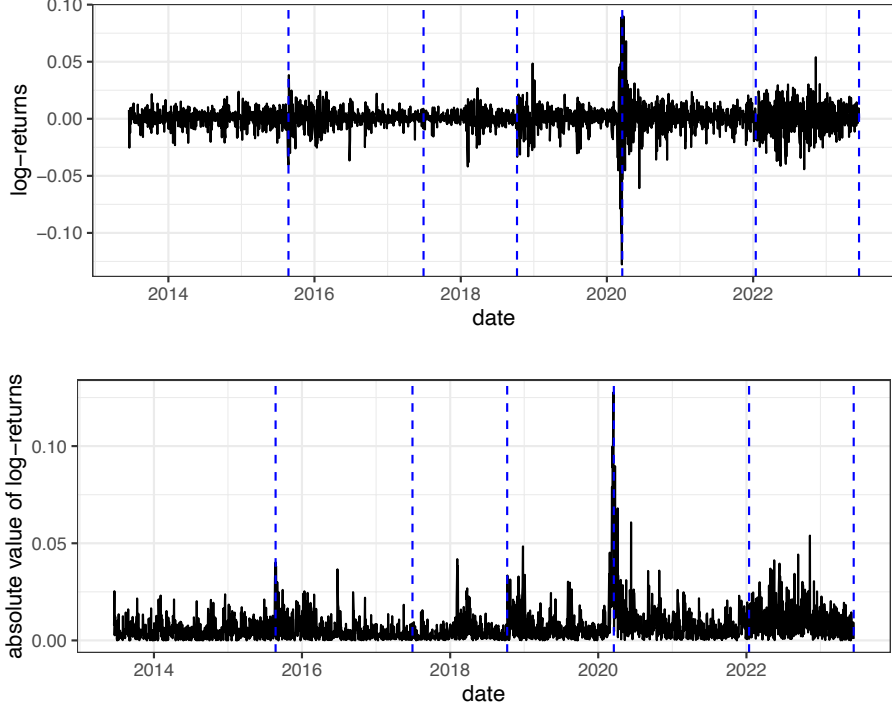


Figure 4: The time series of the daily log returns (X_t) and their absolute values ($|X_t|$) of the S&P 500 index from 2013-06-18 to 2023-06-14. The blue dashed lines represent the segmented results.

for some $0 < \gamma \leq 2$. Then by using the similar arguments as Theorem 2 of [65] and Theorem 2.1 in [52], we have for any $(s, e] \subset (0, T]$ and $\varepsilon > 0$,

$$\mathbb{P} \left(\left| \sum_{i=s+1}^e a_i (X_t - \mathbb{E}X_t) \right| \geq \varepsilon \right) \leq C_{\alpha, \gamma} \exp \left(- \frac{\varepsilon^\gamma}{\exp(1) \gamma 2^{\frac{\gamma}{2}} \alpha} \right) \quad (29)$$

where $\sum_i a_i^2 = 1$, and $C_{\alpha, \gamma}$ is a constant depending on α, γ .

(Inequality 3.) The third measure is for general Markov chains. Let \mathcal{G} be a polish space and $P_i(x, dy)$ be transition kernels satisfying that $P_{i+t}(x_i, dy)$ is a probability distribution for any $x_i \in \mathcal{G}$ and $t \in \mathbb{N}^*$. A Markov chain X_1, X_2, \dots, X_T is a sequence of random variables taking values in \mathcal{G}^T and satisfies that the conditional distribution of X_i given x_1, \dots, x_{i-1} equals to $P_i(x_{i-1}, dy)$. Let $\mathcal{L}_{i+t}(\cdot | x_i)$ denote the conditional distribution of X_{i+t} given $X_i = x_i$, [49] defines the mixing time $\bar{t}_{mix}(s)$ for (inhomogeneous) Markov chain as

$$\bar{t}_{mix}(s) := \min \left\{ t : \max_{1 \leq i \leq T-t} \sup_{x_i, y_i \in \mathcal{G}} \|\mathcal{L}_{i+t}(\cdot | x_i) - \mathcal{L}_{i+t}(\cdot | y_i)\|_{TV} \leq s \right\}. \quad (30)$$

Furthermore, the variance proxy is defined as $\alpha := \inf_{0 < \varepsilon < 1} \bar{t}_{mix}(\varepsilon) \left(\frac{2-\varepsilon}{1-\varepsilon} \right)^2$.

Theorem B.3 (Corollary 2.10 in [49]). *If f satisfies*

$$\exists b_i \text{ s.t. } |f(X) - f(Y)| \leq \sum_{i=1}^T b_i \mathbb{I}(x_i \neq y_i) \text{ for any } X, Y \in \mathcal{G}^T, \quad (31)$$

we have

$$\mathbb{P}(|f(X) - \mathbb{E}f(X)| \geq \varepsilon) \leq 2 \exp\left(-\frac{2\varepsilon^2}{|b|_2^2 \alpha}\right).$$

We now study the concentration inequalities of some important sequences where the f above is a linear function ($f(x_1, \dots, x_n) = \sum_{i=1}^n a_i x_i$ for some coefficients a_i satisfying $\sum_i a_i = 0$ and $\sum_i a_i^2 = 1$). For integer-valued time series INGARCH(p_0, q_0), its tail is heavy so we derive a $h(\varepsilon)$ which is of the polynomial type.

Example 1 (Concentration inequality for m -dependent sequences). *Let $\{X_t\}$ be a m -dependent sub-gaussian sequence with the the maximum ψ_2 -norm be $\sigma = \max_t \|X(t)\|_{\psi_2}$. By Hoeffding's inequality, we have for $\varepsilon > 0, 1 \leq j \leq m$,*

$$\begin{aligned} & \mathbb{P}\left(\left|\sum_{i=1}^{\lfloor \frac{e-s-j}{m} \rfloor + 1} a_{s+m(i-1)+j} (X_{s+m(i-1)+j} - \mathbb{E}X_{s+m(i-1)+j})\right| \geq \varepsilon\right) \\ & \leq 2 \exp\left(-\frac{c\varepsilon^2}{\sigma^2 \sum_{i=1}^{\lfloor \frac{e-s-j}{m} \rfloor + 1} a_{s+m(i-1)+j}^2}\right) \end{aligned}$$

where c is an absolute constant. By Lemma C.3, we have

$$\mathbb{P}\left(\left|\sum_{i=s+1}^e a_i (X_i - \mathbb{E}X_i)\right| \geq \varepsilon\right) \leq 2 \exp\left(-\frac{c\varepsilon^2}{\sigma^2 m}\right).$$

Example 2 (Concentration inequality for contracting Markov chains). *The contracting Markov chain [43] is a Markov chain where*

$$\beta_i := \sup_{x_i, y_i \in \mathcal{G}} \|\mathcal{L}_{i+1}(\cdot|x_i) - \mathcal{L}_{i+1}(\cdot|y_i)\|_{TV} < 1.$$

Denote $\beta = \max_i \beta_i$. [56] proved that for $t \in \mathbb{N}^*$,

$$\max_i \sup_{x_i, y_i \in \mathcal{G}} \|\mathcal{L}_{i+t}(\cdot|x_i) - \mathcal{L}_{i+t}(\cdot|y_i)\|_{TV} \leq \beta^t.$$

Then we can bound the variance proxy as $\alpha \leq \left(\frac{1}{1-\sqrt{\beta}}\right)^2$. By Theorem B.1, we obtain that for any $(s, e) \subset (0, T)$,

$$\mathbb{P}(|f(X_{s+1}, \dots, X_e) - \mathbb{E}f(X_{s+1}, \dots, X_e)| \geq \varepsilon) \leq 2 \exp\left(-\varepsilon^2 \frac{(1-\sqrt{\beta})^2}{2}\right)$$

as long as $\mathcal{G} \subset [0, 1]$ and f is convex and satisfies (28). Notice that the linear f satisfies (28).

Example 3 (Concentration inequality for Φ -mixing processes). *For a random sequence $(X_i)_{i \in \mathbb{Z}}$ and $k \geq 1$, define*

$$\Phi_k := \sup_{j-i \geq k} \sup_{\substack{U \in \sigma(\dots, X_i) \\ V \in \sigma(X_j, \dots) \\ \mathbb{P}(U) > 0}} |\mathbb{P}(V|U) - \mathbb{P}(V)|.$$

[56] showed that $\gamma_{ij} \leq 2\Phi_{j-i}$, and if $\sum_{k=1}^{\infty} \sqrt{\Phi_k} < \infty$, then $\alpha \leq (\sum_{k=1}^{\infty} \sqrt{\Phi_k})^2$. Therefore, by Theorem B.1, we obtain that for any $(s, e) \subset (0, T)$,

$$\mathbb{P}(|f(X_{s+1}, \dots, X_e) - \mathbb{E}f(X_{s+1}, \dots, X_e)| \geq \varepsilon) \leq 2 \exp\left(-\frac{\varepsilon^2}{2\alpha}\right)$$

as long as $\mathcal{G} \subset [0, 1]$ and f is convex and satisfies (28). Notice that the linear f satisfies (28).

Example 4 (Concentration inequality for strong mixing processes). *Let a random sequence $X_i, 1 \leq i \leq n$ satisfy $\max_{1 \leq i \leq n} \mathbb{E}|X_i|^\xi < \infty$ for some odd integer $\xi \geq 3$. Then $C_X := \max_{1 \leq i \leq n} \mathbb{E}|X_i - \mathbb{E}X_i|^\xi < \infty$. Assume further that $\{X_i\}$ is strong mixing [54] with mixing coefficients $\alpha(j) \leq Cr^j$ for some $C > 0$ and $0 < r < 1$. Then by Theorem 3 in [68], for sequence $\{a_i\}$,*

$$\mathbb{E} \left(\sum_{i=1}^n a_i (X_i - \mathbb{E}X_i) \right)^{\xi-1} \leq c_{\xi-1} \left(\sum_{i=1}^n a_i^2 \right)^{\frac{\xi-1}{2}}, \quad (32)$$

where $c_{\xi-1}$ is a constant depending only on ξ . As a result, we have

$$\begin{aligned} \mathbb{P} \left(\left| \sum_{i=1}^n a_i (X_i - \mathbb{E}X_i) \right| \geq \varepsilon \right) &\leq \frac{1}{\varepsilon^{\xi-1}} \mathbb{E} \left(\sum_{i=1}^n a_i (X_i - \mathbb{E}X_i) \right)^{\xi-1} \\ &\leq \frac{c_{\xi-1}}{\varepsilon^{\xi-1}} \left(\sum_{i=1}^n a_i^2 \right)^{\frac{\xi-1}{2}} = \frac{c_{\xi-1}}{\varepsilon^{\xi-1}}, \end{aligned}$$

where the last inequality is due to the fact that $\sum_{i=1}^n a_i^2 = 1$.

Many types of integer-valued GARCH models (INGARCH) are absolute regularity (thus, strong mixing) with geometric decay [1; 12; 46]. We will use the (piecewise) Poisson INGARCH model as an example to provide more detailed illustrations.

Example 5 (Concentration inequality for INGARCH(p_0, q_0) model). *Consider a stationary $\{X_t\}$ satisfying [18]*

$$\begin{aligned} X_t | \mathcal{F}_{t-1} &: \text{Poisson}(\lambda_t) \\ \lambda_t &= \gamma_0 + \sum_{j=1}^{p_0} \gamma_j X_{t-j} + \sum_{k=1}^{q_0} \delta_k \lambda_{t-k} \end{aligned}$$

where $\gamma_0 > 0, \gamma_j > 0, \delta_k > 0, 1 \leq j \leq p_0, 1 \leq k \leq q_0$ and $\sum_{j=1}^{p_0} \gamma_j + \sum_{k=1}^{q_0} \delta_k < 1$. [46] proved that $\mathbb{E}X_t^\xi < \infty$ for all $\xi \geq 0$. Moreover, $\{X_t\}$ is absolutely regular with coefficients decaying geometrically. Thus, $\alpha(j) = O(r^j), 0 < r < 1$. By Example 4, we obtain that for sequence $\{a_i\}$, any even integer $\xi \geq 2$ and any $\varepsilon > 0$,

$$\mathbb{P} \left(\left| \sum_{i=1}^n a_i (X_i - \mathbb{E}X_i) \right| \geq \varepsilon \right) \leq \frac{c_\xi}{\varepsilon^\xi} \left(\sum_{i=1}^n a_i^2 \right)^{\frac{\xi}{2}} = \frac{c_\xi}{\varepsilon^\xi}$$

where c_ξ depends on ξ . We next define the piecewise stationary INGARCH(p_0, q_0) model. For ease of reading, we only derive for Poisson INGARCH model with two segments. Assume that there exists a $\eta \in (0, T)$ such that $\{X_t\}_{t=1}^\eta$ and $\{X_t\}_{t=\eta+1}^T$ are two stationary INGARCH(p_0, q_0)

models with parameters $(\gamma_0, \gamma_j, \delta_k), (\gamma'_0, \gamma'_j, \delta'_k)$. Let $\gamma_0 > 0, \gamma_j > 0, \delta_k > 0, \gamma'_0 > 0, \gamma'_j > 0, \delta'_k > 0, \max\left(\sum_{j=1}^{p_0} \gamma_j + \sum_{k=1}^{q_0} \delta_k, \sum_{j=1}^{p_0} \gamma'_j + \sum_{k=1}^{q_0} \delta'_k\right) < 1$. Then for sequence $\{a_i\}$ and an even number p , by (32) we have

$$\begin{aligned} \left(\mathbb{E}\left(\sum_{i=1}^{\eta} a_i(X_i - \mathbb{E}X_i)\right)^p\right)^{\frac{1}{p}} &\leq (c_p)^{\frac{1}{p}} \left(\sum_{i=1}^{\eta} a_i^2\right)^{\frac{1}{2}} \\ \left(\mathbb{E}\left(\sum_{i=\eta+1}^T a_i(X_i - \mathbb{E}X_i)\right)^p\right)^{\frac{1}{p}} &\leq (c_p)^{\frac{1}{p}} \left(\sum_{i=\eta+1}^T a_i^2\right)^{\frac{1}{2}}. \end{aligned}$$

Thus,

$$\begin{aligned} \mathbb{P}\left(\left|\sum_{i=1}^T a_i(X_i - \mathbb{E}X_i)\right| \geq \varepsilon\right) &\leq \frac{1}{\varepsilon^p} \mathbb{E}\left(\sum_{i=1}^T a_i(X_i - \mathbb{E}X_i)\right)^p \\ &\leq \frac{1}{\varepsilon^p} \left(\left(\mathbb{E}\left(\sum_{i=1}^{\eta} a_i(X_i - \mathbb{E}X_i)\right)^p\right)^{\frac{1}{p}} + \left(\mathbb{E}\left(\sum_{i=\eta+1}^T a_i(X_i - \mathbb{E}X_i)\right)^p\right)^{\frac{1}{p}}\right)^p \\ &\leq \frac{c_p}{\varepsilon^p} \left(\left(\sum_{i=1}^{\eta} a_i^2\right)^{\frac{1}{2}} + \left(\sum_{i=\eta+1}^T a_i^2\right)^{\frac{1}{2}}\right)^p \leq 2^{\frac{p}{2}} \frac{c_p}{\varepsilon^p} \left(\sum_{i=1}^T a_i^2\right)^{\frac{p}{2}}. \end{aligned} \tag{33}$$

Similarly, for the piecewise model with K segments, we have

$$\mathbb{P}\left(\left|\sum_{i=1}^T a_i(X_i - \mathbb{E}X_i)\right| \geq \varepsilon\right) \leq \frac{1}{\varepsilon^p} \mathbb{E}\left(\sum_{i=1}^T a_i(X_i - \mathbb{E}X_i)\right)^p \leq K^{\frac{p}{2}} \frac{c_p}{\varepsilon^p} \left(\sum_{i=1}^T a_i^2\right)^{\frac{p}{2}}.$$

Therefore, let f be a linear function with $\sum_i a_i = 0, \sum_i a_i^2 = 1$, for any (s, e) such that $|(s, e) \cap \eta| \leq 1$ and any even number p , we have

$$\mathbb{P}(|f(X_{s+1}, \dots, X_e) - \mathbb{E}f(X_{s+1}, \dots, X_e)| \geq \varepsilon) \leq \frac{2^{\frac{p}{2}} c_p}{\varepsilon^p}.$$

For arbitrary $(s, e) \subset (0, T)$, we have

$$\mathbb{P}(|f(X_{s+1}, \dots, X_e) - \mathbb{E}f(X_{s+1}, \dots, X_e)| \geq \varepsilon) \leq \frac{c_p}{(\varepsilon/\sqrt{K})^p}.$$

Remark 8. From Example 1 to Example 5, the difference between the case that $|(s, e] \cap \eta| \leq 1$ and the case that $(s, e] \subset (0, T]$ lies in a term of \sqrt{K} . That is, if for $|(s, e] \cap \eta| \leq 1$ we have $|f(X_{s+1}, \dots, X_e) - \mathbb{E}f(X_{s+1}, \dots, X_e)| \leq \mathfrak{J}$ for some \mathfrak{J} with a high probability, then we have for arbitrary $(s, e] \subset (0, T]$, $|f(X_{s+1}, \dots, X_e) - \mathbb{E}f(X_{s+1}, \dots, X_e)| \leq \mathfrak{J}\sqrt{K}$ with the same high probability.

Remark 9. For multivariate data, suppose that there exist functions $f = (f_1, \dots, f_p)^\top$ and $\{h_i\}$ such that $\mathbb{P}(|f_i(X_{s+1,i}, \dots, X_{e,i}) - \mathbb{E}f_i(X_{s+1,i}, \dots, X_{e,i})| \geq \varepsilon) \leq h_i(\varepsilon)$, then by the union bound

argument, we have

$$\begin{aligned}
& \mathbb{P} \left(|f(X_{s+1}, \dots, X_e) - \mathbb{E}f(X_{s+1}, \dots, X_e)|_q \geq \varepsilon \right) \\
& \leq \sum_{i=1}^p \mathbb{P} \left(|f_i(X_{s+1,i}, \dots, X_{e,i}) - \mathbb{E}f_i(X_{s+1,i}, \dots, X_{e,i})| \geq \frac{1}{p^{1/q}} \varepsilon \right) \\
& \leq \sum_{j=1}^p h_j \left(\frac{\varepsilon}{p^{1/q}} \right).
\end{aligned} \tag{34}$$

Therefore, we can derive \mathfrak{J} and \mathfrak{J}^* for models in Table 2, as listed in Table 13.

Type	\mathfrak{J}	\mathfrak{J}^*
m-dependent sub-gaussian	$\Omega \left(p^{1/q} \sqrt{\alpha \log(T \vee p)} \right)$	$\Omega \left(p^{1/q} \sqrt{\alpha \log(T \vee p)} \right)$
Markov chain	$\Omega \left(p^{1/q} \sqrt{\alpha \log(T \vee p)} \right)$	$\Omega \left(p^{1/q} \sqrt{\alpha \log(T \vee p)} \right)$
ϕ -mixing process	$\Omega \left(p^{1/q} \sqrt{\alpha \log(T \vee p)} \right)$	$\Omega \left(p^{1/q} \sqrt{\alpha \log(T \vee p)} \right)$
Piecewise locally stationary time series	$\Omega \left(p^{1/q} (\alpha \log(T \vee p))^{1/\gamma} \right)$	$\Omega \left(p^{1/q} (\alpha \log(T \vee p))^{1/\gamma} \right)$
Strong mixing process	$\Omega \left(T^{4/\xi} p^{1/\xi+1/q} \right)$	$\Omega \left((\Delta T)^{1/\xi} p^{1/\xi+1/q} \right)$
Piecewise stationary Poisson INGARCH(p_0, q_0)	$\Omega \left(T^{4/\xi} p^{1/\xi+1/q} \right)$	$\Omega \left((\Delta T)^{1/\xi} p^{1/\xi+1/q} \right)$

C Appendix for Section 2

C.1 Proof of Theorem 2.2 and Theorem 2.3

Proof of Theorem 2.2. By (3), we have

$$\sup_{(s,e]:|(s,e] \cap \eta| \leq 1} \mathbb{P} \left(\left| |\tilde{f}_{s,e}(X)|_q - |\mathbb{E}\tilde{f}_{s,e}(X)|_q \right| \geq \mathfrak{J} \right) \leq T^{-3}.$$

Therefore, let the event

$$\mathcal{A} := \left\{ \sup_{(s,e]:|(s,e] \cap \eta| \leq 1} \left| |\tilde{f}_{s,e}(X)|_q - |\mathbb{E}\tilde{f}_{s,e}(X)|_q \right| \leq \mathfrak{J} \right\}, \tag{35}$$

we have

$$\begin{aligned}
\mathbb{P}(\mathcal{A}^c) &= \mathbb{P} \left(\sup_{(s,e]:|(s,e] \cap \eta| \leq 1} \left| |\tilde{f}_{s,e}(X)|_q - |\mathbb{E}\tilde{f}_{s,e}(X)|_q \right| \geq \mathfrak{J} \right) \\
&\leq \sum_{(s,e]:|(s,e] \cap \eta| \leq 1} \mathbb{P} \left(\left| |\tilde{f}_{s,e}(X)|_q - |\mathbb{E}\tilde{f}_{s,e}(X)|_q \right| \geq \mathfrak{J} \right) \leq T^{-1},
\end{aligned}$$

which implies that $\mathbb{P}(\mathcal{A}) \geq 1 - T^{-1}$. From (35) and Lemma C.4, we get

$$\mathbb{P}(\mathcal{A} \cap \mathcal{M}) \geq 1 - T^{-1} - \frac{T}{\Delta} \exp \left(-\frac{M\Delta^2}{32T^2} \right),$$

which will tend to 1 as long as $\frac{32T^2}{\Delta^2} \log\left(\frac{T}{\Delta}\right) = o(M)$. All the analysis in the rest of this proof is conducted on $\mathcal{A} \cap \mathcal{M}$. For the random interval (s_m, e_m) , if it contains no change-point, $|\mathbb{E} \tilde{f}_{s_m, e_m}(X)|_q \leq \mathfrak{N}$. Then on event \mathcal{A} , we have $|\tilde{f}_{s_m, e_m}(X)|_q \leq \mathfrak{J} + \mathfrak{N}$. So the choice of $\tau > \mathfrak{J} + \mathfrak{N}$ excludes intervals without change-points. Recall the construction of S in Algorithm 1:

If $|\tilde{f}_{s_m, e_m}(X)|_q > \tau$ then
 $S = S \cup \{(s_m, e_m]\}$
 End if

Therefore, the intervals in S must include at least one change-point. We now prove that $\hat{K} = K$. First, it's obvious that

$$\hat{K} = \max_{\{S' \subset S: \text{intervals in } S' \text{ are disjoint}\}} |S'|.$$

Since every interval in S must cover at least one change-point, it follows from the Pigeonhole Principle that if we select more than K intervals from S , then at least two intervals will cover the same change-point. Therefore, $|S^*| = \hat{K} \leq K$. To prove $\hat{K} \geq K$, we construct a set \mathcal{Q} such that $|\mathcal{Q}| = K$, $\mathcal{Q} \subset S$ and that intervals in \mathcal{Q} are disjoint. Recall the definition of \mathcal{M} , for each $k = 1, \dots, K$, we can pick out an interval (s_k, e_k) such that

$$\eta_k - \frac{1}{4}\Delta < s_k < \eta_k - \frac{1}{8}\Delta, \quad \eta_k + \frac{1}{8}\Delta < e_k < \eta_k + \frac{1}{4}\Delta. \quad (36)$$

Let $\mathcal{Q} = \{(s_1, e_1), \dots, (s_K, e_K)\}$. On event \mathcal{A} , we obtain $|\tilde{f}_{s_k, e_k}(X)|_q \geq |\mathbb{E} \tilde{f}_{s_k, e_k}(X)|_q - \mathfrak{J} \geq \mathfrak{S} - \mathfrak{J}$. Therefore, $(s_k, e_k) \in S$ as long as $\tau < \mathfrak{S} - \mathfrak{J}$. It suffices to show that intervals in \mathcal{Q} are mutually disjoint. Notice that $e_k - \eta_k < \frac{1}{4}\Delta$ and $\eta_k - s_k < \frac{1}{4}\Delta$. Meanwhile, $\Delta \leq \eta_k - \eta_{k-1}$ for all k . This indicates that all (s_k, e_k) are mutually disjoint. Therefore, $\hat{K} = K$.

Recall the construction of r_k and l_k in Line 10 and 17 of Algorithm 1. Since $\eta_1 < r_1 \leq e_1$, $e_1 < s_2$ and every interval covers at least one change-point, we conclude that $\eta_2 < r_2 \leq e_2$. It follows by induction that $\eta_k < r_k \leq e_k$ for $1 \leq k \leq K$. By symmetry, $s_k \leq l_k < \eta_k$ for $1 \leq k \leq K$. So $[l_k, r_k]$ contains η_k only and $r_k - l_k \leq e_k - s_k \leq \frac{\Delta}{2}$. □

Proof of Theorem 2.3. Combining Theorem 2.2 and Lemma C.1, it is straightforward to obtain Theorem 2.3.

Lemma C.1. *Recall Algorithm 2 where we propose the localization procedure. Under Assumption (11), we have for any fixed k ,*

$$\mathbb{P}\left(|\eta_k - \hat{\eta}_k| \leq \frac{2\mathfrak{J}^*}{\mathfrak{R}^*}\right) \geq 1 - T^{-1}.$$

Proof of Lemma C.1. Recall the notation that $S^* = \{(s_k, e_k)\}_{k=1}^{\hat{K}}$. By the definition of \mathfrak{J}^* in (10), similar to the arguments in the proof of Theorem 2.2, we have $\mathbb{P}(\mathcal{A}_k^*) \geq 1 - T^{-1}$ where

$$\mathcal{A}_k^* := \left\{ \sup_{t: s_k < t \leq e_k} \left| |\tilde{g}_{s_k, e_k}^t(X)|_q - |\mathbb{E} \tilde{g}_{s_k, e_k}^t(X)|_q \right| \leq \mathfrak{J}^* \right\}.$$

Therefore, on event \mathcal{A}_k^* , since $\hat{\eta}_k$ is the local maximizer of $|\tilde{g}_{s_k, e_k}^t(X)|_q$, we derive that

$$|\mathbb{E} \tilde{g}_{s_k, e_k}^{\hat{\eta}_k}(X)|_q \geq |\tilde{g}_{s_k, e_k}^{\hat{\eta}_k}(X)|_q - \mathfrak{J}^* \geq |\tilde{g}_{s_k, e_k}^{\eta_k}(X)|_q - \mathfrak{J}^* \geq |\mathbb{E} \tilde{g}_{s_k, e_k}^{\eta_k}(X)|_q - 2\mathfrak{J}^*.$$

Hence,

$$|\mathbb{E}\tilde{g}_{s_k, e_k}^{\eta_k}(X)|_q - |\mathbb{E}\tilde{g}_{s_k, e_k}^{\hat{\eta}_k}(X)|_q \leq 2\mathfrak{J}^*. \quad (37)$$

By (9), $|\mathbb{E}\tilde{g}_{s_k, e_k}^{\eta_k}(X)|_q - |\mathbb{E}\tilde{g}_{s_k, e_k}^{\hat{\eta}_k}(X)|_q \geq \mathfrak{R}^*|\eta_k - \hat{\eta}_k|$. Therefore, $|\eta_k - \hat{\eta}_k| \leq \frac{2\mathfrak{J}^*}{\mathfrak{R}^*}$. \square

\square

C.2 Additional lemmas

Lemma C.2. For any set $S = \{[u_m, v_m]\}_{j=1}^{M^*}$ where M^* is an integer, applying line 8-22 in Algorithm 1 to S , then the output \hat{K} and S^* satisfy $l_j < r_j$ for $1 \leq j \leq \hat{K}$.

Proof of Lemma C.2. We show by contradiction. Assume that $r_j \leq l_j$ for some j . By construction, there are two disjoint intervals in $[1, r_2]$ because we drop the intervals whose left endpoints are less than r_1 in line 12. Therefore, we have $l_2 > r_1$. Similarly, there are j disjoint intervals in $[1, r_j]$ and $\hat{K} + 1 - j$ disjoint intervals in $[l_j, T]$. This leads to a fact that the number of disjoint intervals in $[1, T]$ is $\hat{K} + 1$, which is impossible since \hat{K} is the maximum number of disjoint intervals in $[1, T]$. \square

Lemma C.3. Z_1, \dots, Z_p are random variables (not necessarily independent or zero mean). Suppose there exists a positive sequence $\{\alpha_i\}_{1 \leq i \leq p}$ such that for any $\varepsilon > 0$,

$$\mathbb{P}(|Z_i| > \varepsilon) \leq 2 \exp\left(-\frac{2\varepsilon^2}{\alpha_i}\right) \text{ for every } i = 1, \dots, p.$$

Then for any $\varepsilon > 0$,

$$\mathbb{P}\left(\left|\sum_{i=1}^p Z_i\right| > \varepsilon\right) \leq 12 \exp\left(-\frac{\varepsilon^2}{2p \sum_{i=1}^p \alpha_i}\right).$$

Proof of Lemma C.3. Let $K_i = \sqrt{\alpha_i/2}$, then

$$\mathbb{P}(|Z_i| \geq \varepsilon) \leq 2 \exp\left(-\frac{\varepsilon^2}{K_i^2}\right).$$

For $|\lambda| \leq \frac{1}{\sqrt{1.5}K_i}$,

$$\begin{aligned} \mathbb{E} \exp(\lambda^2 Z_i^2) &= 1 + \sum_{j=1}^{\infty} \frac{1}{j!} \lambda^{2j} \mathbb{E}(Z_i)^{2j} \leq 1 + \sum_{j=1}^{\infty} \frac{2^j \Gamma(j)}{j!} (K_i \lambda)^{2j} \\ &= \frac{1}{1 - (K_i \lambda)^2} \leq 4 \exp(0.5 K_i^2 \lambda^2), \end{aligned} \quad (38)$$

where the first equality comes from Fubini theorem, and the second inequality follows from the proof of $1 \Rightarrow 2$ (especially the $\Gamma(j)$) in Proposition 2.5.2 in [58]. The last inequality follows from the fact that

$$\frac{1}{1-x} \leq 4 \exp\left(\frac{1}{2}x\right) \text{ for } 0 \leq x \leq \frac{2}{3}.$$

Note that

$$e^x < 1.5e^{x^2} \text{ for } x \in \mathbb{R},$$

together with (38), we have that

$$\mathbb{E} \exp(\lambda Z_i) \leq 6 \exp(0.5K_1^2 \lambda^2)$$

provided that $|\lambda| \leq \frac{1}{\sqrt{1.5K_i}}$. For $|\lambda| > \frac{1}{\sqrt{1.5K_i}}$,

$$\begin{aligned} \mathbb{E} \exp(\lambda Z_i) &\leq \mathbb{E} \exp\left(0.75K_i^2 \lambda^2 + \frac{Z_i^2}{3K_i^2}\right) \leq \exp(0.75K_i^2 \lambda^2) \mathbb{E} \exp\left(\frac{Z_i^2}{3K_i^2}\right) \\ &\leq 4 \exp(0.75K_i^2 \lambda^2) \exp\left(\frac{1}{6}\right) < 4 \exp(K_i^2 \lambda^2), \end{aligned} \quad (39)$$

where the first inequality come from the fact that $2ab \leq a^2 + b^2$ for any $a, b \in \mathbb{R}$, the third inequality follows from (38) and the fourth inequality follows from the fact that $1.5K_i^2 \lambda^2 > 1$. Combining (38) and (39), we get that for any λ ,

$$\mathbb{E} \exp(\lambda Z_i) < 6 \exp(K_i^2 \lambda^2), \quad (40)$$

$$\mathbb{E} \exp(-\lambda Z_i) < 6 \exp(K_i^2 \lambda^2).$$

Through iterative utilization of the Cauchy-Schwarz inequality, we derive that for any $\varepsilon_1 \in \mathbb{R}$,

$$\begin{aligned} \mathbb{E} \exp\left(\varepsilon_1 \sum_{i=1}^p Z_i\right) &\leq \left(\prod_{i=1}^p \mathbb{E} \exp(p\varepsilon_1 Z_i)\right)^{\frac{1}{p}} \\ &< \left(\prod_{i=1}^p 6 \exp(K_i^2 p^2 \varepsilon_1^2)\right)^{\frac{1}{p}} = 6 \exp\left(p^2 \varepsilon_1^2 \sum_{i=1}^p K_i^2\right). \end{aligned}$$

We then obtain that for any $\varepsilon > 0$,

$$\begin{aligned} \mathbb{P}\left(\left|\sum_{i=1}^p Z_i\right| \geq \varepsilon\right) &\leq \mathbb{P}\left(\sum_{i=1}^p Z_i \leq -\varepsilon\right) + \mathbb{P}\left(\sum_{i=1}^p Z_i \geq \varepsilon\right) \leq 12 \exp\left(-\frac{\varepsilon^2}{4p \sum_{i=1}^p K_i^2}\right) \\ &= 12 \exp\left(-\frac{\varepsilon^2}{2p \sum_{i=1}^p \alpha_i}\right). \end{aligned}$$

□

Lemma C.4. *Define the event*

$$\mathcal{M} = \bigcap_{k=1}^K \left\{ \exists (s_m, e_m) \text{ s.t. } \eta_k - \frac{1}{4}\Delta < s_m < \eta_k - \frac{1}{8}\Delta, \eta_k + \frac{1}{8}\Delta < e_m < \eta_k + \frac{1}{4}\Delta \right\}. \quad (41)$$

We have

$$\mathbb{P}(\mathcal{M}) \geq 1 - \frac{T}{\Delta} \exp\left(-\frac{M\Delta^2}{32T^2}\right).$$

Proof.

$$\begin{aligned} \mathbb{P}(\mathcal{M}^c) &\leq \sum_{k=1}^K \prod_{m=1}^M \left(1 - \mathbb{P}\left(\eta_k - \frac{1}{4}\Delta < s_m < \eta_k - \frac{1}{8}\Delta, \eta_k + \frac{1}{8}\Delta < e_m < \eta_k + \frac{1}{4}\Delta\right)\right) \\ &= \sum_{k=1}^K \prod_{m=1}^M \left(1 - \mathbb{P}\left(\eta_k - \frac{1}{4}\Delta < s \wedge e < \eta_k - \frac{1}{8}\Delta, \eta_k + \frac{1}{8}\Delta < s \vee e < \eta_k + \frac{1}{4}\Delta\right)\right) \\ &= K \left(1 - 2 \left(\frac{\Delta}{8T}\right)^2\right)^M \leq \frac{T}{\Delta} \exp\left(-\frac{M\Delta^2}{32T^2}\right), \end{aligned}$$

where s, e are two i.i.d. random variables that follow the discrete uniform distribution on $\{1, \dots, T\}$ and the last inequality follows from the fact that $2 \left(\frac{\Delta}{8T}\right)^2 < 1/32$. \square

D Appendix for Section 3

D.1 Detailed derivation of $\mathfrak{N}, \mathfrak{J}, \mathfrak{S}$ and \mathfrak{R}^*

We now give the complete derivations of $\mathfrak{N}, \mathfrak{J}, \mathfrak{S}$ and \mathfrak{R}^* for PC cases. Recall that \tilde{g} is the CUSUM, we already have

$$\mathbb{P}(|\tilde{g}_{s,e,i}^t(X) - \mathbb{E}\tilde{g}_{s,e,i}^t(X)| \geq \varepsilon) \leq h(\varepsilon) \quad (42)$$

for some function $h(\cdot)$ (one can refer to Section B for specific formulas) and any (s, e) such that $|(s, e) \cap \eta| \leq 1$, any $s < t \leq e, i$ and any $\varepsilon > 0$. Moreover, we mention that $\tilde{f}_{s,e,i} = \tilde{g}_{s,e,i}^{t_0}$ where $t_0 = \arg \max_{s < t \leq e} |\tilde{g}_{s,e}^t(X)|_q$. As a result, $|\tilde{f}_{s,e}(X)|_q = \max_{s < t \leq e} |\tilde{g}_{s,e}^t(X)|_q$.

Lemma D.1. *Recall the setting of the PC cases in Section 3.1 and the definition that $\kappa_{\eta_k} := |\mathbb{E}\mathbb{X}_{\eta_k} - \mathbb{E}\mathbb{X}_{\eta_k-1}|_q$, $\kappa_q := \min_k \kappa_{\eta_k}/p$. We have*

1. $\mathfrak{N} = 0$.
2. $\mathfrak{J} = \inf\{\varepsilon : h\left(\frac{\varepsilon}{p^{1/q}}\right) \leq T^{-4}p^{-1}\}$.
3. $\mathfrak{S} \geq \frac{1}{4}\sqrt{\Delta}\kappa_q p - 2\mathfrak{J}$.
4. $\mathfrak{R}^* \geq \frac{(2\sqrt{2}-2)\kappa_q p}{\sqrt{\Delta}}$.

Proof. For \mathfrak{N} . We note that if $(s, e] \cap \eta = \emptyset$, $\mathbb{E}\mathbb{X}_t$ is a constant sequence for $t = s+1, \dots, e$ and $\mathbb{E}\tilde{g}_{s,e,i}^t(X) = 0$ for all $s+1 \leq t \leq e$.

For \mathfrak{J} . By (42), similar to the arguments in (34), we have for any (s, e) such that $|(s, e) \cap \eta| \leq 1$, any $s < t \leq e$ and any $\varepsilon > 0$,

$$\mathbb{P}(||\tilde{g}_{s,e}^t(X)|_q - |\mathbb{E}\tilde{g}_{s,e}^t(X)|_q| \geq \varepsilon) \leq ph\left(\frac{\varepsilon}{p^{1/q}}\right).$$

Therefore,

$$\begin{aligned} \mathbb{P}\left(||\tilde{f}_{s,e}(X)|_q - |\mathbb{E}\tilde{f}_{s,e}(X)|_q| \geq \varepsilon\right) &\leq \mathbb{P}\left(\cup_{s < t \leq e} ||\tilde{g}_{s,e}^t(X)|_q - |\mathbb{E}\tilde{g}_{s,e}^t(X)|_q| \geq \varepsilon\right) \\ &\leq \sum_{t=s+1}^e \mathbb{P}\left(||\tilde{g}_{s,e}^t(X)|_q - |\mathbb{E}\tilde{g}_{s,e}^t(X)|_q| \geq \varepsilon\right) \leq Tph\left(\frac{\varepsilon}{p^{1/q}}\right). \end{aligned}$$

Recall the definition of \mathfrak{J} in (10) and we get that $\mathfrak{J} = \inf\{\varepsilon : h\left(\frac{\varepsilon}{p^{1/q}}\right) \leq T^{-4}p^{-1}\}$.

For \mathfrak{S} . By the arguments above, we have

$$\mathbb{P}\left(\left\{\sup_{|(s,e) \cap \eta| \leq 1} \sup_{s < t \leq e} ||\tilde{g}_{s,e}^t(X)|_q - |\mathbb{E}\tilde{g}_{s,e}^t(X)|_q| \leq \mathfrak{J}\right\}\right) \geq 1 - T^{-1}. \quad (43)$$

As a result, $\mathbb{P}\left(||\tilde{f}_{s,e}(X)|_q \geq |\mathbb{E}\tilde{g}_{s,e}^{\eta_k}(X)|_q - 2\mathfrak{J}\right) \geq 1 - T^{-1}$. Consider the case where $s \in (\eta_k - \Delta/4, \eta_k - \Delta/8)$ and $e \in (\eta_k + \Delta/8, \eta_k + \Delta/4)$ for some k . By the property of CUSUM statistics,

$$\mathbb{E}\tilde{g}_{s,e}^{\eta_k}(X) = \sqrt{\frac{(\eta_k - s)(e - \eta_k)}{e - s}}(\mathbb{E}\mathbb{X}_{\eta_k} - \mathbb{E}\mathbb{X}_{\eta_k-1}).$$

Taking $|\cdot|_q$ for both sides to get that

$$\begin{aligned} |\mathbb{E}\tilde{g}_{s,e}^{\eta_k}(X)|_q &= \sqrt{\frac{1}{2}[(\eta_k - s) \wedge (e - \eta_k)]} |\mathbb{E}\mathbb{X}_{\eta_k} - \mathbb{E}\mathbb{X}_{\eta_k-1}|_q \\ &\geq \sqrt{\frac{1}{2}[(\eta_k - s) \wedge (e - \eta_k)]} |\mathbb{E}\mathbb{X}_{\eta_k} - \mathbb{E}\mathbb{X}_{\eta_k-1}|_q \\ &\geq \frac{1}{4}\sqrt{\Delta} |\mathbb{E}\mathbb{X}_{\eta_k} - \mathbb{E}\mathbb{X}_{\eta_k-1}|_q. \end{aligned}$$

Therefore,

$$|\mathbb{E}\tilde{f}_{s,e}(X)|_q \geq |\mathbb{E}\tilde{g}_{s,e}^{\eta_k}(X)|_q - 2\mathfrak{J} \geq \frac{1}{4}\sqrt{\Delta} |\mathbb{E}\mathbb{X}_{\eta_k} - \mathbb{E}\mathbb{X}_{\eta_k-1}|_q - 2\mathfrak{J}.$$

Let $\kappa_{\eta_k} := |\mathbb{E}\mathbb{X}_{\eta_k} - \mathbb{E}\mathbb{X}_{\eta_k-1}|_q$ and $\kappa_q := \min_k \kappa_{\eta_k}/p$. Then $\mathfrak{S} \geq \frac{1}{4}\sqrt{\Delta}\kappa_q p - 2\mathfrak{J}$.

For \mathfrak{R}^* . By Lemma D.2, for $l \in \mathbb{R}$ and $\gamma \in (0, |\mathbb{E}\tilde{g}_{s,e}^{\eta_k}(X)|_q)$, if $|\mathbb{E}\tilde{g}_{s,e}^{\eta}(X)|_q - |\mathbb{E}\tilde{g}_{s,e}^{\eta+l}(X)|_q \leq \gamma$, then $|l| \leq l^*$ where

$$l^* = \frac{\frac{2\gamma}{\kappa_{\eta_k}} \sqrt{\frac{(\eta_k-s)(e-\eta_k)}{e-s}} - \frac{\gamma^2}{\kappa_{\eta_k}^2}}{1 - \left(\frac{2\gamma}{\kappa_{\eta_k}} \sqrt{\frac{(\eta_k-s)(e-\eta_k)}{e-s}} - \frac{\gamma^2}{\kappa_{\eta_k}^2} \right) \frac{1}{(\eta_k-s) \wedge (e-\eta_k)}}.$$

Therefore,

$$\begin{aligned} \mathfrak{R}^* &\geq \inf_{k=1,\dots,K} \inf_{s \in (\eta_k - \Delta/2, \eta_k)} \inf_{e \in (\eta_k, \eta_k + \Delta/2)} \inf_{\gamma \in (0, |\mathbb{E}\tilde{g}_{s,e}^{\eta_k}(X)|_q)} \frac{\gamma}{l^*} \\ &\geq \inf_{k=1,\dots,K} \inf_{s \in (\eta_k - \Delta/2, \eta_k)} \inf_{e \in (\eta_k, \eta_k + \Delta/2)} \inf_{\gamma \in (0, |\mathbb{E}\tilde{g}_{s,e}^{\eta_k}(X)|_q)} \frac{\kappa_{\eta_k}^2}{2\kappa_{\eta_k} \sqrt{\frac{(\eta_k-s)(e-\eta_k)}{e-s}} - \gamma} - \frac{\gamma}{(\eta_k - s) \wedge (e - \eta_k)} \\ &= \inf_{k=1,\dots,K} \inf_{s \in (\eta_k - \Delta/2, \eta_k)} \inf_{e \in (\eta_k, \eta_k + \Delta/2)} \frac{2\kappa_{\eta_k}}{(\eta_k - s) \wedge (e - \eta_k)} \left(\sqrt{(\eta_k - s) \wedge (e - \eta_k)} - \sqrt{\frac{(\eta_k - s)(e - \eta_k)}{e - s}} \right) \\ &\geq (2\sqrt{2} - 2) \frac{\kappa_q p}{\sqrt{\Delta}}. \end{aligned}$$

□

Lemma D.2. For piecewise constant case, recall the statistics construction of Section 3.1. Suppose $(s, e] \subset (0, T]$ is an interval containing exactly one change-point $\eta + 1$. Then

1. $\eta = \arg \max_t |\mathbb{E}\tilde{g}_{s,e}^t(X)|_q$, and $|\mathbb{E}\tilde{g}_{s,e}^t(X)|_q$ increases in (s, η) , decreases in (η, e) .
2. For $0 < \gamma < |\mathbb{E}\tilde{g}_{s,e}^{\eta}(X)|_q$,

$$\sup \left\{ |l| : |\mathbb{E}\tilde{g}_{s,e}^{\eta}(X)|_q - |\mathbb{E}\tilde{g}_{s,e}^{\eta+l}(X)|_q \leq \gamma \right\} = \frac{H}{1 - \frac{H}{(\eta-s) \wedge (e-\eta)}}$$

where

$$\begin{aligned} H &= \frac{2\gamma}{\kappa_{\eta}} \sqrt{\frac{(\eta-s)(e-\eta)}{e-s}} - \frac{\gamma^2}{\kappa_{\eta}^2} \\ \kappa_{\eta} &= |\mathbb{E}\mathbb{X}_{\eta} - \mathbb{E}\mathbb{X}_{\eta+1}|_q. \end{aligned}$$

Proof. By the definition of CUSUM statistics (13), we have

$$|\mathbb{E}\tilde{g}_{s,e}^t(X)|_q = \begin{cases} \sqrt{\frac{e-t}{(e-s)(t-s)}}(\eta-s)\kappa_\eta, & t \geq \eta \\ \sqrt{\frac{t-s}{(e-s)(e-t)}}(e-\eta)\kappa_\eta, & t < \eta \end{cases}. \quad (44)$$

The monotonicity is then easy to verify.

Consider first the case where $l > 0$. Note that $|\mathbb{E}\tilde{g}_{s,e}^e(X)|_q = 0$ and $g(l) = |\mathbb{E}\tilde{g}_{s,e}^\eta(X)|_q - |\mathbb{E}\tilde{g}_{s,e}^{\eta+l}(X)|_q$ ($l > 0$) is a continuous function. So there is a unique solution to the equation

$$|\mathbb{E}\tilde{g}_{s,e}^\eta(X)|_q - |\mathbb{E}\tilde{g}_{s,e}^{\eta+l}(X)|_q = \gamma \quad (45)$$

Substituting (44) to (45), we get

$$\begin{aligned} & \left[\sqrt{\frac{e-\eta}{(e-s)(\eta-s)}} - \sqrt{\frac{e-\eta-l}{(e-s)(\eta+l-s)}} \right] (\eta-s)\kappa_\eta = \gamma \\ & \Rightarrow \sqrt{\frac{e-\eta}{\eta-s}} - \sqrt{\frac{e-\eta-l}{\eta+l-s}} = \frac{\sqrt{e-s}}{\eta-s} \frac{\gamma}{\kappa_\eta} \end{aligned}$$

With some calculations, the final solution for (45) is

$$l = \frac{\frac{2\gamma}{\kappa_\eta} \sqrt{\frac{(\eta-s)(e-\eta)}{e-s}} - \frac{\gamma^2}{\kappa_\eta^2}}{1 - \left(\frac{2\gamma}{\kappa_\eta} \sqrt{\frac{(\eta-s)(e-\eta)}{e-s}} - \frac{\gamma^2}{\kappa_\eta^2} \right) \frac{1}{\eta-s}}.$$

For the case where $l < 0$, by symmetry (replacing $e - \eta$ with $\eta - s$, and vice versa), we can directly conclude that solution for (45) ($l < 0$) is

$$l = \frac{\frac{2\gamma}{\kappa_\eta} \sqrt{\frac{(\eta-s)(e-\eta)}{e-s}} - \frac{\gamma^2}{\kappa_\eta^2}}{1 - \left(\frac{2\gamma}{\kappa_\eta} \sqrt{\frac{(\eta-s)(e-\eta)}{e-s}} - \frac{\gamma^2}{\kappa_\eta^2} \right) \frac{1}{e-\eta}}.$$

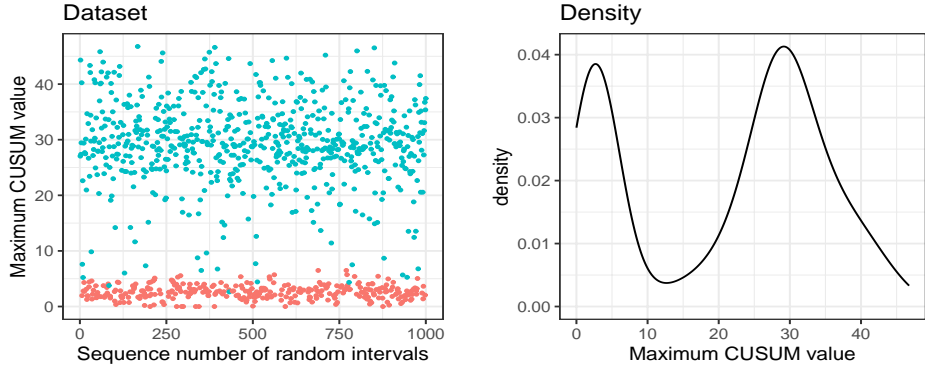
Combining the above two scenarios, we obtain that

$$\sup \left\{ |l| : |\mathbb{E}\tilde{g}_{s,e}^\eta(X)|_q - |\mathbb{E}\tilde{g}_{s,e}^{\eta+l}(X)|_q \leq \gamma \right\} = \frac{\frac{2\gamma}{\kappa_\eta} \sqrt{\frac{(\eta-s)(e-\eta)}{e-s}} - \frac{\gamma^2}{\kappa_\eta^2}}{1 - \left(\frac{2\gamma}{\kappa_\eta} \sqrt{\frac{(\eta-s)(e-\eta)}{e-s}} - \frac{\gamma^2}{\kappa_\eta^2} \right) \frac{1}{(\eta-s) \wedge (e-\eta)}}.$$

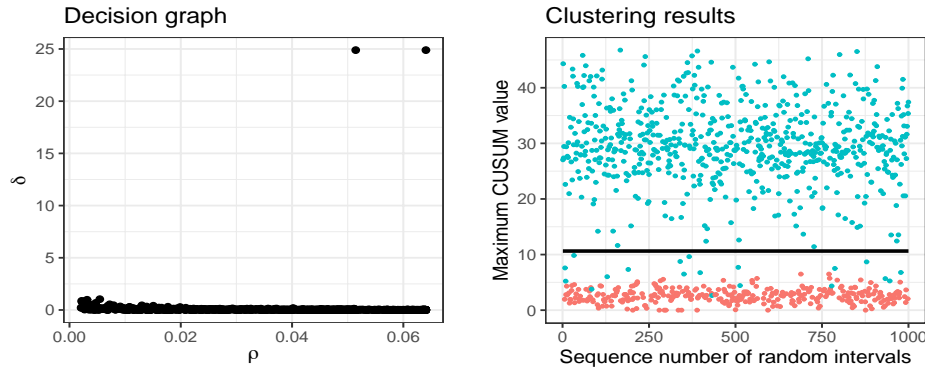
□

D.2 Interpretations and visualizations for threshold choosing

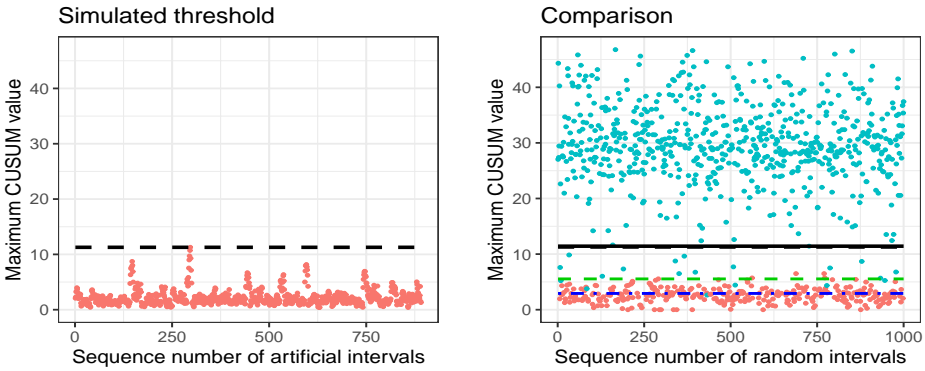
We illustrate the steps and visual representations of our threshold selection method in Figure 5.



(a) Use random intervals to calculate $|f_{s_m, e_m}(X)|_q$ and the $|\tilde{f}_{s_m, e_m}(X)|_q$ v.s. m nel and default bandwidth. plot shows that the vertical coordinates of these points tend to cluster into two groups.



(c) Calculate δ_m according to (18) and draw the decision graph described in [53]. (d) Selecting the number of clusters as 2. The boundary are shown in solid line.



(e) The simulated points are drawn and the reference threshold τ_{ref} is given. (f) The final threshold is presented with solid lines. The black dashed line represents τ_{ref} . For comparison, the threshold obtained by NOT and WBS are shown with the green and blue solid line respectively. Both of them are too small, which is a result of the existence of correlation.

Figure 5: An entire threshold selection process. The original points are sampled from a piecewise AR(1) model with coefficient 0.5 and centered $\chi^2(2)$ innovations.

D.3 Proof of Proposition 1 and Theorem 3.4

To simplify the notations, throughout this section we set $\eta_0 = 1$ and $\eta_{K+1} = T + 1$.

Proof of Proposition 1. Similar to Step 1 in the proof of Theorem 3.7, we have that $\tilde{e}_k - \tilde{s}_k < c_1\Delta$, $\min\{\eta_k - \tilde{s}_k, \tilde{e}_k - \eta_k\} \geq c_2\Delta$ for some $c_1, c_2 > 0$. Then the result follows from Lemma 12 in [60]. \square

Proof of Theorem 3.4. We first prove that under the conditions of Theorem 3.4, we have

- (a) $\mathbb{E} \left(\max_t |\mathbb{E}_X \tilde{g}_{s_m, e_m}^t(X)|_q \middle| \{ |(s_m, e_m] \cap \eta| = 0 \}, \mathcal{A}_* \right) = 0.$
- (b) $\mathbb{E} \left(\max_t |\mathbb{E}_X \tilde{g}_{s_m, e_m}^t(X)|_q \middle| \{ |(s_m, e_m] \cap \eta| = 0 \}, \mathcal{A}_* \right) > b.$
- (c) $\mathbb{P} \left(\bigcup_{m=1}^M \left\{ 0 < \max_t |\mathbb{E}_X \tilde{g}_{s_m, e_m}^t(X)|_q < b \right\} \middle| \mathcal{A}_* \right) \rightarrow 0.$

Then we prove the Theorem itself.

Since $\{(s_l, e_l]\}_{l=1}^M$ are i.i.d. sampled, it suffices to consider one particular random $(s_m, e_m]$ for some m . Let

$$s_m + 1 < \eta_r < \eta_{r+1} < \dots < \eta_{r+q^*} \leq e_m$$

where $\eta_k, k = r, \dots, r+q^*$ are change-points and $q^* \geq -1$ ($q^* = -1$ means there is no change-point in $(s_m, e_m]$). Notice that q^* is determined by s_m and e_m so the above sets are random. Define events

$$\mathcal{A}_1 = \{q^* = -1\}, \mathcal{A}_2^\gamma = \bigcup_{1 \leq r \leq K} \{q^* = 0, (\eta_r - s_m - 1) \wedge (e_m + 1 - \eta_r) \leq \gamma\},$$

$$\mathcal{A}_3^\gamma = \bigcup_{1 \leq r \leq K-1} \{q^* = 1, (\eta_r - s_m - 1) \vee (e_m + 1 - \eta_{r+1}) \leq \gamma\},$$

where $\gamma < \Delta$. \mathcal{A}_1 means that there is no change-point in the interval $(s_m, e_m]$. \mathcal{A}_2^γ indicates that there is only one change-point in $(s_m, e_m]$ and this change-point is close to at least one of the endpoints. \mathcal{A}_3^γ indicates that there are two change-points in $(s_m, e_m]$ and both of them are close to the endpoints. Since the interval $(s_m, e_m]$ is sampled uniformly, we can directly calculate the probabilities of some of these events. For \mathcal{A}_1 , we have

$$\mathbb{P}(\mathcal{A}_1) = \sum_{k=1}^{K+1} \left(\frac{\eta_k - \eta_{k-1}}{T} \right)^2 = \frac{1}{T^2} \sum_{k=1}^{K+1} (\eta_k - \eta_{k-1})^2. \quad (46)$$

To bound (46), we observe that

$$\frac{1}{T^2} \sum_{k=1}^{K+1} (\eta_k - \eta_{k-1})^2 \geq \frac{1}{T^2} \frac{1}{K+1} \left(\sum_{k=1}^{K+1} (\eta_k - \eta_{k-1}) \right)^2 = \frac{1}{K+1}.$$

For the upper bound, since $\sum_{k=1}^{K+1}(\eta_k - \eta_{k-1}) = T$ and $\eta_k - \eta_{k-1} \geq \Delta$, we derive that

$$\begin{aligned} \frac{1}{T^2} \sum_{k=1}^{K+1} (\eta_k - \eta_{k-1})^2 &= \frac{1}{T^2} \left(\sum_{k=1}^{K+1} (\eta_k - \eta_{k-1} - \Delta)^2 - (K+1)\Delta^2 + 2\Delta T \right) \\ &\leq \frac{1}{T^2} \left(\left(\sum_{k=1}^{K+1} (\eta_k - \eta_{k-1}) - (K+1)\Delta \right)^2 - (K+1)\Delta^2 + 2\Delta T \right) \\ &= \frac{1}{T^2} \left((T - (K+1)\Delta)^2 - (K+1)\Delta^2 + 2\Delta T \right) \\ &= \frac{1}{T^2} (K\Delta^2 + (T - K\Delta)^2). \end{aligned}$$

Therefore,

$$\frac{1}{K+1} \leq \mathbb{P}(\mathcal{A}_1) \leq \frac{1}{T^2} (K\Delta^2 + (T - K\Delta)^2). \quad (47)$$

As for \mathcal{A}_2^γ , we have

$$\mathbb{P}(\mathcal{A}_2^\gamma) = \frac{\gamma}{T^2} \sum_{k=1}^K (\eta_{k+1} - \eta_{k-1}) \leq \frac{2\gamma}{T}. \quad (48)$$

For \mathcal{A}_3^γ , similarly we have

$$\mathbb{P}(\mathcal{A}_3^\gamma) = \frac{\gamma^2}{T^2} (K-1). \quad (49)$$

Proof of (a). On \mathcal{A}_1 , i.e., $|(s_m, e_m] \cap \eta| = 0$, from proof of Theorem 2.2 and the fact that $\mathbb{E}_X \tilde{g}_{s_m, e_m}^t(X) = 0$, we have $\max_t |\mathbb{E}_X \tilde{g}_{s_m, e_m}^t(X)|_q = 0$

$$\mathbb{E} \left(\max_t |\mathbb{E}_X \tilde{g}_{s_m, e_m}^t(X)|_q \mid \{ |(s_m, e_m] \cap \eta| = 0 \}, \mathcal{A}_* \right) = 0.$$

Proof of (b). On the event $\{q^* \geq 1\} \cap (\mathcal{A}_3^\gamma)^c$, there exists a change-point η_k such that any other change-point $\eta_{k'}$ and the endpoints s_m, e_m satisfy $\min\{\eta_k - s_m - 1, e_m + 1 - \eta_k, |\eta_k - \eta_{k'}|\} \geq \gamma$. By Lemma D.3,

$$\max_t |\mathbb{E}_X \tilde{g}_{s_m, e_m}^t(X)|_q \geq \frac{1}{4\sqrt{e_m - s_m}} \kappa_q p \gamma \geq \frac{1}{4\sqrt{T}} \kappa_q p \gamma.$$

Recall that \tilde{g}_{s_m, e_m}^t is the CUSUM statistic, therefore, on the event $\{q^* = 0\} \cap (\mathcal{A}_2^{\gamma^2/T})^c$, direct calculations show that

$$\max_t |\mathbb{E}_X \tilde{g}_{s_m, e_m}^t(X)|_q \geq \sqrt{\frac{\gamma^2/T}{2}} \kappa_q p \geq \frac{1}{4\sqrt{T}} \kappa_q p \gamma.$$

As a result, on the event $\mathcal{A}_4 := \{q^* \geq 0\} \cap (\mathcal{A}_2^{\gamma^2/T})^c \cap (\mathcal{A}_3^\gamma)^c$, we have $\max_t |\mathbb{E}_X \tilde{g}_{s_m, e_m}^t(X)|_q \geq$

$\frac{1}{4\sqrt{T}}\kappa_q p\gamma$. We derive that

$$\begin{aligned}
& \mathbb{E} \left(\max_t |\mathbb{E}_X \tilde{g}_{s_m, e_m}^t(X)|_q \mid \{ |(s_m, e_m] \cap \eta| > 0 \}, \mathcal{A}_* \right) \\
& \geq \frac{1}{4\sqrt{T}} \kappa_q p\gamma \frac{\mathbb{P} \left(\{q^* \geq 0\} \cap (\mathcal{A}_2^{\gamma^2/T})^c \cap (\mathcal{A}_3^\gamma)^c \right)}{\mathbb{P}(q^* \geq 0)} \\
& \geq \frac{1}{4\sqrt{T}} \kappa_q p\gamma \left(1 - \frac{2\gamma^2/T^2 + \gamma^2(K-1)/T^2}{1 - \frac{1}{T^2}(K\Delta^2 + (T - K\Delta)^2)} \right) \\
& \geq \frac{1}{4\sqrt{T}} \kappa_q p\gamma \left(1 - \frac{\gamma^2(K+1)}{K\Delta(2T - (K+1)\Delta)} \right) \\
& \geq \frac{1}{4\sqrt{T}} \kappa_q p\gamma \left(1 - \frac{2\gamma^2}{\Delta T} \right).
\end{aligned}$$

We set $\gamma = \frac{8b\sqrt{T}}{\kappa_q p}$ which is of order $o(\Delta)$ by substituting $b = o(\kappa_q p\sqrt{T}/\sqrt{KM})$ and $\frac{32T^2}{\Delta^2} \log(\frac{T}{\Delta}) = o(M)$ which comes from Theorem 3.4 and (8) respectively. Therefore,

$$\mathbb{E} \left(\max_t |\mathbb{E}_X \tilde{g}_{s_m, e_m}^t(X)|_q \mid \{ |(s_m, e_m] \cap \eta| > 0 \}, \mathcal{A}_* \right) \geq \frac{1}{8\sqrt{T}} \kappa_q p\gamma > b.$$

Proof of (c). Define the event

$$\mathcal{A}_5 := \left\{ (\mathcal{A}_2^{\gamma^2/T})^c \cap (\mathcal{A}_3^\gamma)^c \text{ for all } 1 \leq m \leq M \right\}.$$

Note that $(\mathcal{A}_2^{\gamma^2/T})^c \cap (\mathcal{A}_3^\gamma)^c = \left(\{q^* \geq 0\} \cap (\mathcal{A}_2^{\gamma^2/T})^c \cap (\mathcal{A}_3^\gamma)^c \right) \cup \{q^* = -1\}$. Then $\mathbb{P}(\mathcal{A}_5) \geq \left(1 - \frac{\gamma^2(K+1)}{T^2} \right)^M \geq 1 - \frac{M\gamma^2(K+1)}{T^2} \rightarrow 1$ since $\gamma = o(T/\sqrt{KM})$ by the above construction. On \mathcal{A}_5 , we have $\max_t |\mathbb{E}_X \tilde{g}_{s_m, e_m}^t(X)|_q \in 0 \cup [b, \infty)$ for all $1 \leq m \leq M$. Therefore,

$$\mathbb{P} \left(\bigcup_{m=1}^M \left\{ 0 < \max_t |\mathbb{E}_X \tilde{g}_{s_m, e_m}^t(X)|_q < b \right\} \mid \mathcal{A}_* \right) \rightarrow 0.$$

Proof of $\mathbb{P}(\mathcal{A}_*) \geq 1 - T^{-1}$. We need to extend (43) to arbitrary $(s, e] \subset (0, T]$. Recall that \tilde{g} is the CUSUM statistic (13) and X is one of the types in Table 2. In appendix B we derive one by one for these types and Remark 8 concludes that

$$\mathbb{P} \left(\left\{ \sup_{(s, e] \subset (0, T]} \sup_{s < t \leq e} \left| |\tilde{g}_{s, e}^t(X)|_q - |\mathbb{E}_X \tilde{g}_{s, e}^t(X)|_q \right| \leq C_3 \mathfrak{J} \sqrt{K} \right\} \right) \geq 1 - T^{-1}. \quad (50)$$

Therefore,

$$\mathbb{P} \left(\left\{ \sup_{(s, e] \subset (0, T]} \left| \max_t |\tilde{g}_{s, e}^t(X)|_q - \max_t |\mathbb{E}_X \tilde{g}_{s, e}^t(X)|_q \right| \leq C_3 \mathfrak{J} \sqrt{K} \right\} \right) \geq 1 - T^{-1}.$$

Proof of (1-3) in Theorem 3.4. On event \mathcal{A}_* , we have $\left| |\tilde{f}_{s, e}^t(X)|_q - \max_t |\mathbb{E}_X \tilde{g}_{s, e}^t(X)|_q \right| \leq C_3 \mathfrak{J} \sqrt{K}$ for all $(s, e] \subset (0, T]$. Moreover, by Assumption 3.3 we can choose a b such that $\mathfrak{J} \sqrt{K} = o(b)$.

Then (4-6) follows by tracking the previous proof of (a-c). Detailedly, taking the proof of (3) as an example, we derive that on event \mathcal{A}_* ,

$$\bigcup_{m=1}^M \left\{ C_3 \mathfrak{I} \sqrt{K} < \left| \tilde{f}_{s_m, e_m}(X) \right|_q < b/2 \right\} \subset \bigcup_{m=1}^M \left\{ 0 < \max_t |\mathbb{E}_X \tilde{g}_{s_m, e_m}^t(X)|_q < b \right\}.$$

Therefore,

$$\mathbb{P} \left(\bigcup_{m=1}^M \left\{ C_3 \mathfrak{I} \sqrt{K} < \left| \tilde{f}_{s_m, e_m}(X) \right|_q < b/2 \right\} \middle| \mathcal{A}_* \right) \rightarrow 0.$$

□

Lemma D.3. *For change-points detection in the piecewise constant case, suppose $(s, e] \subset (0, T]$ is an interval and there exists a change-point $\eta \in (s, e]$ such that any other change-point η' and the endpoints s, e satisfies $\min\{\eta - s, e - \eta, |\eta - \eta'|\} \geq \gamma$. Then*

$$\max_t |\mathbb{E}_X \tilde{g}_{s, e}^t(X)|_q \geq \frac{1}{4\sqrt{e-s}} \kappa_q p \gamma$$

Proof. Assume without loss of generality that $\sum_{i=s+1}^e \mathbb{E} \mathbb{X}_i = 0$. Due to the triangle inequality and the fact that $\{\mathbb{X}_t\}$ is piecewise constant, we have

$$\begin{aligned} & \max \left\{ \left| \sum_{i=\eta-1-\gamma}^{\eta-1} \mathbb{E} \mathbb{X}_i \right|_q, \left| \sum_{i=\eta}^{\eta+\gamma-1} \mathbb{E} \mathbb{X}_i \right|_q \right\} \geq \frac{1}{2} \left| \sum_{i=\eta-1-\gamma}^{\eta-1} \mathbb{E} \mathbb{X}_i - \sum_{i=\eta}^{\eta+\gamma-1} \mathbb{E} \mathbb{X}_i \right|_q \\ & = \frac{\gamma}{2} |\mathbb{E} \mathbb{X}_{\eta-1} - \mathbb{E} \mathbb{X}_\eta|_q \geq \frac{\gamma}{2} \kappa_q p. \end{aligned}$$

Therefore, by the triangle inequality we have

$$\max \left\{ \left| \sum_{i=s+1}^{\eta-1-\gamma} \mathbb{E} \mathbb{X}_i \right|_q, \left| \sum_{i=s+1}^{\eta-1} \mathbb{E} \mathbb{X}_i \right|_q, \left| \sum_{i=s+1}^{\eta-1+\gamma} \mathbb{E} \mathbb{X}_i \right|_q \right\} \geq \frac{\gamma}{4} \kappa_q p.$$

Without loss of generality, consider that

$$\left| \sum_{i=s+1}^{\eta-1} \mathbb{E} \mathbb{X}_i \right|_q \geq \frac{1}{4} \kappa_q p \gamma,$$

Then it follows from the property of the CUSUM statistic that

$$\max_t |\mathbb{E}_X \tilde{g}_{s, e}^t(X)|_q \geq \sqrt{\frac{e-s}{(e-\eta+1)(\eta-1-s)}} \frac{1}{4} \kappa_q p \gamma \geq \frac{1}{4\sqrt{e-s}} \kappa_q p \gamma.$$

□

D.4 The USVT algorithm and Algorithm 4

We use the USVT algorithm in [61], and our Algorithm for refinement in Markov dynamic networks are shown in Algorithm 4.

Algorithm 3 Universal Singular Value Thresholding in [61]

Require: Symmetric matrix $A \in \mathbb{R}^{n \times n}$, $\tau_2, \tau_3 > 0$.

- 1: $(\kappa_i(A), v_i)$ be the i th eigen-pair of A , with $|\kappa_1(A)| \geq \dots \geq |\kappa_n(A)|$
- 2: $A' = \sum_{i: |\kappa_i(A)| \geq \tau_2} \kappa_i(A) v_i v_i^\top$
- 3: Let $\text{USVT}(A, \tau_2, \tau_3) = (A''_{ij})$ with

$$(A'')_{ij} = \begin{cases} (A')_{ij}, & \text{if } |(A')_{ij}| \leq \tau_3 \\ \text{sign}((A')_{ij})\tau_3, & \text{if } |(A')_{ij}| > \tau_3 \end{cases}$$

- 4: Output $\text{USVT}(A, \tau_2, \tau_3)$.
-

D.5 Proof of Theorem 3.7 and Theorem 3.9

Proof of Theorem 3.7. By Theorem 2.2, after applying Algorithm 1, we have $\mathbb{P}(\hat{K} = K, \mathcal{B}) \rightarrow 1$ where

$$\mathcal{B} := \bigcap_{j=1}^{\hat{K}} \left\{ [l_j, r_j] \text{ covers } \eta_j \text{ and } r_j - l_j \leq \frac{\Delta}{2} \right\}.$$

We start by outlining our proof. In Step 1, we show that the s, v_k, e in Line 5 of Algorithm 4 are well-positioned in that the spacing between them are neither too far nor too close. In Step 2, We show that the Frobenius norm of the expectation of $\tilde{Y}_{s,e}^{v_k}$ in Line 10 of Algorithm 4 is of order $\frac{\kappa_{\eta_k}^2 \Delta}{\tau_3 \log(T)}$. In Step 3, we derive the bound of $\|\tilde{Y}_{s^*,e^*}^t - \mathbb{E}\tilde{Y}_{s^*,e^*}^t\|_{op}$ for any $(s^*, e^*) \subset (0, T)$ and explore the effect the of ‘USVT’. In Step 4, we show that the samples drawn at each $\tau_3 \log(T)$ are nearly independent, and obtained the concentration results required by Step 5. With these concentration inequalities and the results of Step 3, we finish the proof via arguments motivated by [61].

Step 1. We fix for some $k(1 \leq k \leq \hat{K})$. Notice that $\tau_3 \log(T) = o(\Delta)$, we can assume without loss of generality that $\frac{v_k - s - 1}{2\tau_3 \log(T)}, \frac{e - s - 1}{2\tau_3 \log(T)}$ are positive integers. Assume without loss of generality that $l_k - \hat{\Delta}/16, r_k + \hat{\Delta}/16, (l_k + r_k)/2$ are positive integers. Recall that $S^* = \{[l_k, r_k]\}_{k=1}^{\hat{K}}$ and $r_k - l_k \leq \frac{\Delta}{2}$. Since $|\eta_k - v_k| \leq \frac{\Delta}{4}$, we have $\frac{1}{2}\Delta \leq \hat{\Delta} \leq \frac{3}{2}\Delta$.

$$e - \eta_k \geq e - r_k \geq \frac{\Delta}{32},$$

similarly, $\eta_k - s \geq \frac{\Delta}{32}, e - s \geq \frac{\Delta}{16}, e - s \leq \frac{3\Delta}{4}, e - v_k \geq \frac{\Delta}{32}, e - v_k \leq \frac{\Delta}{2}, v_k - s \geq \frac{\Delta}{32}$.

Step 2. Let $\kappa_{\eta_k} = |\mathbb{E}A(\eta_k) - \mathbb{E}A(\eta_k - 1)|_F$. It’s obvious that $\frac{e - s - 1}{\tau_3 \log(T)} + 1 \geq \frac{\Delta}{16\tau_3 \log(T)}$. As a result,

$$\tilde{\Delta}_k^2 \geq \frac{1}{2} \min \left(\frac{v_k - s - 1}{2\tau_3 \log(T)} + 1, \frac{e - v_k}{2\tau_3 \log(T)} \right) \geq \frac{1}{4} \left(\frac{\Delta/32}{2\tau_3 \log(T)} \right) \geq \frac{\Delta}{128\tau_3 \log(T)}.$$

Assume without loss of generality that $v_k \leq \eta_k$. By some direct calculations and the previous inequality, we have

$$|\mathbb{E}\tilde{Y}_{s,e}^{v_k}|_F^2 = \tilde{\Delta}_k^2 \left(\frac{e - \eta_k}{e - v_k} \right)^2 \kappa_{\eta_k}^2 \geq \frac{\Delta}{128\tau_3 \log(T)} \frac{1}{16^2} \kappa_{\eta_k}^2 = \frac{\kappa_{\eta_k}^2 \Delta}{32768\tau_3 \log(T)}. \quad (51)$$

Step 3. Let $Y(t) = A(s + 1 + 2\tau_3 \log(T)(t - 1)), 1 \leq t \leq 1 + \frac{e - s - 1}{2\tau_3 \log(T)}, \bar{Y}(t) = Y(t) - \mathbb{E}Y(t)$. For any $1 \leq i, j \leq n, Y_{ij}(t)$ is a Markov chain. By the definition of β in Assumption 3.6 and Example 2

Algorithm 4 Local refinement in dynamic networks

Require: $\{A(t)\}_{t=1}^T$, S^* , τ_2, τ_3

1: $k = 1, \hat{K} = |S^*|$. Suppose $S^* = \{[l_k, r_k]\}_{k=1}^{\hat{K}}$.

2: $\hat{\Delta} = \min_{2 \leq k \leq \hat{K}} \left(\frac{l_k + r_k}{2} - \frac{l_{k-1} + r_{k-1}}{2} \right) \wedge \left(T + 1 - \frac{l_{\hat{K}} + r_{\hat{K}}}{2} \right) \wedge \left(\frac{l_1 + r_1}{2} - 1 \right)$

3: **while** $k \leq \hat{K}$ **do**

4: $s = \lfloor l_k - \hat{\Delta}/16 \rfloor, e = \lfloor r_k + \hat{\Delta}/16 \rfloor, v_k = \lfloor (l_k + r_k)/2 \rfloor$

5: **if** $\lfloor \frac{e-s-1}{2\tau_3 \log(T)} \rfloor$ is an odd number **then**

6: $e = e + \tau_3 \log(T)$

7: **end if**

8: $\tilde{\Delta}_k = \sqrt{\left(\lfloor \frac{v_k - s - 1}{2\tau_3 \log(T)} \rfloor + 1 \right) \left(\lfloor \frac{e - s - 1}{2\tau_3 \log(T)} \rfloor - \lfloor \frac{v_k - s - 1}{2\tau_3 \log(T)} \rfloor \right) / \left(\lfloor \frac{e - s - 1}{2\tau_3 \log(T)} \rfloor + 1 \right)}$

9:

$$\begin{aligned} \tilde{Y}_{s,e}^{v_k} &= \frac{\tilde{\Delta}_k}{\lfloor \frac{v_k - s - 1}{2\tau_3 \log(T)} \rfloor + 1} \sum_{i=0}^{\lfloor \frac{v_k - s - 1}{2\tau_3 \log(T)} \rfloor} A(s + 1 + 2\tau_3 \log(T)i) \\ &\quad - \frac{\tilde{\Delta}_k}{\lfloor \frac{e - s - 1}{2\tau_3 \log(T)} \rfloor - \lfloor \frac{v_k - s - 1}{2\tau_3 \log(T)} \rfloor} \sum_{i=1 + \lfloor \frac{v_k - s - 1}{2\tau_3 \log(T)} \rfloor}^{\lfloor \frac{e - s - 1}{2\tau_3 \log(T)} \rfloor} A(s + 1 + 2\tau_3 \log(T)i) \end{aligned}$$

10: $\hat{Y}_k = \text{USVT}(\tilde{Y}_{s,e}^{v_k}, \tau_2, \tilde{\Delta}_k)$

11: **Let**

$$\begin{aligned} \tilde{Z}_{s,e}^t &= \sqrt{\frac{\lfloor \frac{e-s-1}{2\tau_3 \log(T)} - \frac{1}{2} \rfloor - \lfloor \frac{t-s-1}{2\tau_3 \log(T)} - \frac{1}{2} \rfloor}{\left(1 + \lfloor \frac{e-s-1}{2\tau_3 \log(T)} - \frac{1}{2} \rfloor\right) \left(1 + \lfloor \frac{t-s-1}{2\tau_3 \log(T)} - \frac{1}{2} \rfloor\right)}}^{\lfloor \frac{t-s-1}{2\tau_3 \log(T)} - \frac{1}{2} \rfloor} \sum_{i=0} A(s + 1 + \tau_3 \log(T)(2i + 1)) \\ &\quad - \sqrt{\frac{1 + \lfloor \frac{t-s-1}{2\tau_3 \log(T)} - \frac{1}{2} \rfloor}{\left(1 + \lfloor \frac{e-s-1}{2\tau_3 \log(T)} - \frac{1}{2} \rfloor\right) \left(\lfloor \frac{e-s-1}{2\tau_3 \log(T)} - \frac{1}{2} \rfloor - \lfloor \frac{t-s-1}{2\tau_3 \log(T)} - \frac{1}{2} \rfloor\right)}} \\ &\quad \sum_{i=1 + \lfloor \frac{t-s-1}{2\tau_3 \log(T)} - \frac{1}{2} \rfloor}^{\lfloor \frac{e-s-1}{2\tau_3 \log(T)} - \frac{1}{2} \rfloor} A(s + 1 + \tau_3 \log(T)(2i + 1)) \end{aligned}$$

12: $b_k = \arg \max_{s+(e-s)/100 < t \leq e-(e-s)/100} \langle \tilde{Z}_{s,e}^t, \hat{Y}_k \rangle$

13: $k = k + 1$

14: **end while**

15: **Output** $\{b_k\}_{k=1}^{\hat{K}}$

in Appendix B, we have

$$\|\mathbb{P}(\cdot | Y_{ij}(t-1) = 1) - \mathbb{P}(\cdot | Y_{ij}(t-1) = 0)\|_{TV} \leq \beta^{2\tau_3 \log(T)} \leq T^{-2c_7} \leq \frac{1}{4}. \quad (52)$$

Then equation (2.8) in [56] becomes $\|\Gamma\|^2 \leq \left(\frac{1}{1 - \sqrt{\beta^{2\tau_3 \log(T)}}} \right)^2 \leq 4$. Let w_t be a sequence of weights that satisfy $\sum w_t = 0, \sum w_t^2 = 1$. Since $\sum_t w_t \bar{Y}_{ij}(t)$ and $\|\sum_t w_t \bar{Y}(t)\|_{op}$ are both 1-Lipschitz. By

Corollary 4 of [56], for any $\varepsilon > 0$, we have

$$\mathbb{P} \left(\left\| \sum_t w_t \bar{Y}(t) \right\|_{op} \geq \mathbb{E} \left\| \sum_t w_t \bar{Y}(t) \right\|_{op} + 2\varepsilon \right) \leq e^{-\frac{\varepsilon^2}{2}}, \quad (53)$$

$$\mathbb{P} \left(\left| \sum_t w_t \bar{Y}_{ij}(t) \right| \geq 2\varepsilon \right) \leq 2e^{-\frac{\varepsilon^2}{2}}. \quad (54)$$

By Definition 3.5, $\{\sum_t w_t \bar{Y}_{ij}(t)\}_{1 \leq i, j \leq n}$ are independent. By (54) and Corollary 3.2 in [6], we get

$$\mathbb{E} \left\| \sum_t w_t \bar{Y}(t) \right\|_{op} \leq C_8^*(\sqrt{n} + \sqrt{\log n}) \leq C_8 \sqrt{n}, \quad (55)$$

where $C_8^*, C_8 > 8$ are two absolute constants. Combine (55) with (53) and set $\varepsilon = \frac{C_8}{2} \sqrt{\log(T)}$, then we have

$$\mathbb{P} \left(\left\| \sum_t w_t \bar{Y}(t) \right\|_{op} \geq C_8(\sqrt{n} + \sqrt{\log(T)}) \right) \leq T^{-8}. \quad (56)$$

Define the event

$$\mathcal{A} = \left\{ \sup_{0 \leq s^* < t \leq e^* \leq T} \|\tilde{Y}_{s^*, e^*}^t - \mathbb{E} \tilde{Y}_{s^*, e^*}^t\|_{op} \leq C_8(\sqrt{n} + \sqrt{\log(T)}) \right\},$$

by the union bound argument and (56), we have $\mathbb{P}(\mathcal{A}) \geq 1 - T^{-5}$. Let $\tau_2 = \frac{4}{3}C_8(\sqrt{n} + \sqrt{\log(T)})$. On event \mathcal{A} , by Lemma 1 (applying it with $\delta = \frac{1}{3}$) in [66], we have

$$\sup_{0 \leq s^* < t \leq e^* \leq T} |\text{USVT}(\tilde{Y}_{s^*, e^*}^t, \tau_2, \infty) - \mathbb{E} \tilde{Y}_{s^*, e^*}^t|_F \leq 4\tau_2 \sqrt{r}. \quad (57)$$

Let \mathcal{B} denote the above event. Similar to (51), we have

$$\mathbb{E}(\tilde{Y}_{s^*, e^*}^{v_k})_{ij} = \tilde{\Delta}_k \left(\frac{e^* - \eta_k}{e^* - v_k} \right) \leq \tilde{\Delta}_k. \quad (58)$$

Therefore, for any $1 \leq i, j \leq n$, we have

$$|(\text{USVT}(\tilde{Y}_{s, e}^{v_k}, \tau_2, \tilde{\Delta}_k))_{ij} - (\mathbb{E} \tilde{Y}_{s, e}^{v_k})_{ij}| \leq |(\text{USVT}(\tilde{Y}_{s, e}^{v_k}, \tau_2, \infty))_{ij} - (\mathbb{E} \tilde{Y}_{s, e}^{v_k})_{ij}|.$$

So on event \mathcal{B} , we have

$$|\hat{Y}_k - \mathbb{E} \tilde{Y}_{s, e}^{v_k}|_F \leq |\text{USVT}(\tilde{Y}_{s, e}^{v_k}, \tau_2, \infty) - \mathbb{E} \tilde{Y}_{s, e}^{v_k}|_F \leq 4\tau_2 \sqrt{r}.$$

By Assumption 3.6 and (51), we have

$$|\hat{Y}_k|_F \geq |\mathbb{E} \tilde{Y}_{s, e}^{v_k}|_F - 4\tau_2 \sqrt{r} \geq \frac{\kappa \eta_k \sqrt{\Delta}}{200 \sqrt{\tau_3} \log(T)} \quad (59)$$

when T is large enough. As a result, similarly to the derivations in [61] (using the inequality above (40) therein), we have when T is large enough,

$$\left\langle \frac{\mathbb{E} \tilde{Y}_{s, e}^{v_k}}{|\mathbb{E} \tilde{Y}_{s, e}^{v_k}|_F}, \frac{\hat{Y}_k}{|\hat{Y}_k|_F} \right\rangle \geq \frac{1}{2}.$$

Therefore,

$$\left\langle \mathbb{E}\tilde{Y}_{s,e}^{v_k}, \frac{\hat{Y}_k}{|\hat{Y}_k|_F} \right\rangle \geq \frac{1}{2} |\mathbb{E}\tilde{Y}_{s,e}^{v_k}|_F \geq \frac{\kappa_{\eta_k} \sqrt{\Delta}}{400 \sqrt{\tau_3 \log(T)}}. \quad (60)$$

Step 4. Let $Z(t) = A(s+1 + \tau_3 \log(T)(2t-1))$, $1 \leq t \leq \frac{e-s-1}{2\tau_3 \log(T)}$. By Lemma D.4, Conditional on $\{Y(t)\}$, we get that $\{Z(t)\}$ are independent. By Bernstein inequality, for any $\varepsilon > 0$,

$$\begin{aligned} & \mathbb{P} \left(\left| \frac{1}{\sqrt{\frac{e-s-1}{2\tau_3 \log(T)}}} \sum_{t=1}^{\frac{e-s-1}{2\tau_3 \log(T)}} \left\langle \mathbb{E}(Z(t)|\{Y(t)\}) - Z(t), \frac{\hat{Y}_k}{|\hat{Y}_k|_F} \right\rangle \right| \geq \varepsilon \middle| \{Y(t)\} \right) \\ & \leq 2 \exp \left(- \frac{1.5\varepsilon^2}{3 + \varepsilon \frac{1}{\sqrt{\frac{e-s-1}{2\tau_3 \log(T)}}} \frac{|\hat{Y}_k|_\infty}{|\hat{Y}_k|_F}} \right). \end{aligned}$$

By (58), (59), we get that on event \mathcal{A} ,

$$\frac{1}{\sqrt{\frac{e-s-1}{2\tau_3 \log(T)}}} \frac{|\hat{Y}_k|_\infty}{|\hat{Y}_k|_F} \leq \frac{200 \sqrt{\tau_3 \log(T)}}{\kappa_{\eta_k} \sqrt{\Delta}}.$$

Notice that the right hand side of the above inequality is $o(1)$ because of Assumption 3.6 and the fact that $\tilde{\kappa} = \min_k \kappa_{\eta_k}/n$ (recall that we define $\kappa_{\eta_k} = |\mathbb{E}A(\eta_k) - \mathbb{E}A(\eta_k - 1)|_F$ and $\tilde{\kappa} = \min_{1 \leq k \leq K} |\mathbb{E}A(\eta_k) - \mathbb{E}A(\eta_k - 1)|_F/n$). Setting $\varepsilon = 3 \log(T)$, we obtain that when T is large enough,

$$\begin{aligned} & \mathbb{P} \left(\left| \frac{1}{\sqrt{\frac{e-s-1}{2\tau_3 \log(T)}}} \sum_{t=1}^{\frac{e-s-1}{2\tau_3 \log(T)}} \left\langle \mathbb{E}(Z(t)|\{Y(t)\}) - Z(t), \frac{\hat{Y}_k}{|\hat{Y}_k|_F} \right\rangle \right| \geq 3 \log(T) \middle| \mathcal{A} \right) \leq 2T^{-4.5}, \\ & \mathbb{P} \left(\left| \frac{1}{\sqrt{\frac{e-s-1}{2\tau_3 \log(T)}}} \sum_{t=1}^{\frac{e-s-1}{2\tau_3 \log(T)}} \left\langle \mathbb{E}(Z(t)|\{Y(t)\}) - Z(t), \frac{\hat{Y}_k}{|\hat{Y}_k|_F} \right\rangle \right| \geq 3 \log(T) \right) \leq 2T^{-4.5}. \quad (61) \end{aligned}$$

We then bound

$$I_1 = \left| \frac{1}{\sqrt{\frac{e-s-1}{2\tau_3 \log(T)}}} \sum_{t=1}^{\frac{e-s-1}{2\tau_3 \log(T)}} \left\langle \mathbb{E}(Z(t)|\{Y(t)\}) - \mathbb{E}Z(t), \frac{\hat{Y}_k}{|\hat{Y}_k|_F} \right\rangle \right|.$$

By the derivation of (52), we can use Lemma D.5 with $\beta^* = T^{-c\tau}$ and the Cauchy-Schwarz inequal-

ity, so that

$$\begin{aligned}
I_1 &= \frac{1}{\sqrt{\frac{e-s-1}{2\tau_3 \log(T)}}} \left| \left\langle \sum_{t=1}^{\frac{e-s-1}{2\tau_3 \log(T)}} (\mathbb{E}(Z(t)|\{Y(t)\}) - \mathbb{E}Z(t)), \frac{\hat{Y}_k}{|\hat{Y}_k|_F} \right\rangle \right| \tag{62} \\
&\leq \frac{1}{\sqrt{\frac{e-s-1}{2\tau_3 \log(T)}}} \left| \sum_{t=1}^{\frac{e-s-1}{2\tau_3 \log(T)}} (\mathbb{E}(Z(t)|\{Y(t)\}) - \mathbb{E}Z(t)) \right|_F \\
&= \frac{1}{\sqrt{\frac{e-s-1}{2\tau_3 \log(T)}}} \sqrt{\sum_{i,j=1}^n \left(\sum_{t=1}^{\frac{e-s-1}{2\tau_3 \log(T)}} (\mathbb{E}(Z_{ij}(t)|\{Y(t)\}) - \mathbb{E}Z_{ij}(t)) \right)^2} \\
&\leq \frac{1}{\sqrt{\frac{e-s-1}{2\tau_3 \log(T)}}} \sqrt{\sum_{i,j=1}^n \left(3\beta^* \frac{e-s-1}{2\tau_3 \log(T)} \right)^2} = 3n\beta^* \sqrt{\frac{e-s-1}{2\tau_3 \log(T)}}.
\end{aligned}$$

Recall that $n\sqrt{\Delta}T^{-c\tau} \leq 1$, combining (61) with (62), we have that

$$\mathbb{P} \left(\left| \frac{1}{\sqrt{\frac{e-s-1}{2\tau_3 \log(T)}}} \sum_{t=1}^{\frac{e-s-1}{2\tau_3 \log(T)}} \left\langle \mathbb{E}Z(t) - Z(t), \frac{\hat{Y}_k}{|\hat{Y}_k|_F} \right\rangle \right| \geq \sqrt{\frac{3}{2\tau_3 \log(T)}} + 3 \log(T) \right) \leq 2T^{-4.5}.$$

Since $\tau_3 \geq 1/(-\log(0.5)) \geq 1$, we have that

$$\mathbb{P} \left(\left| \frac{1}{\sqrt{\frac{e-s-1}{2\tau_3 \log(T)}}} \sum_{t=1}^{\frac{e-s-1}{2\tau_3 \log(T)}} \left\langle \mathbb{E}Z(t) - Z(t), \frac{\hat{Y}_k}{|\hat{Y}_k|_F} \right\rangle \right| \geq 4 \log(T) \right) \leq 2T^{-4.5} \tag{63}$$

when T is large enough. Similar arguments show that for $s + (e-s)/100 < t \leq e - (e-s)/100$,

$$\mathbb{P} \left(\left| \left\langle \mathbb{E}\tilde{Z}_{s,e}^t - \tilde{Z}_{s,e}^t, \frac{\hat{Y}_k}{|\hat{Y}_k|_F} \right\rangle \right| \geq 4 \log(T) \right) \leq 2T^{-4.5}. \tag{64}$$

Step 5. Consider the one dimensional time series $a(t) = \langle Z(t), \frac{\hat{Y}_k}{|\hat{Y}_k|_F} \rangle$. By Lemma S.2.4. in the supplemental material of [62], using (60), (63) and (64), we have that $|b_k^* - \eta_k| \leq C_{10} \frac{\log^2(T)}{\tilde{\kappa}_{\eta_k}^2}$, and $\sup_k |b_k^* - \eta_k| \leq C_{10} \frac{\log^2(T)}{\tilde{\kappa}^2 n^2}$, where b_k^* is $\arg \max_t \langle \tilde{Z}(t), \hat{Y}_k \rangle$ and $\tilde{Z}(t)$ is the CUSUM statistic on $Z(t)$. Recall that $Z(t) = A(s+1 + \tau_3 \log(T)(2t-1))$. So finally we get

$$\sup_k |b_k - \eta_k| \leq C_4^* \frac{c_7 \log^3(T)}{-(\log \beta) \tilde{\kappa}^2 n^2}$$

when T is large enough. We comment that when $\beta \leq 1 - \delta$ for some $\delta > 0$, this result almost recover the minimax localization lower bound which is proposed in Lemma 2 in [61]. \square

Proof of Theorem 3.9. By tracking the proof of Theorem 3.7, it suffices to show that Step 3 in the proof of Theorem 3.7 still holds. Moreover, the entire derivation is similar to the proof of Theorem 3 in [61], so we omit the proof. \square

Lemma D.4. Assume that $\{X_i\}_{i=1}^{2n+1}$, $n \geq 1$ is a discrete Markov chain with state space \mathcal{S} . Then conditional on $X_1, X_3, \dots, X_{2n+1}$, the sequence X_2, X_4, \dots, X_{2n} is independent.

Proof. For any $x_1, x_2, \dots, x_{2n+1} \in \mathcal{S}$,

$$\begin{aligned} & \mathbb{P}(X_2 = x_2, X_4 = x_4, \dots, X_{2n} = x_{2n} | X_1 = x_1, X_3 = x_3, \dots, X_{2n+1} = x_{2n+1}) \\ &= \frac{\mathbb{P}(X_{2n+1} = x_{2n+1} | X_{2n} = x_{2n}) \cdots \mathbb{P}(X_2 = x_2 | X_1 = x_1) \mathbb{P}(X_1 = x_1)}{\mathbb{P}(X_{2n+1} = x_{2n+1} | X_{2n-1} = x_{2n-1}) \cdots \mathbb{P}(X_3 = x_3 | X_1 = x_1) \mathbb{P}(X_1 = x_1)} \\ & \mathbb{P}(X_2 = x_2 | X_1 = x_1, X_3 = x_3, \dots, X_{2n+1} = x_{2n+1}) \\ &= \frac{\mathbb{P}(X_{2n+1} = x_{2n+1} | X_{2n-1} = x_{2n-1}) \cdots \mathbb{P}(X_5 = x_5 | X_3 = x_3) \mathbb{P}(X_3 = x_3 | X_2 = x_2) \mathbb{P}(X_2 = x_2 | X_1 = x_1)}{\mathbb{P}(X_{2n+1} | X_{2n-1}) \cdots \mathbb{P}(X_3 = x_3 | X_1 = x_1)} \\ &= \frac{\mathbb{P}(X_3 = x_3 | X_2 = x_2) \mathbb{P}(X_2 = x_2 | X_1 = x_1)}{\mathbb{P}(X_3 = x_3 | X_1 = x_1)}. \\ & \mathbb{P}(X_4 = x_4, \dots, X_{2n} = x_{2n} | X_1 = x_1, X_3 = x_3, \dots, X_{2n+1} = x_{2n+1}) \\ &= \frac{\mathbb{P}(X_{2n+1} = x_{2n+1} | X_{2n} = x_{2n}) \cdots \mathbb{P}(X_5 = x_5 | X_4 = x_4) \mathbb{P}(X_4 = x_4 | X_3 = x_3)}{\mathbb{P}(X_{2n+1} = x_{2n+1} | X_{2n-1} = x_{2n-1}) \cdots \mathbb{P}(X_5 = x_5 | X_3 = x_3)}. \end{aligned}$$

Therefore, conditional on $X_1, X_3, \dots, X_{2n+1}$, X_2 and (X_4, \dots, X_{2n}) are independent. By induction we get the desired result. \square

Lemma D.5. Assume that X_1, X_2, X_3 is a Markov chain taking values in $\{0, 1\}$. Let $\beta^* = \max_{x \in \{0, 1\}, i=1, 2} |\mathbb{P}(X_{i+1} = x | X_i = 0) - \mathbb{P}(X_{i+1} = x | X_i = 1)|$. Assume that $\beta^* \leq \frac{1}{2}, \beta^* \leq \mathbb{P}(X_i = 1) \leq 1 - \beta^*, i = 1, 2, 3$, then for any $x_1, x_3 \in \{0, 1\}$,

$$|\mathbb{P}(X_2 = 1 | X_1, X_3) - \mathbb{P}(X_2 = 1)| \leq 3\beta^*.$$

Proof. Let $\theta = \mathbb{P}(X_2 = 1)$. For any $x_1, x_2, x_3 \in \{0, 1\}$,

$$\begin{aligned} & \mathbb{P}(X_2 = 1 | X_1 = x_1, X_3 = x_3) \\ &= \frac{\mathbb{P}(X_3 = x_3 | X_2 = 1) \mathbb{P}(X_2 = 1 | X_1 = x_1)}{\mathbb{P}(X_3 = x_3 | X_2 = 1) \mathbb{P}(X_2 = 1 | X_1 = x_1) + \mathbb{P}(X_3 = x_3 | X_2 = 0) \mathbb{P}(X_2 = 0 | X_1 = x_1)} \\ &:= \frac{A}{A + B}. \end{aligned}$$

For $i = 1, 2$,

$$\begin{aligned} & |\mathbb{P}(X_{i+1} = x_{i+1} | X_i = x_i) - \mathbb{P}(X_{i+1} = x_{i+1})| \\ &= |\mathbb{P}(X_{i+1} = x_{i+1} | X_i = x_i)(1 - \mathbb{P}(X_i = x_i)) - \mathbb{P}(X_{i+1} = x_{i+1} | X_i = 1 - x_i) \mathbb{P}(X_i = 1 - x_i)| \\ &\leq \beta^* \mathbb{P}(X_i = 1 - x_i). \end{aligned}$$

So we have

$$\begin{aligned} & (\mathbb{P}(X_3 = x_3) - \beta^*(1 - \theta))(\theta - \beta^* \mathbb{P}(X_1 = 1 - x_1)) \leq A \leq (\mathbb{P}(X_3 = x_3) + \beta^*(1 - \theta))(\theta + \beta^* \mathbb{P}(X_1 = 1 - x_1)), \\ & (\mathbb{P}(X_3 = x_3) - \beta^* \theta)(1 - \theta - \beta^* \mathbb{P}(X_1 = 1 - x_1)) \leq B \leq (\mathbb{P}(X_3 = x_3) + \beta^* \theta)(1 - \theta + \beta^* \mathbb{P}(X_1 = 1 - x_1)). \end{aligned}$$

We first derive the upper bound of $A/(A + B)$.

$$\begin{aligned} \frac{A}{A + B} &\leq \frac{(\mathbb{P}(X_3 = x_3) + \beta^*(1 - \theta))(\theta + \beta^* \mathbb{P}(X_1 = 1 - x_1))}{\mathbb{P}(X_3 = x_3) + \beta^{*2} \mathbb{P}(X_1 = 1 - x_1)} \\ &\leq \theta + \beta^* \frac{\theta(1 - \theta) + (1 - \beta^*)(1 - 2\theta\beta^*)}{(1 + \beta^{*2})(1 - \beta^*)} \\ &\leq \theta + \beta^* \left(\frac{2}{1 + \beta^{*2}} + \frac{\beta^*}{(1 + \beta^{*2})(1 - \beta^*)} \right) < \theta + 3\beta^* \end{aligned}$$

Similarly, $\frac{A}{A+B} \geq \theta - \beta^* \frac{2-\beta^*}{(1+\beta^{*2})(1-\beta^*)} \geq \theta - 3\beta^*$. Then the proof is complete. \square

D.6 Proof of Proposition 2

Proof. Following the proof of the Theorem 4.4 in [15], using the Burkholder inequality in $\mathcal{L}^{\bar{q}}$ norm (see for example [65] and similar arguments as given in Lemma 3 of [73]),

$$\|\tilde{\sigma}_i^2(u) - \mathbb{E}\tilde{\sigma}_i^2(u)\|_{\mathcal{L}^{\bar{q}}} = O\left(\sqrt{\frac{m}{T\tau_T}}\right)$$

where $\tilde{\sigma}_i^2(u) = \sum_{j=1}^T \frac{m(\tilde{\Delta}_j^{(i)})^2}{2} \omega(u, j)$, $\tilde{\Delta}_j^{(i)} = \frac{\tilde{S}_{j-m+1, j}^{(i)} - \tilde{S}_{j+1, j+m}^{(i)}}{m}$, $\tilde{S}_{k, r}^{(i)} = \sum_{t=k}^r X_{t, i} - \mathbb{E}X_{t, i}$. By Proposition B.1 in [16], we have

$$\|\sup_{u \in [0, 1]} |\tilde{\sigma}_i^2(u) - \mathbb{E}\tilde{\sigma}_i^2(u)|\|_{\mathcal{L}^{\bar{q}}} = O\left(\sqrt{\frac{m}{T\tau_T}} \tau_T^{-\frac{1}{\bar{q}}}\right).$$

Notice that $\max_{1 \leq i \leq n} |a_i|^{\bar{q}} \leq \sum_{i=1}^n |a_i|^{\bar{q}}$ for any real numbers (a_i) , we then obtain that

$$\|\max_i \sup_{u \in [0, 1]} |\tilde{\sigma}_i^2(u) - \mathbb{E}\tilde{\sigma}_i^2(u)|\|_{\mathcal{L}^{\bar{q}}} = O\left(p^{\frac{1}{\bar{q}}} \sqrt{\frac{m}{T\tau_T}} \tau_T^{-\frac{1}{\bar{q}}}\right).$$

Notice that for some large enough constant C , $\omega(u, j) \leq \frac{C}{T\tau_T}$ for any t and j . Moreover, there are at most $2Km$ non-zero terms in $\{\Delta_j^{(i)} - \tilde{\Delta}_j^{(i)}\}_{j=1}^T$, and they are bounded due to Assumption 3.10 (1). Therefore, for some large constant $C^* > 0$ we have

$$\begin{aligned} \|\sup_u |\tilde{\sigma}_i^2(u) - \hat{\sigma}_i^2(u)|\|_{\mathcal{L}^{\frac{\bar{q}}{2}}} &\leq \|C \sum_{j=1}^T \frac{m}{2T\tau_T} |(\Delta_j^{(i)})^2 - (\tilde{\Delta}_j^{(i)})^2|\|_{\mathcal{L}^{\frac{\bar{q}}{2}}} \\ &\leq C \sum_{j=1}^T \frac{m}{2T\tau_T} \|\Delta_j^{(i)} - \tilde{\Delta}_j^{(i)}\|_{\mathcal{L}^{\bar{q}}} \|\Delta_j^{(i)} + \tilde{\Delta}_j^{(i)}\|_{\mathcal{L}^{\bar{q}}} \leq C^* \frac{m^2 K}{2T\tau_T}. \end{aligned}$$

So we have $\max_i \sup_u |\tilde{\sigma}_i^2(u) - \hat{\sigma}_i^2(u)| = O_p\left(p^{\frac{2}{\bar{q}}} \frac{m^2 K}{T\tau_T}\right)$. By the equation after (B.37) in the proof of Theorem 4.4 in [15], we have

$$\max_i \sup_u |\mathbb{E}\tilde{\sigma}_i^2(u) - \sigma_i^2(u)| = O\left(p^{\frac{1}{\bar{q}}} \left(\sqrt{\frac{m}{T}} + \frac{1}{m} + \tau_T\right)\right).$$

Then the result follows. \square

E Appendix for Section 4

E.1 The signal-to-noise ratio condition for PP case

Define

$$\mathfrak{P} := \inf_{1 \leq k \leq K} \inf_{\substack{s \in (\eta_k - \Delta/(4H_T), \eta_k - \Delta/(8H_T)) \\ e \in (\eta_k + \Delta/(8H_T), \eta_k + \Delta/(4H_T))}} |\mathbb{E}\tilde{f}_{s, e}(X)|_q.$$

To calculate \mathfrak{P} , consider the case where $s \in (\eta_k - \Delta/(4H_T), \eta_k - \Delta/(8H_T))$ and $e \in (\eta_k + \Delta/(8H_T), \eta_k + \Delta/(4H_T))$ for some k . Let $a_l = (0, \dots, 0, 1^l, \dots, (e - \eta_k)^l)^\top$. Then

$$\begin{aligned}\mathbb{E}\tilde{g}_{s,e}^{\eta_k}(X) &= \sum_{r=s+1}^e \tilde{w}_{s,e}^{\eta_k}(r) \mathbb{E}X_r \\ &= \begin{pmatrix} \mathbb{E}X_{s+1,1} & \cdots & \mathbb{E}X_{e,1} \\ \vdots & \ddots & \vdots \\ \mathbb{E}X_{s+1,p} & \cdots & \mathbb{E}X_{e,p} \end{pmatrix} \frac{(I - P_U)a_l}{\sqrt{a_l^\top (I - P_U)a_l}}.\end{aligned}$$

Notice that $(I - P_U)a_l$ is orthogonal to any polynomial with degree up to l , and the interval (s, e) only contains one change-point η_k . By Lemma E.1, we have that

$$\begin{aligned}& (\mathbb{E}X_{s+1,1}, \dots, \mathbb{E}X_{e,1}) \frac{(I - P_U)a_l}{\sqrt{a_l^\top (I - P_U)a_l}} \\ &= (a_l^{(\eta_k)})_1 \sqrt{a_l^\top (I - P_U)a_l} = \Omega \left((a_l^{(\eta_k)})_1 (e - s)^{l+\frac{1}{2}} \right) \\ &= \Omega \left((a_l^{(\eta_k)})_1 \left(\frac{\Delta}{H_T} \right)^{l+\frac{1}{2}} \right)\end{aligned}$$

where $(a_l^{(\eta_k)})_1$ is the first component of vector $a_l^{(\eta_k)}$. Hence, $\mathbb{E}\tilde{g}_{s,e}^{\eta_k}(X) = \Omega \left(a_l^{(\eta_k)} \left(\frac{\Delta}{H_T} \right)^{l+\frac{1}{2}} \right)$. Then it suffices to follow the same derivation as in Appendix D.1. Finally, we get

$$\mathfrak{P} \geq \frac{1}{2} \left(C_l |a_l^{(\eta_k)}|_q \left(\frac{\Delta}{H_T} \right)^{l+\frac{1}{2}} - \mathfrak{J} \right)$$

where C_l is a constant depending on l . Similar to Lemma D.1, we have that $\mathfrak{N} = 0$. Therefore, the signal-to-noise ratio condition (5) reduces to $\frac{H_T^{l+\frac{1}{2}} \mathfrak{J}}{\min_{k=1, \dots, K} |a_l^{(\eta_k)}|_q \Delta^{l+\frac{1}{2}}} \rightarrow 0$ as $T \rightarrow \infty$.

Lemma E.1. *Let e, b be two positive integers, such that $\chi_e = \frac{b}{e} \rightarrow \chi \in [\delta, 1 - \delta]$ for some fixed small constant δ as $e \rightarrow \infty$. Let p be an integer such that $1 \leq p \leq 50$. Let*

$$\begin{aligned}U &= \begin{pmatrix} 1 & 1 & 1^2 & \cdots & 1^p \\ 1 & 2 & 2^2 & \cdots & 2^p \\ \vdots & \vdots & \vdots & \vdots & \vdots \\ 1 & e & e^2 & \cdots & e^p \end{pmatrix}, \\ P_U &= U(U^\top U)^{-1}U^\top, \\ a_k &= (0, \dots, 0, 1^k, \dots, (e - b)^k)^\top \text{ for } 0 \leq k \leq p.\end{aligned}$$

Then as $e \rightarrow \infty$, we have

$$\frac{a_k^\top (I - P_U)a_p}{e^{k+p+1}} \rightarrow c(p, k, \chi)$$

where $c(p, k, \chi)$ is an constant depending on p, k, χ . Moreover, when $p = k$, we have $c(p, p, \chi) = \frac{(\chi(1-\chi))^{2p+1}}{2^{p+1}} > 0$.

Proof. Let $H_e(k) = \sum_{j=1}^e j^k$. It's well known that $H_e(k) = \frac{1}{k+1}e^{k+1}(1 + o(1))$ for fixed k and $e \rightarrow \infty$. Therefore,

$$\begin{aligned} U^\top U &= \begin{pmatrix} H_e(0) & H_e(1) & \cdots & H_e(p) \\ \vdots & \vdots & \ddots & \vdots \\ H_e(p) & \cdots & \cdots & H_e(2p) \end{pmatrix}_{(p+1) \times (p+1)} \\ &= \begin{pmatrix} e(1 + o(1)) & \frac{1}{2}e^2(1 + o(1)) & \cdots & \frac{1}{p+1}e^{p+1}(1 + o(1)) \\ \vdots & \vdots & \ddots & \vdots \\ \frac{1}{p+1}e^{p+1}(1 + o(1)) & \cdots & \cdots & \frac{1}{2p+1}e^{2p+1}(1 + o(1)) \end{pmatrix}_{(p+1) \times (p+1)}. \end{aligned}$$

By the continuity of the inverse operation, we get

$$\left((U^\top U)^{-1} \right)_{ij} = f_{ij} e^{1-i-j} (1 + o(1))$$

where $(\cdot)_{ij}$ is the element of the i th row and j th column, and f_{ij} is the entity of the inverse of the Hilbert matrix $\begin{pmatrix} 1 & \cdots & \frac{1}{p+1} \\ \vdots & \ddots & \vdots \\ \frac{1}{p+1} & \cdots & \frac{1}{2p+1} \end{pmatrix}$. We briefly mention that Hilbert matrix is positive definite. On

the other hand, for fixed $0 \leq k \leq p, 0 \leq i \leq p$, let $G_\chi(k, i) = \int_0^1 u^k ((1 - \chi)u + \chi)^i du$. Then

$$\sum_{s=1}^{e-b} s^k (s+b)^i = (1 - \chi)^{k+1} e^{k+i+1} G_\chi(k, i) (1 + o(1)).$$

So we have

$$\begin{aligned} a_k^\top P_U a_p &= (a_k^\top U) (U^\top U)^{-1} (U^\top a_p) \\ &= (1 - \chi)^{k+p+2} e^{k+p+1} \begin{pmatrix} G_\chi(k, 0) \\ \vdots \\ G_\chi(k, p) \end{pmatrix}^\top \begin{pmatrix} f_{11} & f_{12} & \cdots & f_{1,p+1} \\ \vdots & \vdots & \ddots & \vdots \\ f_{p+1,1} & \cdots & \cdots & f_{p+1,p+1} \end{pmatrix} \begin{pmatrix} G_\chi(p, 0) \\ \vdots \\ G_\chi(p, p) \end{pmatrix} (1 + o(1)). \end{aligned}$$

Since $a_k^\top a_p = \frac{1}{k+p+1} (1 - \chi)^{k+p+1} e^{k+p+1} (1 + o(1))$, we have that as $e \rightarrow \infty$,

$$\frac{a_k^\top (I - P_U) a_p}{e^{k+p+1}} \rightarrow \frac{(1 - \chi)^{k+p+1}}{k + p + 1} \mathbb{G}$$

where

$$\mathbb{G} = 1 - (k + p + 1)(1 - \chi) \begin{pmatrix} G_\chi(k, 0) \\ \vdots \\ G_\chi(k, p) \end{pmatrix}^\top \begin{pmatrix} f_{11} & f_{12} & \cdots & f_{1,p+1} \\ \vdots & \vdots & \ddots & \vdots \\ f_{p+1,1} & \cdots & \cdots & f_{p+1,p+1} \end{pmatrix} \begin{pmatrix} G_\chi(p, 0) \\ \vdots \\ G_\chi(p, p) \end{pmatrix}. \quad (65)$$

Notice that \mathbb{G} only relies on p, k, χ , and it is a polynomial in χ with degree no more than $2p + 1$. It's clear that \mathbb{G} can be calculated directly, and we verified one by one that for $1 \leq p \leq 50$, $\mathbb{G} = \chi^{2p+1}$. We also conjecture that $\mathbb{G} = \chi^{2p+1}$ when $p > 50$ and leave the rigorous proof to our future work. Therefore, when $k = p \in \{1, \dots, 50\}$, we have $c(p, k, \chi) = \frac{(\chi(1-\chi))^{2p+1}}{2p+1}$. \square

E.2 Proof of Theorem 4.1

Proof. Consider the event

$$\mathcal{M}^* = \bigcap_{k=1}^K \left\{ \exists (s_m, e_m) \text{ s.t. } \eta_k - \frac{\Delta}{4H_T} < s_m < \eta_k - \frac{\Delta}{8H_T}, \eta_k + \frac{\Delta}{8H_T} < e_m < \eta_k + \frac{\Delta}{4H_T} \right\}.$$

$$\begin{aligned} \mathbb{P}(\mathcal{M}^{*c}) &\leq \sum_{k=1}^K \prod_{m=1}^M \left(1 - \mathbb{P} \left(\eta_k - \frac{\Delta}{4H_T} < s_m < \eta_k - \frac{\Delta}{8H_T}, \eta_k + \frac{\Delta}{8H_T} < e_m < \eta_k + \frac{\Delta}{4H_T} \right) \right) \\ &= K \left(1 - 2 \left(\frac{\Delta}{8H_T T} \right)^2 \right)^M \leq \frac{T}{\Delta} \exp \left(-\frac{M\Delta^2}{32(TH_T)^2} \right) \end{aligned}$$

So when $\frac{32T^2H_T^2}{\Delta^2} \log \left(\frac{T}{\Delta} \right) = o(M)$, we have $\mathbb{P}(\mathcal{M}^*) \rightarrow 1$. Recall the event \mathcal{A} in (35), we have $\mathbb{P}(\mathcal{A} \cap \mathcal{M}^*) \rightarrow 1$. Following the statements in Proof C.1 and use the notations there, we easily have that $\hat{K} = K$, $[l_k, r_{K+1-k}]$ contains η_{K+1-k} only and $r_{K+1-k} - l_k \leq \frac{\Delta}{2H_T}$. Then the proof is complete. □